KINETICS AND MECHANISMS OF CATALYSED REDUCTION OF AMINOCARBOXYLATO-COBALT(III) COMPLEXES BY L-ASCORBIC ACID AND HYDRAZINE IN AQUEOUS ACIDIC MEDIUM

BY

YAKADI BALA ABITI

DEPARTMENT OF CHEMISTRY
FACULTY OF PHYSICAL SCIENCES
AHMADU BELLO UNIVERSITY,
ZARIA NIGERIA

MARCH, 2018

KINETICS AND MECHANISMS OF CATALYSED REDUCTION OF AMINOCARBOXYLATO-COBALT(III) COMPLEXES BY L-ASCORBIC ACID AND HYDRAZINE IN AQUEOUS ACIDIC MEDIUM

BY

Yakadi Bala ABITI, B.Sc Pure Chemistry (Uni Jos) 2012
P14SCCH8006

A THESIS SUBMITTED TO THE SCHOOL OF POSTGRADUATE STUDIES, AHMADU BELLO UNIVERSITY, ZARIA

IN PARTIAL FULFILLMENT OF THE REQUIREMENTS FOR THE AWARD OF MASTER OF SCIENCE DEGREE IN INORGANIC CHEMISTRY

DEPARTMENT OF CHEMISTRY
FACULTY OF PHYSICAL SCIENCES
AHMADU BELLO UNIVERSITY,
ZARIA, NIGERIA

MARCH, 2018

Declaration

I hereby declare that the work in this dissertation entitled "Kinetics and Mechanisms of Catalysed Reduction of Aminocarboxylato-cobalt(III) Complexes by L-Ascorbic Acid and Hydrazine in Aqueous Acidic Medium" was carried out by me in the Department of Chemistry of Ahmadu Bello University Zaria under the supervision of Dr A. D. Onu and Prof. S. O. Idris. To the best of my knowledge, no part of this work has been previously presented for the award of another degree or diploma at any institution. All information obtained from literature has been duly acknowledged in the text and a list of references has been provided.

Yakadi Bala ABITI _____ _____

Signature Date

Certification

This dissertation entitled: "Kinetics and Mechanisms of Catalysed Reduction of Aminocarboxylato-cobalt(III) Complexes by L-Ascorbic Acid and Hydrazine in Aqueous Acidic Medium" by Yakadi Bala ABITI, meets the regulations governing the award of the degree of Master of Science in Inorganic Chemistry of Ahmadu Bello University Zaria, and is approved for its contribution to knowledge and literary presentation.

Dr. A. D. Onu Chairman, Supervisory Committee	_____ Signature	_____ Date
Prof. S. O. Idris Member, Supervisory Committee	_____ Signature	_____ Date
Prof. A. O. Oyewale Head of Department	_____ Signature	_____ Date
Prof. S. Z. Abubakar Dean, School of Postgraduate Studies	_____ Signature	_____ Date

Acknowledgment

My profound gratitude goes to God almighty, for His provision, guidance and protection. Having kept me in a sound mind throughout the course of this research, I give Him all the glory.

The efforts of my esteemed supervisors, Dr. A. D. Onu and Prof. S. O. Idris in terms of supervision, tolerance and mentorship can never be over emphasized. The success of this work was a product of their unending support.

My appreciation is also extended to the Head of Department, Prof. A. O. Oyewale for providing a convenient avenue for this research to take place and the lecturers of the Department for their support. The assistance rendered by the technical staff of the department is also acknowledged.

My research mates, Ahmed Y. and Sulaiman I. S. have left a warm memory of our laboratory experience which will be hard for me to forget.

I wish to deeply appreciate the tireless effort of my family, especially my parents Dada and Ango Bala Garba Abiti, and my siblings; in terms of financial, moral, prayers and advice, which fuelled me through this programme. My friends also were encouraging and for this I am grateful.

Dedication

In memory of Mrs. Hannatu Abiti (1950 - 2015), a loving and caring mother who lived as a role model to many.

Table of Contents

List of Tables

List of Figures

Abbreviations

Abbreviation	Name
BDH	British Drug House
D	Dielectric Constant
DHA/ HA/ A	Dehydroascorbic Acid
EDTA	Ethylenediaminetetraacetate
GSH	Glutathione
H_2A	Ascorbic Acid
HEDTA	n–(2–hydroxylethyl)ethylenediaminetetraacetate
I	Ionic Strength
In	Natural Logarithm
k	Rate Constant
K	Equilibrium Constant
M & B	May and Baker
obs	Observed
Redox	Reduction – Oxidation
t	Time
T	Temperature
tmc	1,4,8,11–tetramethyl–1,4,8,11–tetraazacyclodecane
TU	Thiourea
UV – visible	Ultra Violet – visible
λ_{max}	Wavelength of Maximum Absorption

Abstract

Copper(II) catalysed reduction of aminocarboxylatocobaltate(III) ion (hereafter referred to as $[CoEDTA]^-$) and aminocarboxylatocobalt(III) complex (hereafter referred to as $[Co(HEDTA)OH_2]$) by L-ascorbic acid (hereafter referred to as H_2A) and Hydrazine (hereafter referred to as N_2H_4) have been spectrophotometrically studied in aqueous acidic medium. Stoichiometric studies gave a mole ratio of 2:1 for $[CoEDTA]^-$: H_2A, $[CoEDTA]^-$: N_2H_4, and $[Co(HEDTA)OH_2]$: N_2H_4 systems, but 1:1 for the $[Co(HEDTA)OH_2]$: H_2A system respectively. A first order with respect to the concentrations of each reactant was obtained for the $[CoEDTA]^-$ – H_2A, $[CoEDTA]^-$ – N_2H_4, and $[Co(HEDTA)OH_2]$ – N_2H_4 systems. For the $[Co(HEDTA)OH_2]$ – H_2A system, a first order with respect to $[Co(HEDTA)OH_2]$ and a half order with respect to $[H_2A]$ was obtained. Further kinetic studies on the effect of $[H^+]$ and $[Cu^{2+}]$ gave result which conforms to the following rate equations:

$$-\frac{d[Co^{III}(EDTA)^-]}{dt} = b[Cu^{2+}]\,[Co^{III}(EDTA)^-]\,[H_2A]$$

$$-\frac{d[Co^{III}(EDTA)^-]}{dt} = c[Cu^{2+}]\,[Co^{III}(EDTA)^-]\,[N_2H_4]$$

$$-\frac{d[Co^{III}(HEDTA)OH_2]}{dt} = d[Cu^{2+}]^2\,[Co^{III}(HEDTA)OH_2]\,[H_2A]^{1/2}$$

$$-\frac{d[Co^{III}(HEDTA)OH_2]}{dt} = a[H^+]^{-1}\,e[Cu^{2+}]\,[Co^{III}(HEDTA)OH_2]\,[N_2H_4]$$

a = 3.47×10^{-4} s^{-1} , b = 4.9 s^{-1}, c = 18.25 s^{-1}, d = 4.47 $s^{-1/2}$ and e = 1.8×10^2 s^{-1}.

Negative salt effects were observed for $[Co(EDTA)]^-$ – H_2A and $[Co(EDTA)]^-$ – N_2H_4 systems while neutral salt effect were obtained for $[Co(HEDTA)OH_2]$ – H_2A and $[Co(HEDTA)OH_2]$– N_2H_4 systems respectively. The test for the effect of added ions showed catalysis for

$[Co(EDTA)]^{-}$ – H_2A, $[Co(HEDTA)OH_2]$ – H_2A and $[Co(HEDTA)OH_2]$ – N_2H_4 systems, and no effect on $[Co(EDTA)]^{-}$ – N_2H_4 reaction. Results from the thermodynamic measurements indicated that $\Delta H^{\ddagger}$ = 72.75 kJ mol^{-1} and $\Delta S^{\ddagger}$ = □ 43.65 JK^{-1} mol^{-1} for $[Co(EDTA)]^{-}$ – H_2A system, $\Delta H^{\ddagger}$ = 31.46 kJ mol^{-1} and $\Delta S^{\ddagger}$ = –175.58 JK^{-1} mol^{-1} for $[Co(EDTA)]^{-}$ – N_2H_4 system, $\Delta H^{\ddagger}$ = 85.21 kJ mol^{-1} and $\Delta S^{\ddagger}$ = 7.02 JK^{-1} mol^{-1} for $[Co(HEDTA)OH_2]$ – H_2A system, $\Delta H^{\ddagger}$ = 82.89 kJ mol^{-1} and $\Delta S^{\ddagger}$ = 17.13 JK^{-1} mol^{-1} for $[Co(HEDTA)OH_2]$ – N_2H_4 system respectively. The zero intercept obtained from the Michaelis – Menten plots, enhanced rate from added ions, and the absence of spectroscopically determinable intermediates led to the proposal that the $[Co(EDTA)]^{-}$ – H_2A and $[Co(HEDTA)OH_2]$ – N_2H_4 reactions occurred via the outer – sphere mechanism. However, the non – zero intercept on the Michaelis – Menten plot, the presence of a spectroscopically determinable intermediate, negative values of the entropy of activation and non – catalysis by added ions led to the suggestion that the $[Co(EDTA)]^{-}$ – N_2H_4 reaction occurred via the inner –sphere mechanism. Both the outer – sphere and inner – sphere mechanisms have been proposed for the $[Co(HEDTA)OH_2]$ – H_2A reaction due to non –zero intercept on the Michaelis – Menten plot, catalysis by added ions and positive values of activation entropy.

CHAPTER ONE

1.0 INTRODUCTION

Many electron transfer reactions occur naturally, and they have vast applications in modern chemistry, thus making the kinetic study in this area ever promising. In various kinetic studies, the rate of the reaction is often monitored by changing experimental conditions such as temperature, concentrations and pressure (Asperger, 2003). These changes in experimental conditions give good information that sheds light on the mechanism of such reactions and these mechanisms are generally classified into the outer – sphere and inner – sphere mechanisms (Twigg, 1983; Miessler *et al*., 2014). Of the many mechanisms obtained from kinetic studies, those involving metal complexes are of great interest, due to the wide applications of such metal complexes (Davies, 1982; Bazhko, 2009; Gamenera *et al*., 2013; Joseph *et al*., 2013; Jiewei *et al*., 2014). Many researchers investigated reduction of these metal complexes with various reductants in order to gain kinetic data, of the various reductants used; L-ascorbic acid and hydrazine have proven to be very potent. Works exist on the reduction of these metal complexes by L-ascorbic acid (Laurence and Ellis, 1972; Kustin and Toppen, 1973; Pelizzetti *et al.,* 1978; Lappin, 1981; Brzyska and Krol, 1988; El-Zaru and Hodali, 1990; Davis, 1992; Leal *et al*., 1993; Saha *et al*.,1995; Abdur-Rashid, 1996) and hydrazine (Carl *et al.,* 1975; Sadagopa *et al*., 1975; Micheal *et al*., 1978; David, 1984; Sultan *et al*., 1985; Patapati *et al.,* 1986; Zagal *et al*., 1986; Max *et al*, 1998; 1999; Rupa *et al.,* 1999; Larsen *et al.,* 2001; Jhimli *et* al., 2004; Zheng *et al*., 2005; Mshelia *et al.,* 2010; Ravi and Brian, 2012; Cantillo *et al.,* 2013; Ghanbari *et al*., 2013; Streszewski *et al.,* 2014; Shirin *et al.,* 2016). In fact, there is a growing interest on the redox activity of these reductants with Co(III) complexes (Mondal and Banerjee, 2009; Majumdar, 2010; Gain *et al*., 2011; Sadhana *et al*., 2014; 2015), due to the inert nature of some Co(III)

complexes towards redox reactions (Davis, 1992; Hemzeh, 2001) which in turn provides a promising field for researchers to explore the use of catalysts in enhancing reaction rates (Luty-Blocho *et al.*, 2013; Singh *et al*., 2014).

1.1 Statement of Research Problem

Co(III) aminocarboxylato complexes have vast industrial and pharmaceutical applications and are important antimicrobial agents. Their antimicrobial activities have been attributed to series of redox reactions involving the metal complexes with electron sensitive substrates accessible within intracellular bio – molecules of these microbes, which often leads to oxidative stress (Liu, 2002; Joseph *et al*., 2013). Furthermore, these complexes are useful in agricultural industries, as they have been used for top dressing in Co – deficient pastures. These complexes when mixed in little amount with fertilizers can be assimilated by Co – deficient plants, which is subsequently involved in important redox activities to facilitate effective plant growth (Sherrell, 1990; Sekhon, 2003). Co(III) aminocarboxylato complexes can also be useful and can serve as models for vitamin B_{12} (cobalamine). The Co – N bonds found in both Co(III) aminocarboxylato complexes as well as cobalamine, and the fact that the central Co(III) metal ion in cobalamine is often reduced to Co(II) during bioactive processes makes Co(III) aminocarboxylato complexes useful models for studying redox processes as it relays to cobalamine.

It is of interest to note however that even though there exist vast applications of these complexes which are in turn related to their redox activaties, the kinetic data on the redox reactions of these cobalt(III) aminocarboxylato complexes are scanty. The paucity of information as to their redox reactions have been linked to the slow rate and sometimes kinetically unfavourable nature of their redox reactions (Hamzeh, 2001; Sadhana *et al*., 2015). Therefore,

kinetic studies of the reaction of these complexes with ascorbic acid and hydrazine which involves the use of catalyst is embarked upon to get full insight into the mechanism that underlie the reaction.

1.2 Justification of the Research

It is established that Co(III) aminocarboxylato complexes have vast uses which are based on their redox properties. In spite of this, kinetic data on their redox reactions are scanty, there is therefore the need to study the kinetics of their reaction and consequently establish the mechanisms of these reactions. This will go a long way in enhancing their activities by effectively altering their reaction conditions and hence, optimising their usefulness. Moreover, the data generated from this study would satisfy the need to understand the redox processes involving Co(III) complexes in biological systems. In addition, unveiling the mechanism behind the redox processes of these stable cobalt(III) complexes hold great importance in the kinetic community, this is partly because the complexes are widely common. As inorganic reaction mechanism forms a basic curriculum of inorganic chemistry in various graduate and undergraduate courses, the findings in this study would therefore come in handy in bridging the ambiguity encountered while addressing the kinetics and mechanisms of Co(III) aminocarboxylato complexes.

1.3 Aim of the Study

The aim of this work is to study catalysed electron transfer reactions of $[Co(EDTA)]^{-}$ and $[Co(HEDTA)OH_2]$ complexes with L-ascorbic acid and hydrazine monohydrate respectively.

1.4 Objectives of the Study

The stated aim would be achieved via the following objectives:

a. To determine the stoichiometry and analyse the products of the reactions.

b. To carry out kinetic and temperature dependent studies.

c. To propose plausible mechanism for the reactions.

CHAPTER TWO

2.0 LITERATURE REVIEW

2.1 Ascorbic Acid

Ascorbic acid commonly known as vitamin C with the molecular formula $C_6H_8O_6$, is a white solid which dissolves in water to give a mildly acidic solution. It is a naturally occurring organic compound, since it is a biosynthetic product of many plants (Carlos *et al*., 2000). The compound forms an essential part of a daily requirement of micronutrients in humans. Although many animals can synthesize the vitamin on their own, humans and other primates cannot, hence, a need for a daily intake of the vitamin (Lachapelle and Drouin, 2010). Ascorbic acid has a wide range of medicinal applications, from enhancing the response of body's immune system and pulmonary function, to high degree of anticancer activity (Juan *et al.,* 2012).

The structure of ascorbic acid is given as;

L-ascorbic Acid. $C_6H_8O_6$

2.1.1 Reactions of L-ascorbic acid

The ability of ascorbic acid to serve as a good reductant is due to the presence of the group C(OH)=C(OH)-C=O, containing conjugated double bonds (Sadhana *et al*., 2015). Electron transfer reactions of ascorbic acid are of great interest in chemical and biological processes. Hence, works that seek to explore the reducing ability of ascorbic acid in both acidic and basic media with various inorganic and organic substrates exist (Lemma *et al*., 2002; Khan *et al*., 2005; Pap *et al*., 2011; Sailani *et al*; 2011; Lawrence *et al*., 2012; Luty-Blocho *et al*., 2013). The reduction of Ni(IV), Ni(III), hexacynoferate(III) and oxime complexes by ascorbic acid have been well documented (Leal *et al*., 1993; Saha *et al*.,1995), also many works have been carried out on the reduction of some forms of Co(III) metal complexes by ascorbic acid (Majumdar, 2010; Sadhana *et al*., 2014; 2015)**.**

The kinetics and mechanism of the reduction of $[Co(en)_2(1\text{-amino-propane-2-ol})(OH_2)](ClO_4)_3$ by ascorbic acid has been reported by Sadhana *et al.,* (2015). The reaction was studied under pseudo – first order condition and the stoichiometry was found to be 1:1 of cobalt(III) complex to ascorbic acid. Temperature dependence study was carried out and the outer-sphere mechanism was proposed for the reaction. A similar mechanism was proposed for the Cu^{2+} catalysed reduction of bis(ethylenediamine)(1-amino-propane-2-ol)cobalt(III) perchlorate by ascorbic acid (Sadhana *et al.,* 2014).

2.2 Hydrazine Monohydrate

Hydrazine monohydrate is a colourless liquid with a boiling point of 118 – 119 ^{0}C and a vapour pressure of 5 mmHg at 25 ^{0}C. The chemical formula for hydrazine monohydrate is $N_2H_4.H_2O$, with a molecular structure given as:

Hydrazine monohydrate has a wide range of applications as a raw material in the synthesis of organic (Jean-Pierre and Paul, 2002; Manolis and Mercouri, 2009) and industrial chemicals especially hydrogen gas (Sanjay and Qiang, 2013; Jiang *et al.,* 2015), agricultural products (Patil and Tanu, 2014), medical drugs (Muhammad *et al.,* 2013; Anca *et al*., 2015) as well as a propellant in board space vehicles (Suggs *et al*., 1979; Vieira *et al*., 2002).

2.2.1 Reactions of hydrazine monohydrate

It is generally understood that hydrazine is slightly basic in water, as it dissociates to give a hydroxide ion depicted in Equation (2.1)

$$N_2H_4 + H_2O \rightarrow N_2H_5^+ + OH^- \quad (2.1)$$

The hydrazinium ion ($N_2H_5^+$) serves as a good reductant and in the presence of atmospheric oxygen, the major products are nitrogen gas, hydrogen gas, water and probably ammonia (Micheal *et al*., 1978). The catalytic reduction and decomposition of hydrazine was investigated by several researchers (Max *et al,* 1998; Larsen *et al.,* 2001; Cantillo *et al.,* 2013; Ghanbari *et al*., 2013; Shirin *et al.,* 2016). Interestingly, an important aspect of this catalytic reduction was observed not to follow a fixed chemical stoichiometry. This was attributed to the nature of catalyst and temperature of the electron transfer reaction (Zheng *et al*., 2005; Ghanbari *et al*., 2013).

Mechanism of the oxidation of hydrazine by tris(biguanide)manganese(IV) in aqueous acidic medium exists (Basab *et al.,* 2005). In the report, Mn(IV) is reduced to Mn(II), the stoichiometry of 2:1 (Mn(IV) : hydrazine) was obtained. The kinetic study showed a first order with respect to the concentration of Mn(IV) complex. As expected, increasing the reaction pH resulted in an increase in the k_{obs} values. The overall increase in rate accompanied by an increase in ionic strength ($NaClO_4$), led to the suggestion that the active specie at the rate determining step is $N_2H_5^+$ rather than the neutral N_2H_4. The inner – sphere mechanism was proposed for this reaction. Streszewski *et al.,* (2014) established a similar mechanism while investigating the reaction of tetrachloroaurate(III) ions with hydrazine, the reaction was monitored using a combination of the classical UV–visible spectrophotometry and the stopped – flow technique. The reaction was first order with respect to Au(III) concentration, and activation enthalpy ($\Delta H^{\ddagger}$ = 30.9 ± 2.9 kJ mol^{-1}) and entropy ($\Delta S^{\ddagger}$ = −174.7 ± 9.5 JK^{-1} mol^{-1}) were obtained from a temperature dependent study.

2.3 Cobalt(III) Complexes

2.3.1 Reactions of cobalt(III) complexes

The reactions of cobalt(III) complexes involves majorly a one electron transfer to a single cobalt(III) ion in the complex, thereby reducing the Co^{III} to Co^{II}. The rate of the reduction of cobalt(III) complexes is a function of the nature and size of the ligands (Hamzeh, 2001), and also depends greatly on the identity of the reductant (Tobe and Burgess, 1999). In most cases, the reactions of Co(III) complexes are often slow (Olayinka *et al.,* 2006), this could be attributed to the high magnitude of Δ_{oct} that accompanies +3 cobalt ions. Notwithstanding, several works have been documented for the reduction of cobalt(III) complexes with both organic and inorganic

reductants (Hamzeh, 2001; Olayinka *et al.*, 2006; Asemave *et al.*, 2012; Mandal *et al*., 2013; Sadhana *et al.*, 2014; Singh *et al*., 2014).

Kinetics and mechanism of electron transfer reaction of cobalt(III) complex by Fe^{2+} ions in liposome (dipalmitoylphosphotidylcholine) vesicles has been studied (Nagaraj *et al.*, 2015). The rate of the reaction was measured spectrophotometrically and the temperature was controlled using a water Peltier system. From the stoichiometric study, one mole of Co(III) reacted with one mole of Fe(II), the kinetic study indicated a first order dependence on Fe(II) and a second order overall. The temperature dependence study was carried out over a temperature range of 298 K to 323 K, where the activation parameters where obtained. The comparison of $[Fe(CN)_6]^{4-}$ and Fe^{2+} ions as oxidants showed that the greater rate was observed with $[Fe(CN)_6]^{4-}$ as oxidant, compared with Fe^{2+} ions. This was attributed to the strong π-acidic character of $[Fe(CN)_6]^{4-}$ compared to Fe^{2+} ions. The complexes used in this study are inert to substitution due to the non-availability of a free coordination site for inner-sphere electron transfer reaction, an outer – sphere electron transfer process was hence proposed. Mohanty *et al.,* (2014) also investigated the kinetics and mechanism of the oxidation of glutathione (GSH) by cis-(diaqua)-bis-(ethylenediamine) cobalt(III) ion spectrophotometrically and proposed the outer – sphere mechanism for the reaction.

The kinetics and mechanism of thiourea (TU) oxidation by $[Co_2(O_2)(NH_3)_{10}]^{5+}$ complex was successfully studied by Osunlaja *et al.*,(2013). The stoichiometry established for the reaction conform to the overall Equation (2.2).

$$(NH_3)_5Co(O_2)Co(NH_3)_5^{4+} + (NH_2)_2C{=}S + 5H_2O \rightarrow 2Co^{2+} + (NH_2)_2C{=}O + 2H^+ + 10NH_3 + SO_4^{2-}. \qquad (2.2)$$

Evaluating the evidences adduced for the reaction led to the conclusion that the reaction follows an outersphere mechanism.

However, the ruthenium(III) catalyzed oxidation of d-glucose by 12–tungstocobaltate(III) gave a stoichiometry which conform to Equation (2.3).

$$C_6H_{12}O_6 + 2[Co^{III}W_{12}O_{40}]^{5-} \rightarrow C_5H_{10}O_5 + 2[Co^{II}W_{12}O_{40}]^{6-} + CO + 2H^+ \quad (2.3)$$

Kinetic study showed a first order with respect to both Co(III) oxidant and Ru(III) catalyst, and a second order overall. Increase in the pH, ionic strength and dielectric constants of the reaction were accompanied by an increase in the respective rates. The temperature dependence study was carried out at 298 K – 313 K and the activation parameters ($\Delta H^{\ddagger}$ = 20.92 ± 3 kJ mol^{-1}, $\Delta S^{\ddagger}$ = –120.44 ± 2 JK^{-1} mol and $\Delta G^{\ddagger}$ = 87.60 ± 2 kJ K^{-1} mol^{-1}) for the reaction were obtained. The outersphere mechanism was proposed and the rate of the of the reaction was expressed as

$$Rate = k_{obs}[Co^{III}W_{12}O_{40}{}^{5-}] \quad (2.4)$$

2.3.2 Cobalt(III) complexes of aminocarboxylates

Aminocarboxylates are forms of ligands having one or more amine group(s) bonded to two or more carboxylic groups, such ligands have been documented in earlier works (Juranic *et al*., 2006; Curie *et al.*,2009). Thus cobalt(III) Complexes of aminocarboxylates that are considered in this work are aminocarboxylatocobaltate(III) ion $[Co(EDTA)]^{-}$ and aminocarboxylatocobalt(III) complex $[Co(HEDTA)OH_2]$.

$[Co(EDTA)]^-$ $(C_{10}H_{12}CoN_2O_8)$

$[Co(HEDTA)OH_2]$ $(C_{10}H_{17}CoN_2O_8)$

The reduction of these metal complexes has been studied (Liu *et al*., 2002; Paraneeiswaran *et al.*,2014; Singh *et al*., 2015; Paraneeiswaran *et al.,* 2015; 2016). However, these studies were concerned with the reduction of cobalt(III) aminocarboxylato complexes by active microorganisms such as *Pseudomonas aeruginosa*, *Bacillus licheniformis*, etc. It is of interest to note that literature on the mechanism of the kinetic reduction of $[Co(EDTA)]^-$ and $[Co(HEDTA)OH_2]$ by either organic or inorganic reductants are scanty. William *et al.,* (1991) successfully studied the kinetics of aqueous $[Co(HEDTA)OH_2]^-$ oxidation by $[Co(EDTA)]^-$ at varied pressure. In this study, kinetic data were obtained spectrophotometrically, at a constant

ionic strength of 0.5 mol dm^{-3} ($NaClO_4$). It was found that the order was first order with respect to both Co^{II} and Co^{III}, and a second order overall, the mechanism of this reaction was rationalized to follow the outer – sphere scheme.

Most reactions of cobalt(III)aminocarboxylato complexes are relatively slow; this is due to high stability of these complexes as they are made up of good chelating polydentate ligands. The nature and size of these ligands coupled with the high oxidation state of the metal that form such complexes causes a large magnitude of splitting (Δ_{oct}), thus electron donated by a reductant has to be filled into a higher energy *eg* orbital, this is less likely to occur hence a slow nature of the redox process. Furthermore, the large and bulky size of aminocarboxylato ligands makes electron tunneling through it an entirely slow process, since rate of electron transfer reactions depend on rate of electron tunneling, these ligands contribute to the slow rate observed in these complexes (Hamzeh, 2001; James, 2002).

CHAPTER THREE

3.0 MATERIALS AND METHODS

3.1 Materials

All solutions were prepared with distilled water. Analytical grade reagents were used throughout the period of investigation. Cobaltous nitrate, hydrogen peroxide and disodium salt of EDTA (Sigma-Aldrich) were used to prepare $[Co(EDTA)]^-$, while cobaltous chloride, hydrogen peroxide, sodium hydroxide and HEDTA salt (M & B) were used to prepare $[Co(HEDTA)OH_2]$, the reductants used were L-ascorbic acid (BDH) and 98 % hydrazine monohydrate (Sigma-Aldrich).

Sulphuric acid (Sigma-Aldrich) was used to maintain $[H^+]$ for the $[Co(EDTA)]^- – H_2A$ system, while perchloric acid (Sigma-Aldrich) was used for the reactions of $[Co(EDTA)]^- – N_2H_4$, $[Co(HEDTA)OH_2] – H_2A$, and $[Co(HEDTA)OH_2] – N_2H_4$. Sodium sulphate was used to maintain a constant ionic strength for each run in the $[Co(EDTA)]^- – H_2A$ system, while sodium perchlorate was used for $[Co(EDTA)]^- – N_2H_4$, $[Co(HEDTA)OH_2] – H_2A$, and $[Co(HEDTA)OH_2] – N_2H_4$, systems. Copper sulphate was used as catalyst, and acrylamide with methanol was used to test for free radical in all the reactions.

Kinetic investigations were carried out using a Corning Colorimetre 252 model equipped with a Grant JB1 thermostated water bath. Rate of the reaction was monitored with a digital stop watch.

3.1.1 Preparation of cobalt(III) complex solutions

3.1.1.1 *Preparation of $[Co(EDTA)]^-$ solution*

The complex was prepared from cobaltous nitrate and ethylenediaminetetraacetic acid disodium salt, according to the method of Szabolcs *et al*,. (2005). Accurately weighed 7.29 g of $[Co(H_2O)_6](NO_3)_2$ and 9.32 g of $Na_2.H_2EDTA.2H_2O$ were added to 50 cm^3 of water, 3.0 ml of 30 % H_2O_2 was added to oxidise the Co(II) to Co(III). The solution was then boiled for an hour and transferred into a 100 cm^3 volumetric flask and made up to the mark to obtain 0.5 mol dm^{-3} Na[Co(EDTA)]. The complex was characterised using UV/Visible spectrophotometre between wavelength ranges of 300 – 600 nm.

3.1.1.2 *Preparation of $[Co(HEDTA)OH_2]$ solution*

The complex was prepared according to the method of Dézsi *et al*,.(1976), with some minor modification. A 10.0 g of $CoCl_2.6H_2O$ was dissolved in a beaker containing 100 cm^3 of distilled water, the solution was then oxidised using 3.0 ml of 30 % H_2O_2. About 3.36 g of NaOH was then dissolved and added into the solution, and $Co(OH)_3$ was formed as a precipitate, which was washed with ice cold water and dried in a desiccator. The dried $Co(OH)_3$ (2.76 g) was mixed with 7.2 g of HEDTA in 60 cm^3 of distilled water and was boiled for an hour. The solution was cooled, transferred into a 100 cm^3 volumetric flask and made up to the mark with distilled water to obtain a 0.25 mol dm^{-3} $[Co(HEDTA)OH_2]$. The complex was characterised using UV/Visible spectrophotometre with the UV/Visible spectrum scanned between wavelength ranges of 300 – 600 nm.

3.1.2 Preparation of stock L-ascorbic acid solution

Solution of ascorbic acid was prepared by dissolving 8.8 g of the solid ascorbic acid in 20 cm^3 of distilled water. The solution was then carefully transferred into a 50 cm^3 volumetric flask and made up to the mark with freshly prepared distilled water to get a 1 mol dm^{-3} ascorbic acid solution.

3.1.3 Preparation of stock hydrazine solution

Desired stock solution of hydrazine monohydrate was prepared by measuring 1.24 cm^3 into a 25 cm^3 volumetric flask. It was then made up to the mark with freshly prepared distilled water to give a 1.0 mol dm^{-3} solution.

3.1.4 Preparation of standard perchloric acid solution

A 0.5 mol dm^{-3} stock solution of perchloric acid was made from 70 % perchloric acid (Sigma-Aldrich) of density 1.66 g cm^{-3}. The acid was prepared by transferring 4.32 cm^3 of the 70 % perchloric acid into 20 cm^3 of water contained in a 100 cm^3 volumetric flask and further made up to the mark with distilled water. The prepared acid was then standardised volumetrically using sodium carbonate as primary standard and phenolphthalein as indicator.

3.1.5 Preparation of standard sulphuric acid solution

A 0.05 mol dm^{-3} stock solution of sulphuric acid (analar grade) was made by diluting 98% sulphuric acid of specific gravity 1.84 g cm^{-3}. The sulphuric acid was then standardised volumetrically using sodium carbonate as primary standard and phenolphthalein indicator.

3.1.6 Preparation of stock copper sulphate solution

$CuSO_4$ (0.1 mol dm^{-3}) was prepared by dissolving 2.5 g of $CuSO_4.5H_2O$ with a molecular weight of 249.61 g mol^{-1} in 40 cm^3 of distilled water; this was then transferred into a 100 cm^3 volumetric flask and made up to the mark with distilled water.

3.1.7 Preparation of stock sodium perchlorate solution

Stock solution of sodium perchlorate was prepared by dissolving 35.13 g of $NaClO_4.H_2O$ salt into 100 cm^3 of distilled water contained in a beaker, the solution was then transferred into a 250 cm^3 volumetric flask and the beaker was serially rinsed into the flask, the transferred solution was made up with distilled water to obtain 2.0 mol dm^{-3} salt solution.

3.1.8 Preparation of stock sodium sulphate solution

A 14.20 g of weighted salt was transferred into a beaker and dissolved in 50 cm^3 of distilled water; the solution was transferred to a 100 cm^3 volumetric flask and made up to the mark with freshly prepared distilled water to obtain a 2.0 mol dm^{-3} salt solution.

3.1.9 Preparation of sodium carbonate solution

Stock solution of 0.10 mol dm^{-3} sodium carbonate was obtained by dissolving 1.06 g of Na_2CO_3 in 100 cm^3 of distilled water. This solution was used as a primary standard in the standardisation of sulphuric and perchloric acids.

3.1.10 Preparation of salt solutions

Stock solutions of sodium acetate, sodium formate, potassium perchlorate, lithium sulphate and zinc sulphate were prepared by dissolving a known weight of each salt in a known volume of distilled water.

3.2 Methods

3.2.1 Stoichiometric studies

The stoichiometry of the reactions were determined by spectrophotometric titration, using the mole ratio method for both $[Co(EDTA)]^-$ and $[Co(HEDTA)OH_2]$ systems. The concentration of $[Co(EDTA)]^-$ and $[Co(HEDTA)OH_2]$ were kept constant at 3.0×10^{-3} mol dm^{-3} and 6.0×10^{-3} mol dm^{-3} respectively , $[H^+] = 1.0 \times 10^{-2}$ mol dm^{-3} (for $[Co(EDTA)]^-$ each with N_2H_4 and H_2A systems) and 2.0×10^{-2} mol dm^{-3} (for $[Co(HEDTA)OH_2]$ with N_2H_4 and H_2A systems). I = 0.05 mol dm^{-3} and T = 25 ± 1^0C for all the systems. Decrease in absorbance was monitored after every six (6) hours at λ_{max} = 535 nm for $[Co(EDTA)]^-$ systems, and λ_{max} = 550 nm for $[Co(HEDTA)OH_2]$ systems. $[H_2A]$ and $[N_2H_4]$ ranged from (0.6 to 6.0) $\times 10^{-3}$ mol dm^{-3} for $[Co(EDTA)]^-$ systems and (1.2 to 12.0) $\times 10^{-3}$ mol dm^{-3} for $[Co(HEDTA)OH_2]$ systems respectively.

The reacting mixtures were allowed to go to completion often indicated by steady value of absorbance observed over a period of two days. The final absorbances were taken and the graphs of absorbance against mole ratio were plotted, the stoichiometry was then evaluated from these graphs.

3.2.2 Kinetic measurements

The rates of the reaction were monitored following the rate of decrease in absorbance of the complexes at λ_{max} = 535 nm for $[Co(EDTA)]^-$ systems and 550 nm for $[Co(HEDTA)OH_2]$ systems on a Corning Colorimetre 252 model. All kinetic measurements were performed under pseudo first order conditions with the concentration of both complexes maintained at 3.0×10^{-3} mol dm^{-3} and 6.0×10^{-3} mol dm^{-3} for $[Co(EDTA)]^-$ and $[Co(HEDTA)OH_2]$ respectively, the reductants were varied at least 10 – 20 folds in excess over that of the complexes. The following experimental conditions were maintained for the respective systems studied.

–$[Co(EDTA)]^-$ – H_2A system:

$[H_2A] = (0.3 – 2.4) \times 10^{-1}$ mol dm^{-3}, $[H^+] = 1.0 \times 10^{-3}$ mol dm^{-3} (H_2SO_4), $[Cu^{2+}] = 5.0 \times 10^{-3}$ mol dm^{-3} ($CuSO_4$), I = 0.4 mol dm^{-3} (Na_2SO_4) and T = 299 ± 1K.

–$[Co(EDTA)]^-$ – N_2H_4 system:

$[N_2H_4] = (0.6 – 4.2) \times 10^{-1}$ mol dm^{-3}, $[H^+] = 2.0 \times 10^{-3}$ mol dm^{-3} ($HClO_4$), $[Cu^{2+}] = 6.0 \times 10^{-4}$ mol dm^{-3} ($CuSO_4$), I = 0.45 mol dm^{-3} ($NaClO_4$) and T = 298 ± 1K.

–$[Co(HEDTA)OH_2]$ – H_2A system:

$[H_2A] = (1.2 – 8.4) \times 10^{-1}$ mol dm^{-3}, $[H^+] = 2.0 \times 10^{-3}$ mol dm^{-3} ($HClO_4$), $[Cu^{2+}] = 7.0 \times 10^{-3}$ mol dm^{-3}($CuSO_4$), I = 0.9 mol dm^{-3} ($NaClO_4$) and T = 299 ± 1K.

–$[Co(HEDTA)OH_2]$ – N_2H_4 system:

$[N_2H_4] = (0.6 – 4.2) \times 10^{-1}$ mol dm^{-3}, $[H^+] = 2.0 \times 10^{-3}$ mol dm^{-3} ($HClO_4$), $[Cu^{2+}] = 5.0 \times 10^{-4}$ mol dm^{-3} ($CuSO_4$), I = 0.5 mol dm^{-3} ($NaClO_4$) and T = 298 ± 1K.

From the plots of log ($A_t - A_\infty$) against time (where A_∞ and A_t are the absorbances at the end of the reaction and at time, t respectively), the slopes of the plots were obtained and the pseudo – first order rate constants (k_{obs}) were determined. The second order rate constants (k_2) were subsequently evaluated from the relation:

$$k_2 = k_{obs}/[\text{reductant}]^n \quad (3.1)$$

where [reductant] = $[H_2A]$ or $[N_2H_4]$ and n = order with respect to the reductant.

3.2.3 Effect of $[H^+]$ on the reaction rate

The effect of $[H^+]$ on the rate of the reactions was investigated by keeping the concentration of all other reactants constant while varying the $[H^+]$. The following experimental conditions were maintained for the four systems:

–$[Co(EDTA)]^-$ – H_2A system:

$[H_2A] = 0.21$ mol dm^{-3}, $[H^+] = (0.5 – 10.0) \times 10^{-3}$ mol dm^{-3} (H_2SO_4), $[Cu^{2+}] = 5.0 \times 10^{-3}$ mol dm^{-3} ($CuSO_4$), I = 0.4 mol dm^{-3} (Na_2SO_4) and T = 299 ± 1K.

–$[Co(EDTA)]^-$ – N_2H_4 system:

$[N_2H_4] = 0.36$ mol dm^{-3}, $[H^+] = (0.5 – 3.5) \times 10^{-3}$ mol dm^{-3} ($HClO_4$), $[Cu^{2+}] = 6.0 \times 10^{-4}$ mol dm^{-3} ($CuSO_4$), I = 0.2 mol dm^{-3} ($NaClO_4$) and T = 298 ± 1K.

–$[Co(HEDTA)OH_2]$ – H_2A system:

$[H_2A] = 0.12$ mol dm^{-3}, $[H^+] = (2.5 – 40.0) \times 10^{-4}$ mol dm^{-3} ($HClO_4$), $[Cu^{2+}] = 7.0 \times 10^{-3}$ mol dm^{-3} ($CuSO_4$), I = 0.2 mol dm^{-3} ($NaClO_4$) and T = 299 ± 1K.

–[Co^{III}(HEDTA)OH_2] – N_2H_4 system:

[N_2H_4] = 0.12 mol dm^{-3}, [H^+] = (1.0 – 7.0) × 10^{-3} mol dm^{-3} ($HClO_4$), [Cu^{2+}] = 5.0 × 10^{-4} mol dm^{-3} ($CuSO_4$), I = 0.5 mol dm^{-3} ($NaClO_4$) and T = 298 ± 1K.

From the slope of the plot of log k_{obs} against log [H^+], the order with respect to hydrogen ion concentration in each reaction was obtained. Variations of acid dependent rate constants with [H^+] were obtained by plotting a graph of k_2 against [H^+].

3.2.4 Effect of catalyst on the rate of the reaction

The effect of [Cu^{2+}] was studied while keeping all other conditions constant, the observed experimental conditions are as outlined;

–[Co(EDTA)]$^-$ – H_2A system:

[H_2A] = 0.21 mol dm^{-3}, [H^+] = 1.0 × 10^{-3} mol dm^{-3} (H_2SO_4), [Cu^{2+}] = (3.0 – 15.0) × 10^{-3} mol dm^{-3} ($CuSO_4$), I = 0.4 mol dm^{-3} (Na_2SO_4) and T = 299 ± 1K.

–[Co(EDTA)]$^-$ – N_2H_4 system:

[N_2H_4] = 0.36 mol dm^{-3}, [H^+] = 1.0 × 10^{-3} mol dm^{-3} ($HClO_4$), [Cu^{2+}] = (1.0 – 7.0) × 10^{-4} mol dm^{-3} ($CuSO_4$), I = 0.2 mol dm^{-3} ($NaClO_4$) and T = 298 ± 1K.

–[Co(HEDTA)OH_2] – H_2A system:

[H_2A] = 0.12 mol dm^{-3}, [H^+] = 2.0 × 10^{-3} mol dm^{-3} ($HClO_4$), [Cu^{2+}] = (6.0 – 9.0) × 10^{-3} mol dm^{-3} ($CuSO_4$), I = 0.2 mol dm^{-3} ($NaClO_4$) and T = 299 ± 1K.

–$[Co(HEDTA)OH_2]$ – N_2H_4 system:

$[N_2H_4]$ = 0.12 mol dm^{-3}, $[H^+]$ = 2.0 × 10^{-3} mol dm^{-3} ($HClO_4$), $[Cu^{2+}]$ = (3.0 – 6.0) × 10^{-4} mol dm^{-3} ($CuSO_4$), I = 0.5 mol dm-3 ($NaClO_4$) and T = 298 ± 1K.

3.2.5 Effect of ionic strength on the reaction rate

The effect of change in ionic strength of the reaction medium on the rate of the reaction was investigated over a range of (0.30 – 0.55) mol dm^{-3} using Na_2SO_4 for $[Co(EDTA)]^-$ – H_2A system. However, $NaClO_4$ was used in the other three systems as follows; (0.20 – 0.55) mol dm^{-3} for $[Co(EDTA)]^-$ – N_2H_4 system, (0.3 – 0.9) mol dm^{-3} for $[Co(HEDTA)OH_2]$ – H_2A system and (0.3 – 0.6) mol dm^{-3} for $[Co(HEDTA)OH_2]$ – N_2H_4 system. All other experimental conditions were kept constant during these studies.

3.2.6 Effect of dielectric constant of reaction medium on the rate of the reaction

The effect of changes in dielectric constant of the reaction medium on the reaction rate was investigated using acetone – water mixture by adding 0 – 0.12 cm^3 of acetone (for H_2A systems) and 0 – 0.10 cm^3 of acetone (for N_2H_4 systems) to water in a 5 cm^3 reaction vessel, while all other conditions were kept constant.

The dielectric constant for the reaction medium was calculated as:

$$D = \frac{D_{Water} \times V_{Water} + D_{Acetone} \times V_{Acetone}}{V_{Water} + V_{Acetone}} \quad (3.2)$$

3.2.7 Effect of change in temperature on the reaction rate

The temperatures were varied across 313 K – 333 K for $[Co(EDTA)]^-$ – H_2A system, 293 K – 313 K for $[Co(EDTA)]^-$ – N_2H_4 system, 303 K – 323 K for $[Co(HEDTA)OH_2]$ – H_2A system and 293 K – 313 K for $[Co(HEDTA)OH_2]$ – N_2H_4 system. All other experimental conditions were maintained, and a plot of ln k/T versus 1/T (using Eyring – Polanyi equation):

$$\ln \frac{k}{T} = \ln \frac{k_B}{h} + \frac{\Delta S^{\ddagger}}{R} - \frac{\Delta H^{\ddagger}}{RT} \quad (3.3)$$

this gave a slope and an intercept from which the activated parametres were estimated.

3.2.8 Effect of added ions on the reaction rate

The effect of added ions on the reaction rate was studied by adding different ions of varied concentrations to the reaction systems, while keeping all other parametres constant. The ions added in each of the systems include:

–$[Co(EDTA)]^-$ – H_2A system:

$CHOO^-$ (0.5 – 7.5) × 10^{-2} mol dm^{-3} (CHOONa), CH_3COO^- (0.5 – 10.0) × 10^{-2} mol dm^{-3} (CH_3COONa), Li^+ (0.5 – 8.5) × 10^{-2} mol dm^{-3} (Li_2SO_4), and Zn^{2+} (0.5 – 8.5) × 10^{-2} mol dm^{-3} ($ZnSO_4$).

– $[Co(EDTA)]^-$ – N_2H_4 system:

(0 – 2.5) × 10^{-2} mol dm^{-3} for $CHOO^-$ (CHOONa), CH_3COO^- (CH_3COONa) and K^+ ($KClO_4$).

–[Co(HEDTA)OH_2] – H_2A system:

$CHOO^-$ (1.5 – 10.0) × 10^{-2} mol dm^{-3} (CHOONa) and CH_3COO^- (CH_3COONa), K^+ (0.5 – 3.5) × 10^{-2} mol dm^{-3} ($KClO_4$).

–[Co(HEDTA)OH_2] – N_2H_4 system:

(0 – 2.0) × 10^{-2} mol dm^{-3} for $CHOO^-$ (CHOONa), CH_3COO^- (CH_3COONa) and K^+ ($KClO_4$).

3.2.9 Test for intermediate complex

The spectra of the reaction mixtures were obtained over a wavelength range of 400 – 650 nm. This was carried out in order to determine whether there is significant shift in λ_{max} or enhancement of peak as the reaction progressed. Michaelis-Menten plot of $1/k_{obs}$ versus 1/[reductant] were also made.

3.2.10 Test for free radical

To a partially reduced reaction mixture containing various concentrations of reductant and hydrogen ion for each system, about 5 cm^3 of acrylamide was added and after 2 – 3 minutes, excess of methanol was added to initiate free radical polymerisation. A control experiment was carried out by repeating the process on each of the reactants separately. Formation of gelatinous precipitate in the partially reduced mixture indicates presence of free radicals.

3.2.11 Products analysis

3.2.11.1 *Qualitative methods*

Qualitative test was carried out to determine if Co^{2+} ions were present in the product mixtures using potassium thiocynate according to the method developed by Hahn and Welcher (1963). Furthermore, test was carried out on the products of the N_2H_4 systems to check for the presence of NH_3, according to the methods of Richard and Renfrow (1952). The method of Tipson (1945) was used to check for the presence of dehydroascorbic acid as a possible product of H_2A oxidation, this involved reacting the final reaction product with pyrrole in excess trichloroacetic acid at 50 ^{0}C.

3.2.11.2 ***Spectrophotometric methods***

The UV – visible spectrophotometre was used to scan the spectrum of the reaction product in the wavelengths range of 300 to 650 nm.

CHAPTER FOUR

4.0 RESULTS

4.1 Stoichiometry

The results obtained from the stoichiometric investigations showed that two moles of $[Co(EDTA)]^-$ were consumed by one mole of H_2A and one mole of N_2H_4 respectively, while one mole $[Co(HEDTA)OH_2]$ was consumed by one mole of H_2A, and two moles of $[Co(HEDTA)OH_2]$ were consumed by a mole of N_2H_4 respectively. The overall equations for these reactions are expressed by Equations 4.1 – 4.4. The titration curves from which these stoichiometries were obtained are also shown in Figures 4.1 – 4.4.

$$2[Co(EDTA)]^- + H_2A \rightarrow 2[Co(EDTA)]^{2-} + A + 2H^+ \quad (4.1)$$

$$2[Co(EDTA)]^- + N_2H_4 + {}^1/_2O_2 \rightarrow 2[Co(EDTA)]^{2-} + N_2 + H_2O + 2H^+ \quad (4.2)$$

$$[Co(HEDTA)OH_2] + H_2A \rightarrow [Co(HEDTA)OH_2]^- + HA + H^+ \quad (4.3)$$

$$2[Co(HEDTA)OH_2] + N_2H_4 + {}^1/_2O_2 \rightarrow 2[Co(HEDTA)OH_2]^- + N_2 + H_2O + 2H^+ \quad (4.4)$$

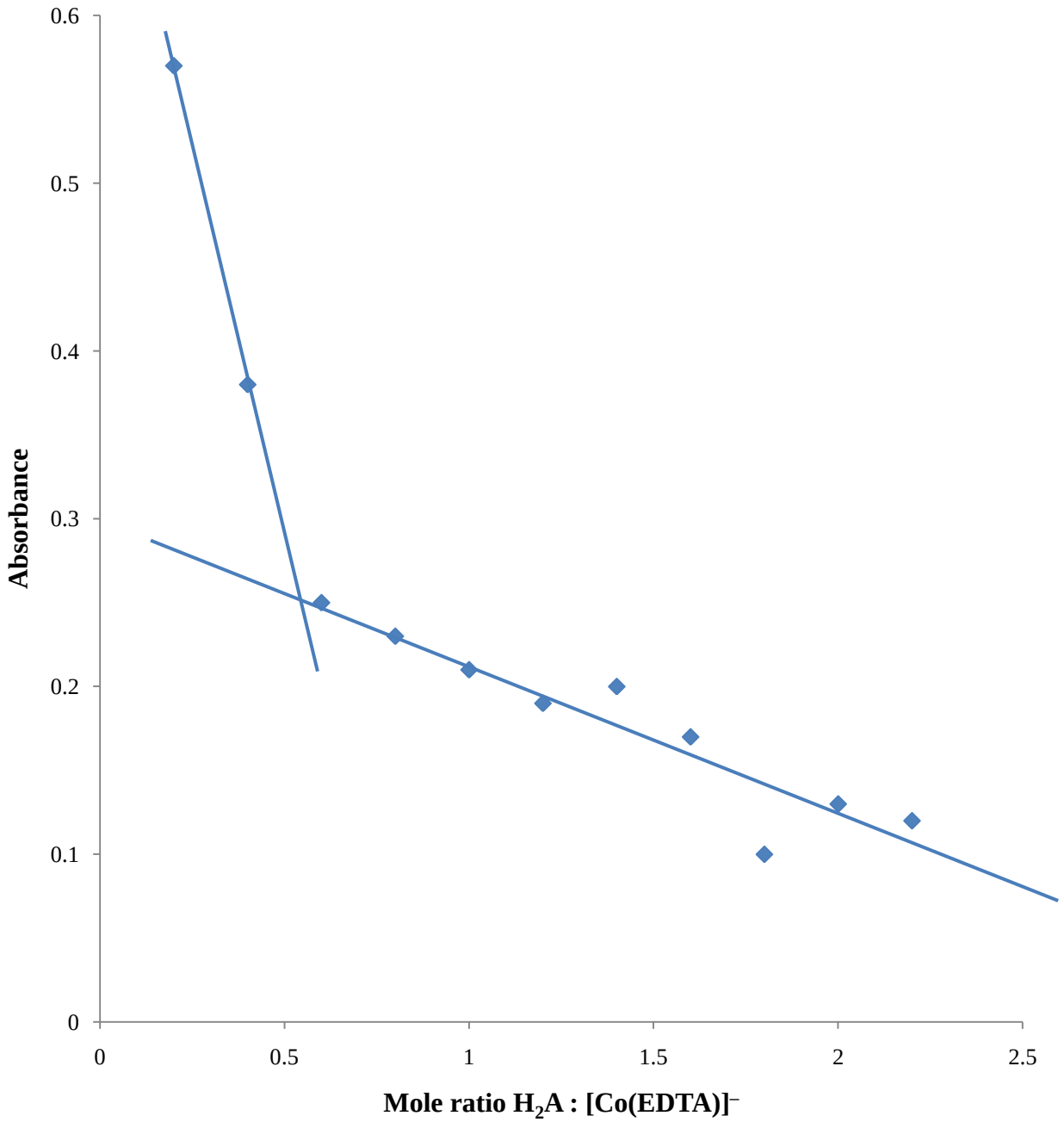
0.6
0.5
0.4
0.3
0.2
0.1
0
Absorbance
0
0.5
1
1.5
2
2.5
Mole ratio H2A : [Co(EDTA)]–

Figure 4.1: **Stoichiometric plot for the reduction of [Co(EDTA)]$^{-}$ (3.0×10^{-3} mol dm^{-3}) by H_2A (0.6 – 6.6) $\times 10^{-3}$ mol dm^{-3}, $[H^+] = 1.0 \times 10^{-3}$ mol dm^{-3}, I = 0.05 mol dm^{-3} (Na_2SO_4), $CuSO_4 = 2.0 \times 10^{-3}$ mol dm^{-3}, λ_{max} = 535 nm, T = 299 ± 1K**

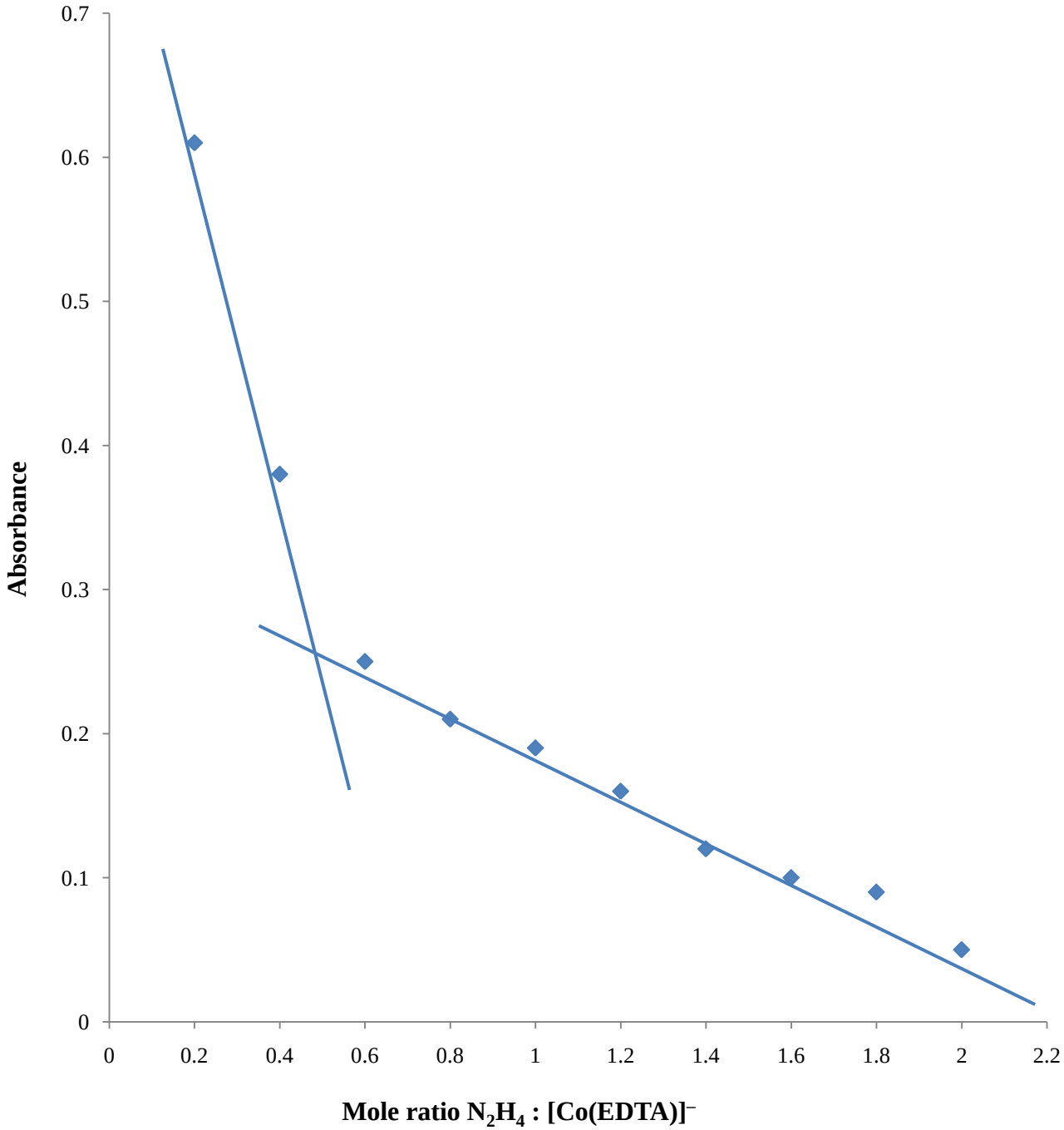

Figure 4.2: **Stoichiometric plot for the reduction of [Co(EDTA)]$^{-}$ (3.0×10^{-3} mol dm^{-3}) by N_2H_4 (0.6 – 6.6) $\times 10^{-3}$ mol dm^{-3}, $[H^+] = 1.0 \times 10^{-3}$ mol dm^{-3}, I = 0.05 mol dm^{-3} ($NaClO_4$), $CuSO_4 = 5.0 \times 10^{-4}$ mol dm^{-3}, λ_{max} = 535 nm, T = 298 ± 1K**

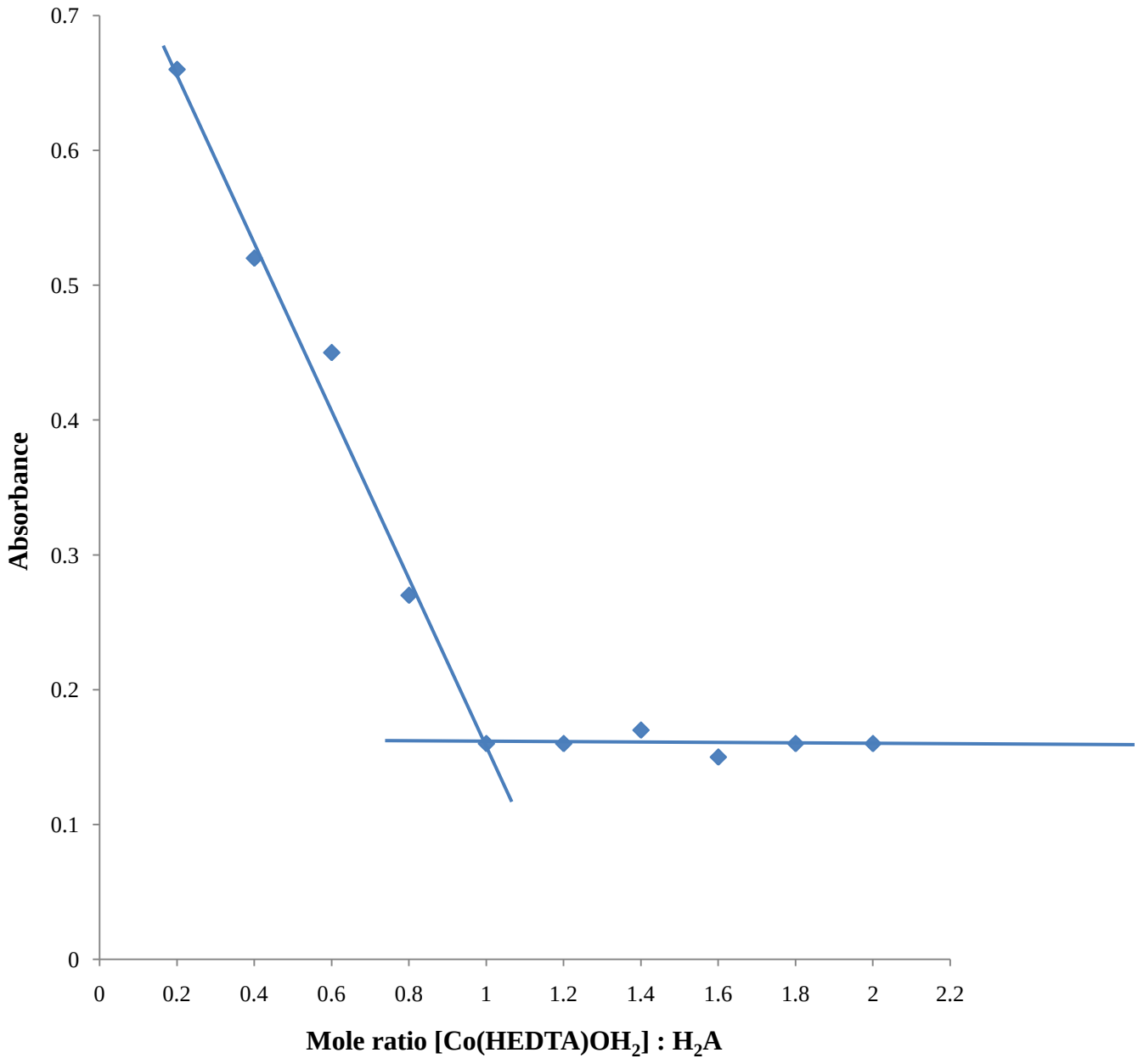

Figure 4.3: **Stoichiometric plot for the reduction of $[Co(HEDTA)OH_2]$ (6.0×10^{-3} mol dm^{-3}) by H_2A ($0.12 - 1.2$) $\times10^{-2}$ mol dm^{-3}, $[H^+]= 2.0 \times 10^{-3}$ mol dm^{-3}, I = 0.05 mol dm^{-3} ($NaClO_4$), $CuSO_4$=5.0×10^{-4} mol dm^{-3}, λ_{max} = 550 nm, T = 299 ± 1K**

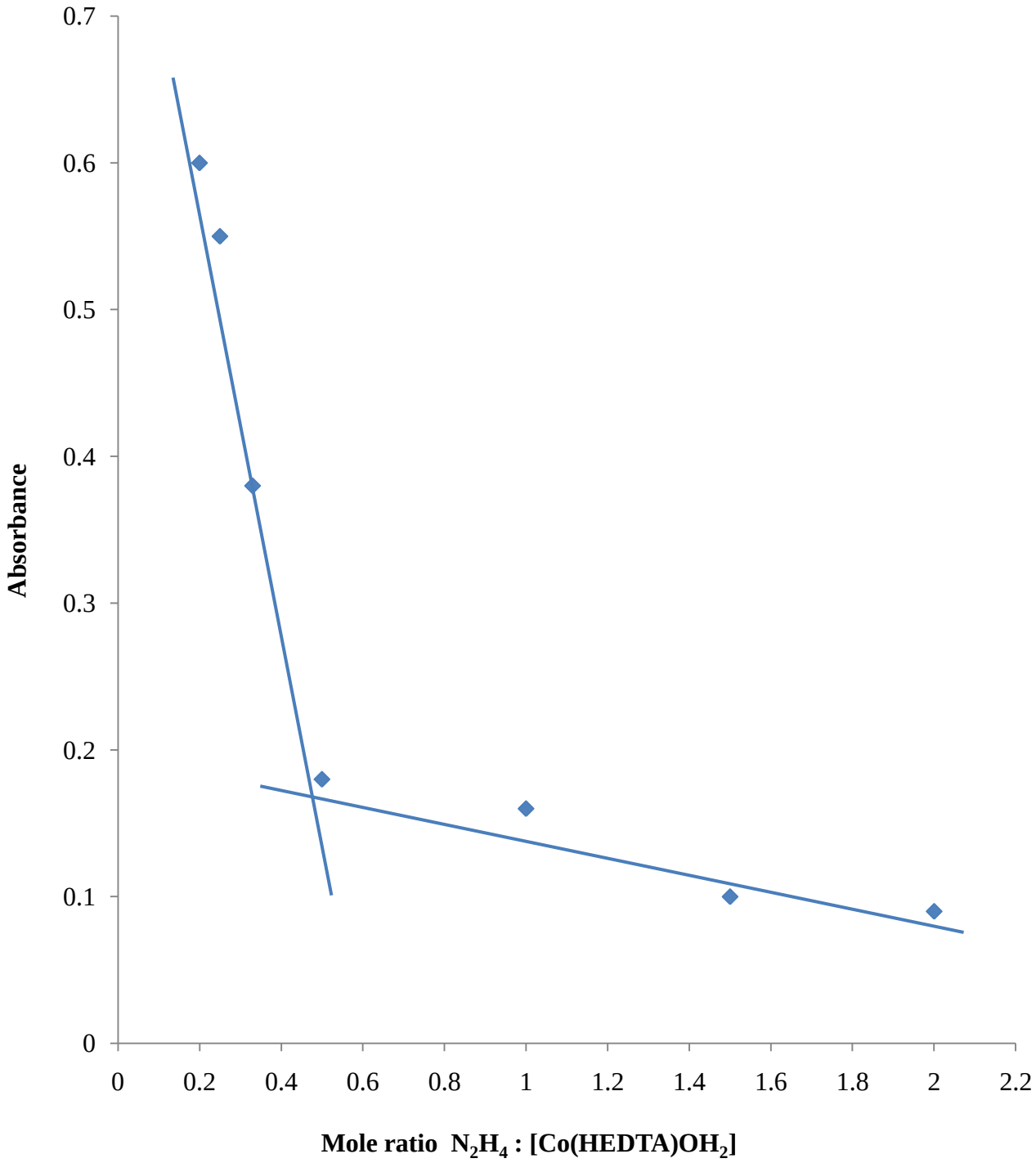

Figure 4.4: **Stoichiometric plot for the reduction of $[Co(HEDTA)OH_2]$ (6.0×10^{-3} mol dm^{-3}) by N_2H_4 ($0.12 - 1.2$) $\times 10^{-2}$ mol dm^{-3}, $[H^+] = 2.0 \times 10^{-3}$ mol dm^{-3}, I = 0.05 mol dm^{-3} ($NaClO_4$), $CuSO_4 = 5.0 \times 10^{-4}$ mol dm^{-3}, λ_{max} = 550 nm, T = 298 ± 1K**

4.2 Determination of Order of the Reactions with Respect to the Reactants

The typical pseudo – first order plots of log ($A_t - A_\infty$) versus time were linear and are shown in Figures 4.5 – 4.8. The linearity of these plot show that the order of reaction with respect to the complexes is one each. The pseudo – first order rate constants, k_{obs} were evaluated from the slopes of these plots. From the k_{obs} obtained, the second order rate constants k_2 were evaluated. The respective values of k_{obs} and k_2 for all the systems are reported on Tables 4.1 – 4.4 accordingly.

The order of the reaction with respect to the concentration of the reductant for each of the system was obtained from the slope of the plots of log k_{obs} versus log [reductants] (Figures 4.9 – 4.12). The slopes obtained were: 1.02 for $[Co(EDTA)]^-$ –H_2A, 0.77 for $[Co(EDTA)]^-$ – N_2H_4, 0.48 for $[Co(HEDTA)OH_2]$ – H_2A and 1.03 for $[Co(HEDTA)OH_2]$ − N_2H_4 respectively.

These observations showed that the order of the reaction with respect to the reductants for the $[Co(EDTA)]^-$ –H_2A, $[Co(EDTA)]^-$ – N_2H_4 and $[Co(HEDTA)OH_2]$ − N_2H_4 systems is one each, and their reaction with the Co(III) complexes is second order overall. The order of the reaction with respect to the reductant for the $[Co(HEDTA)OH_2]$ – H_2A system is however half order, and the reaction is one and half order overall. On the basis of the above observations, the rate laws for these reactions can therefore be written as:

$$-\frac{d[Co^{III}(EDTA)^-]}{dt} = k_2[Co^{III}(EDTA)^-]\,[H_2A] \quad (4.6)$$

$$-\frac{d[Co^{III}(EDTA)^-]}{dt} = k_2[Co^{III}(EDTA)^-]\,[N_2H_4] \quad (4.7)$$

$$-\frac{d[Co^{III}(HEDTA)OH_2]}{dt} = k_2[Co^{III}(HEDTA)OH_2]\,[H_2A]^{1/2} \quad (4.8)$$

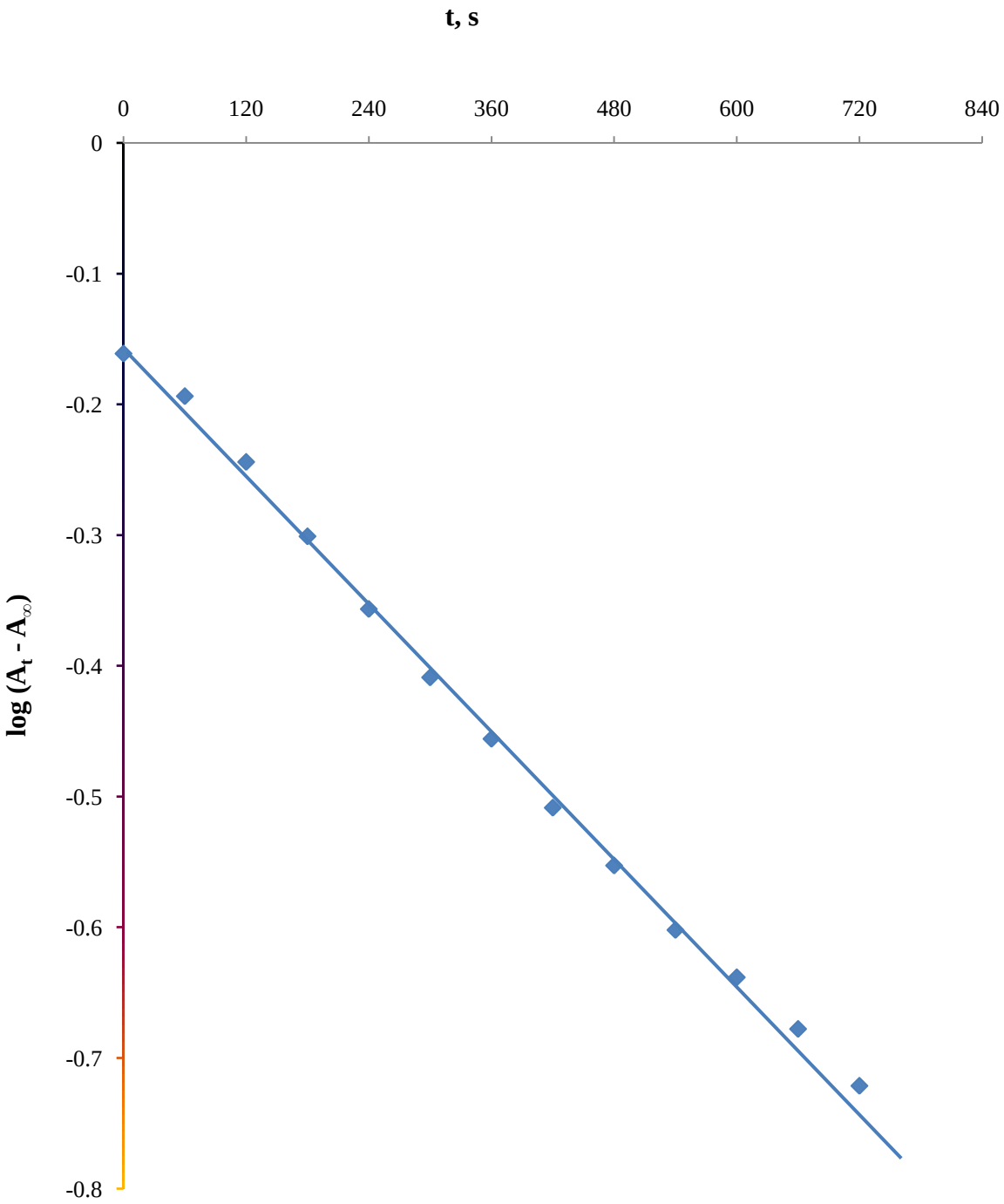

Figure 4.5: Typical pseudo – first order plot for the redox reaction of $[Co(EDTA)]^-$ with H_2A at $[Co^{3+}] = 3.0 \times 10^{-3}$ mol dm^{-3}, $[H_2A] = 0.18$ mol dm^{-3}, $[H^+] = 1.0 \times 10^{-3}$ mol dm^{-3}, I = 0.40 mol dm^{-3} (Na_2SO_4), $[Cu^{2+}] = 5.0 \times 10^{-3}$ mol dm^{-3}, $\lambda_{max} = 535$ nm and T = 299 ± 1K

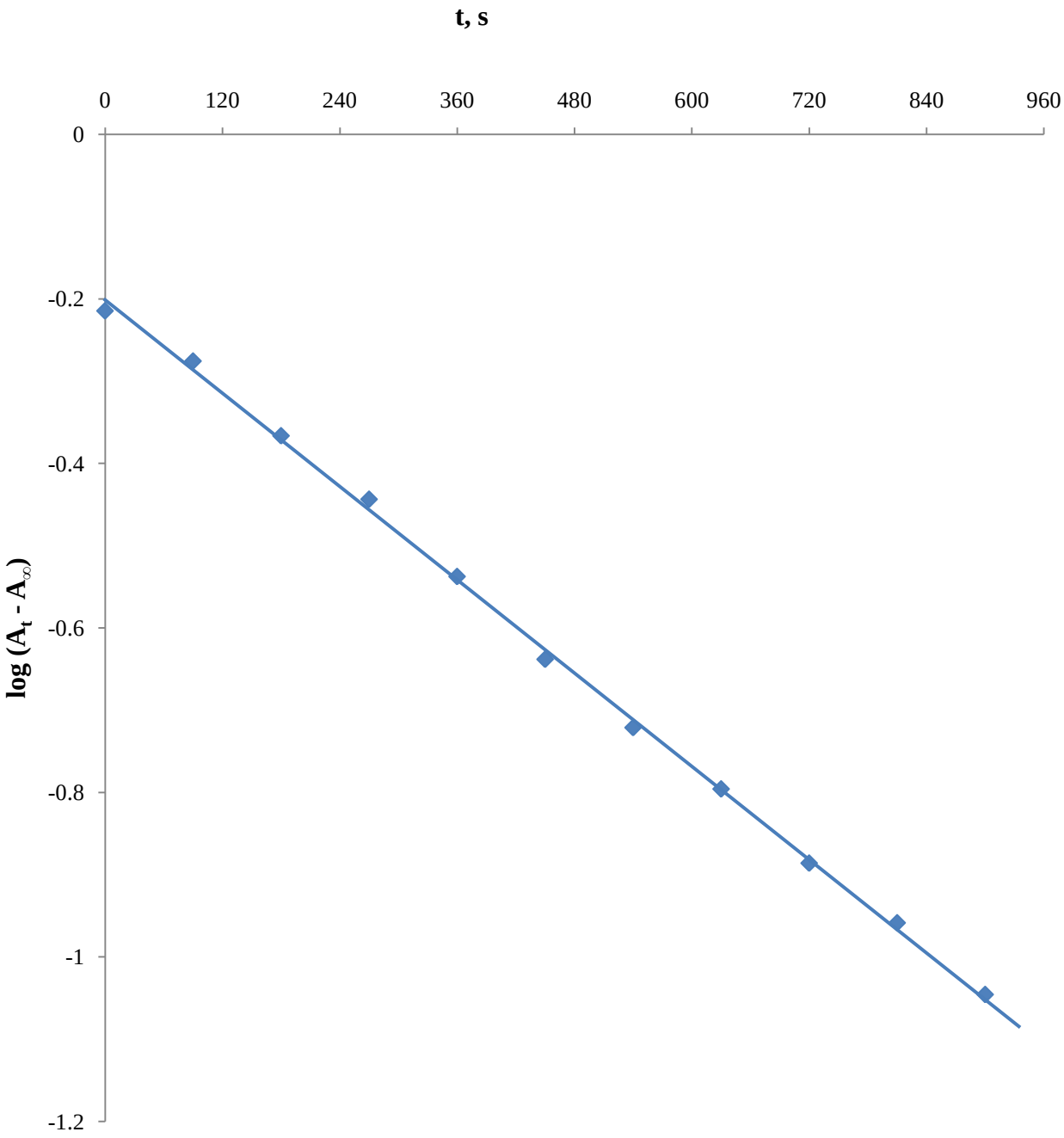

Figure 4.6: **Typical pseudo – first order plot for the redox reaction of $[Co(EDTA)]^{-}$ with N_2H_4 at $[Co^{3+}] = 3.0 \times 10^{-3}$ mol dm^{-3}, $[N_2H_4] = 0.12$ mol dm^{-3}, $[H^{+}] = 1.0 \times 10^{-3}$ mol dm^{-3}, I = 0.45 mol dm^{-3} ($HClO_4$), $[Cu^{2+}] = 6.0 \times 10^{-4}$ mol dm^{-3}, λ_{max} = 535 nm and T = 298 ± 1K**

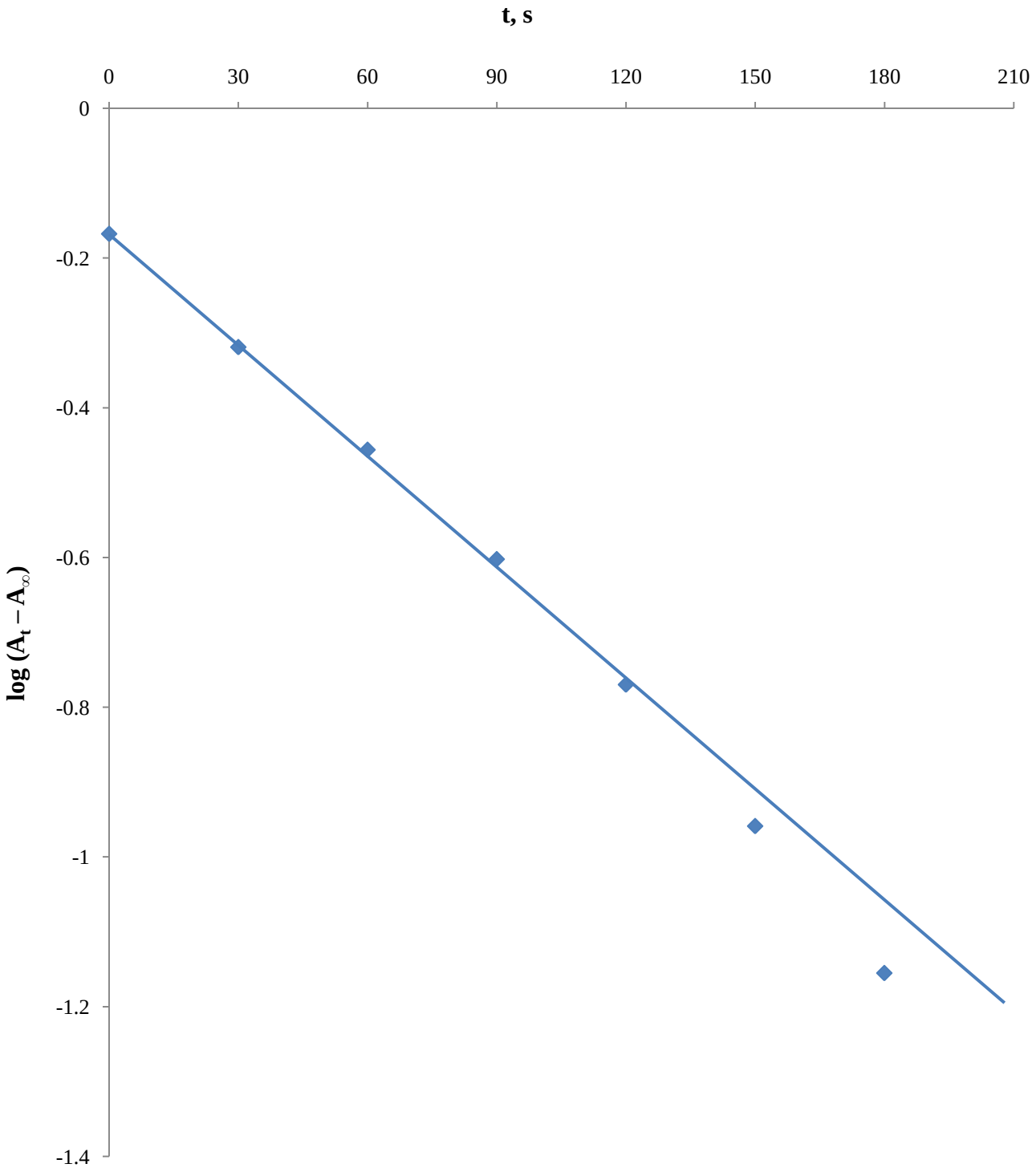

Figure 4.7: **Typical pseudo-first order plot for the redox reaction $[Co(HEDTA)OH_2]$ with H_2A at $[Co^{3+}] = 6.0 \times 10^{-3}$ mol dm^{-3}, $[H_2A] = 0.72$ mol dm^{-3}, $[H^+] = 2.0 \times 10^{-3}$ mol dm^{-3}, I = 0.9 mol dm^{-3} ($HClO_4$),$[Cu^{2+}] = 7.0 \times 10^{-3}$ mol dm^{-3}, λ_{max} = 550 nm and T = 299 ± 1K**

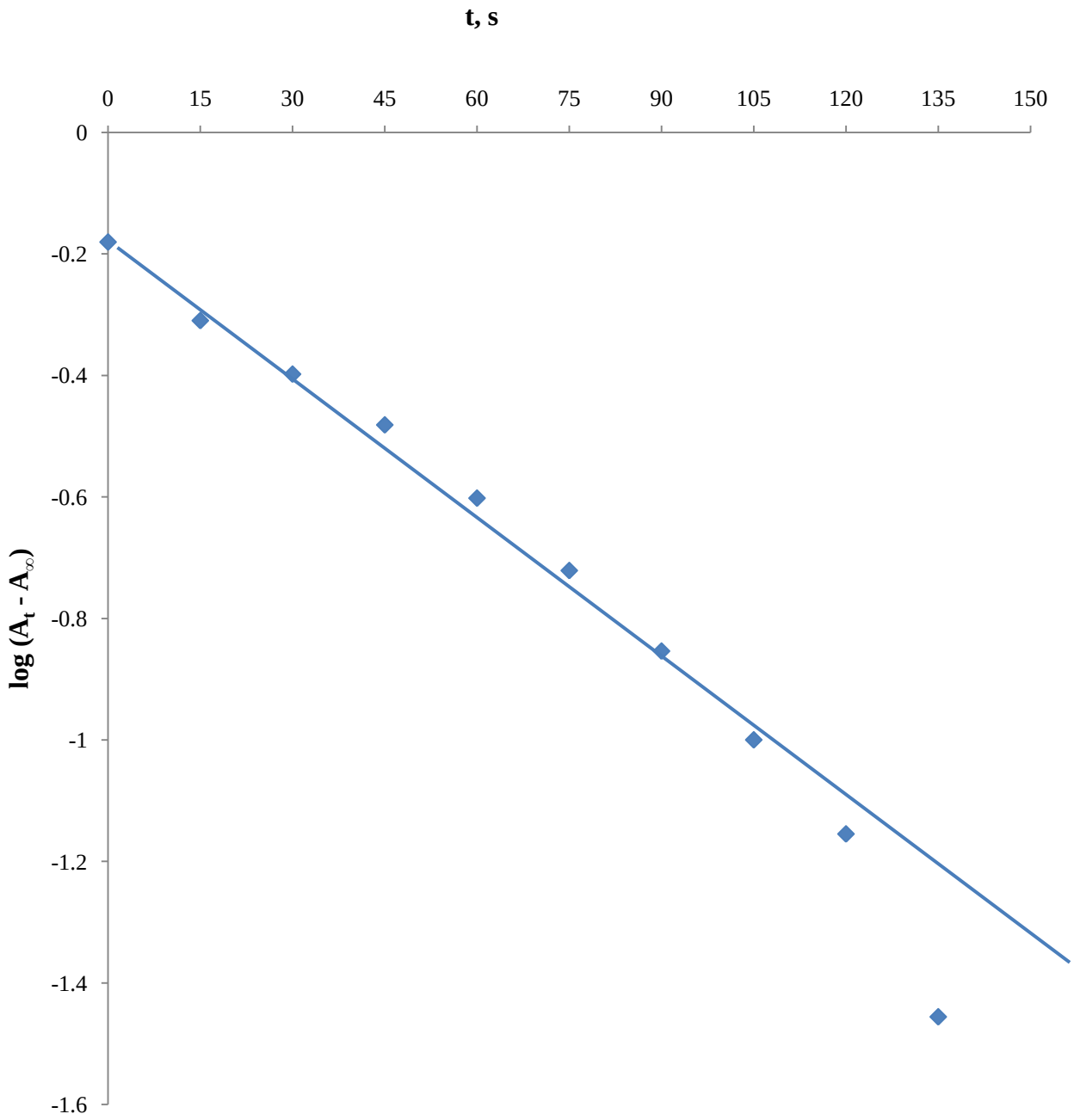

Figure 4.8: **Typical pseudo – first order plot for the redox reaction of $[Co(HEDTA)OH_2]$ with N_2H_4 at $[Co^{3+}] = 6.0 \times 10^{-3}$ mol dm^{-3}, $[N_2H_4] = 0.24$ mol dm^{-3}, $[H^+] = 4.0 \times 10^{-3}$ mol dm^{-3}, I = 0.5 mol dm^{-3} ($HClO_4$), $[Cu^{2+}] = 5.0 \times 10^{-4}$ mol dm^{-3}, λ_{max} = 550 nm and T = 298 ± 1K**

Table 4.1: Pseudo – first order and second order rate constants for the reduction of $[Co(EDTA)]^-$ by H_2A in aqueous H_2SO_4 medium at $[Co^{3+}] = 3.0 \times 10^{-3}$ mol dm^{-3}, $\lambda_{max} = 535$ nm and T = 299 ± 1K

$10[H_2A]$, mol dm^{-3}	$10^3[H^+]$, mol dm^{-3}	$10^3[Cu^{2+}]$, mol dm^{-3}	$10[I]$, mol dm^{-3}	$10^3\ k_{obs}$, s^{-1}	$10^2 k_2$, $dm^3mol^{-1}s^{-1}$
0.30	1.00	5.00	4.00	0.29	0.97
0.60	1.00	5.00	4.00	0.58	0.97
0.90	1.00	5.00	4.00	0.88	0.98
1.20	1.00	5.00	4.00	1.18	0.98
1.50	1.00	5.00	4.00	1.48	0.99
1.80	1.00	5.00	4.00	1.82	1.00
2.10	1.00	5.00	4.00	2.14	1.02
2.40	1.00	5.00	4.00	2.38	0.99
2.10	0.50	5.00	4.00	1.98	0.94
2.10	1.00	5.00	4.00	2.14	1.02
2.10	2.00	5.00	4.00	1.94	0.92
2.10	4.00	5.00	4.00	2.23	1.06
2.10	6.00	5.00	4.00	2.12	1.00
2.10	8.00	5.00	4.00	2.17	1.03
2.10	10.00	5.00	4.00	2.26	1.07
2.10	1.00	3.00	4.00	1.33	0.63
2.10	1.00	5.00	4.00	2.14	1.02
2.10	1.00	7.00	4.00	3.25	1.55
2.10	1.00	9.00	4.00	4.56	2.17
2.10	1.00	11.00	4.00	5.74	2.73

2.10	1.00	13.00	4.00	6.93	3.30
2.10	1.00	5.00	3.00	5.36	2.55
2.10	1.00	5.00	3.50	2.99	1.42
2.10	1.00	5.00	4.00	2.14	1.02
2.10	1.00	5.00	4.50	1.43	0.68
2.10	1.00	5.00	5.00	1.18	0.56
2.10	1.00	5.00	5.50	1.06	0.51

Table 4.2: Pseudo – first order and second order rate constants for the reduction of $[Co(EDTA)]^-$ by N_2H_4 in aqueous $HClO_4$ medium at $[Co^{3+}] = 3.0 \times 10^{-3}$ mol dm^{-3}, λ_{max} = 535 nm and T = 298 ± 1K

$10[N_2H_4]$, mol dm^{-3}	$10^3[H^+]$, mol dm^{-3}	$10^4[Cu^{2+}]$, mol dm^{-3}	10[I], mol dm^{-3}	$10^3\ k_{obs}$, s^{-1}	$10^2 k_2$, $dm^3\ mol^{-1}\ s^{-1}$
0.06	1.00	6.00	4.50	1.20	1.03
0.12	1.00	6.00	4.50	2.14	1.08
0.18	1.00	6.00	4.50	2.97	1.10
0.24	1.00	6.00	4.50	3.75	1.12
0.30	1.00	6.00	4.50	4.32	1.09
0.36	1.00	6.00	4.50	4.73	1.03
0.42	1.00	6.00	4.50	5.31	1.03
1.80	0.50	6.00	4.50	2.99	1.11
1.80	1.00	6.00	4.50	2.97	1.10

1.80	1.50	6.00	4.50	3.01	1.12
1.80	2.00	6.00	4.50	2.96	1.10
1.80	2.50	6.00	4.50	2.93	1.09
1.80	3.00	6.00	4.50	3.01	1.12
1.80	3.50	6.00	4.50	2.90	1.08
1.80	1.00	5.00	4.50	2.50	0.93
1.80	1.00	6.00	4.50	2.97	1.10
1.80	1.00	7.00	4.50	3.61	1.34
1.80	1.00	8.00	4.50	3.99	1.48
1.80	1.00	9.00	4.50	4.54	1.69
1.80	1.00	10.00	4.50	4.90	1.82
1.80	1.00	11.00	4.50	5.48	2.04
1.80	1.00	6.00	2.00	4.48	1.67
1.80	1.00	6.00	2.50	3.93	1.46
1.80	1.00	6.00	3.00	3.75	1.39
1.80	1.00	6.00	3.50	3.39	1.26
1.80	1.00	6.00	4.00	3.19	1.19
1.80	1.00	6.00	4.50	2.97	1.10
1.80	1.00	6.00	5.00	2.57	0.96

Table 4.3: Pseudo – first order and second order rate constants for the reduction of [Co(HEDTA)OH_2] by H_2A in aqueous $HClO_4$ medium at [Co^{3+}] = 6.0 × 10^{-3} mol dm^{-3}, λ_{max} = 550 nm and T = 299 ± 1K

$10[H_2A]$, mol dm^{-3}	$10^3[H^+]$, mol dm^{-3}	$10^3[Cu^{2+}]$, mol dm^{-3}	$10[I]$, mol dm^{-3}	$10^3\ k_{obs}$, s^{-1}	$10^2 k_{3/2}$, $dm^{3/2}\ mol^{-1/2}\ s^{-1/2}$
1.2	2.00	7.00	9.00	4.82	1.39
1.8	2.00	7.00	9.00	5.87	1.38
2.4	2.00	7.00	9.00	6.84	1.39
3.0	2.00	7.00	9.00	7.64	1.39
3.6	2.00	7.00	9.00	8.23	1.37
4.2	2.00	7.00	9.00	8.81	1.36
4.8	2.00	7.00	9.00	9.38	1.36
1.2	0.25	7.00	2.00	5.41	1.56
1.2	0.50	7.00	2.00	5.36	1.55
1.2	0.75	7.00	2.00	5.11	1.48
1.2	1.00	7.00	2.00	4.97	1.44
1.2	1.25	7.00	2.00	4.90	1.42
1.2	2.00	7.00	2.00	4.86	1.40
1.2	4.00	7.00	2.00	4.83	1.39
1.2	2.00	6.00	2.00	3.14	0.91
1.2	2.00	6.50	2.00	3.81	1.10
1.2	2.00	7.00	2.00	4.81	1.39
1.2	2.00	7.50	2.00	5.15	1.49
1.2	2.00	8.00	2.00	6.32	1.83
1.2	2.00	8.50	2.00	7.20	2.08
1.2	2.00	9.00	2.00	7.60	2.20
1.2	2.00	7.00	3.00	4.13	1.19

1.2	2.00	7.00	4.00	4.57	1.32
1.2	2.00	7.00	5.00	4.72	1.36
1.2	2.00	7.00	6.00	4.65	1.34
1.2	2.00	7.00	7.00	4.96	1.43
1.2	2.00	7.00	8.00	4.83	1.39
1.2	2.00	7.00	9.00	4.85	1.40

Table 4.4: Pseudo – first order and second order rate constants for the reduction of $[Co(HEDTA)OH_2]$ by N_2H_4 in aqueous $HClO_4$ medium at $[Co^{3+}] = 6.0 \times 10^{-3}$ mol dm^{-3}, λ_{max} = 550 nm and T = 298 ± 1K

$10[N_2H_4]$, mol dm^{-3}	$10^3[H^+]$, mol dm^{-3}	$10^4[Cu^{2+}]$, mol dm^{-3}	10[I], mol dm^{-3}	$10^2\ k_{obs}$, s^{-1}	$10^2 k_2$, $dm^3\ mol^{-1}\ s^{-1}$
0.60	4.00	5.00	5.00	0.58	9.67
1.20	4.00	5.00	5.00	1.14	9.49
1.80	4.00	5.00	5.00	1.76	9.79
2.40	4.00	5.00	5.00	2.36	9.82
3.00	4.00	5.00	5.00	2.95	9.83
3.60	4.00	5.00	5.00	3.41	9.46
4.20	4.00	5.00	5.00	4.45	10.59
1.20	1.00	5.00	5.00	4.28	35.64
1.20	2.00	5.00	5.00	2.07	17.25
1.20	3.00	5.00	5.00	1.61	13.38

1.20	4.00	5.00	5.00	1.14	9.51
1.20	5.00	5.00	5.00	0.95	7.87
1.20	6.00	5.00	5.00	0.78	6.51
1.20	7.00	5.00	5.00	0.65	5.43
1.20	4.00	2.50	5.00	0.61	5.06
1.20	4.00	5.00	5.00	1.14	9.50
1.20	4.00	7.50	5.00	1.60	13.37
1.20	4.00	10.00	5.00	2.07	17.22
1.20	4.00	12.50	5.00	2.66	22.13
1.20	4.00	15.00	5.00	3.40	28.35
1.20	4.00	5.00	3.00	1.11	9.25
1.20	4.00	5.00	3.50	1.13	9.42
1.20	4.00	5.00	4.00	1.16	9.64
1.20	4.00	5.00	4.50	1.15	9.61
1.20	4.00	5.00	5.00	1.14	9.51
1.20	4.00	5.00	5.50	1.14	9.51
1.20	4.00	5.00	6.00	1.11	9.25

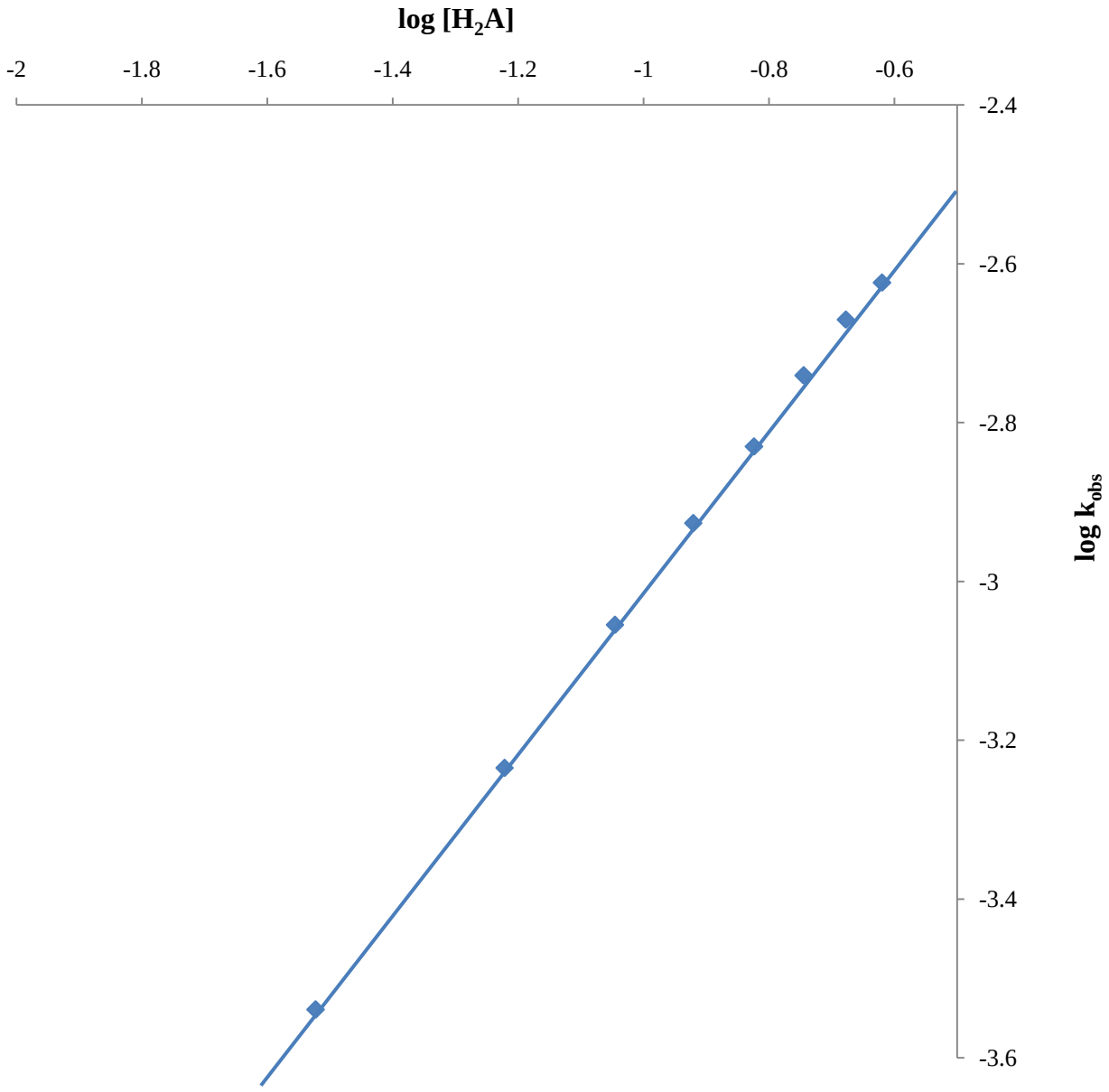

Figure 4.9: **Plot of log k_{obs} versus log [H_2A] for the redox reaction of $[Co(EDTA)]^-$ with H_2A at $[Co^{3+}] = 3.0 \times 10^{-3}$ mol dm^{-3}, $[H^+] = 1.0 \times 10^{-3}$ mol dm^{-3}, I = 0.40 mol dm^{-3} (Na_2SO_4), $[Cu^{2+}] = 5.0 \times 10^{-3}$ mol dm^{-3}, λ_{max} = 535 nm and T = 299 ± 1K**

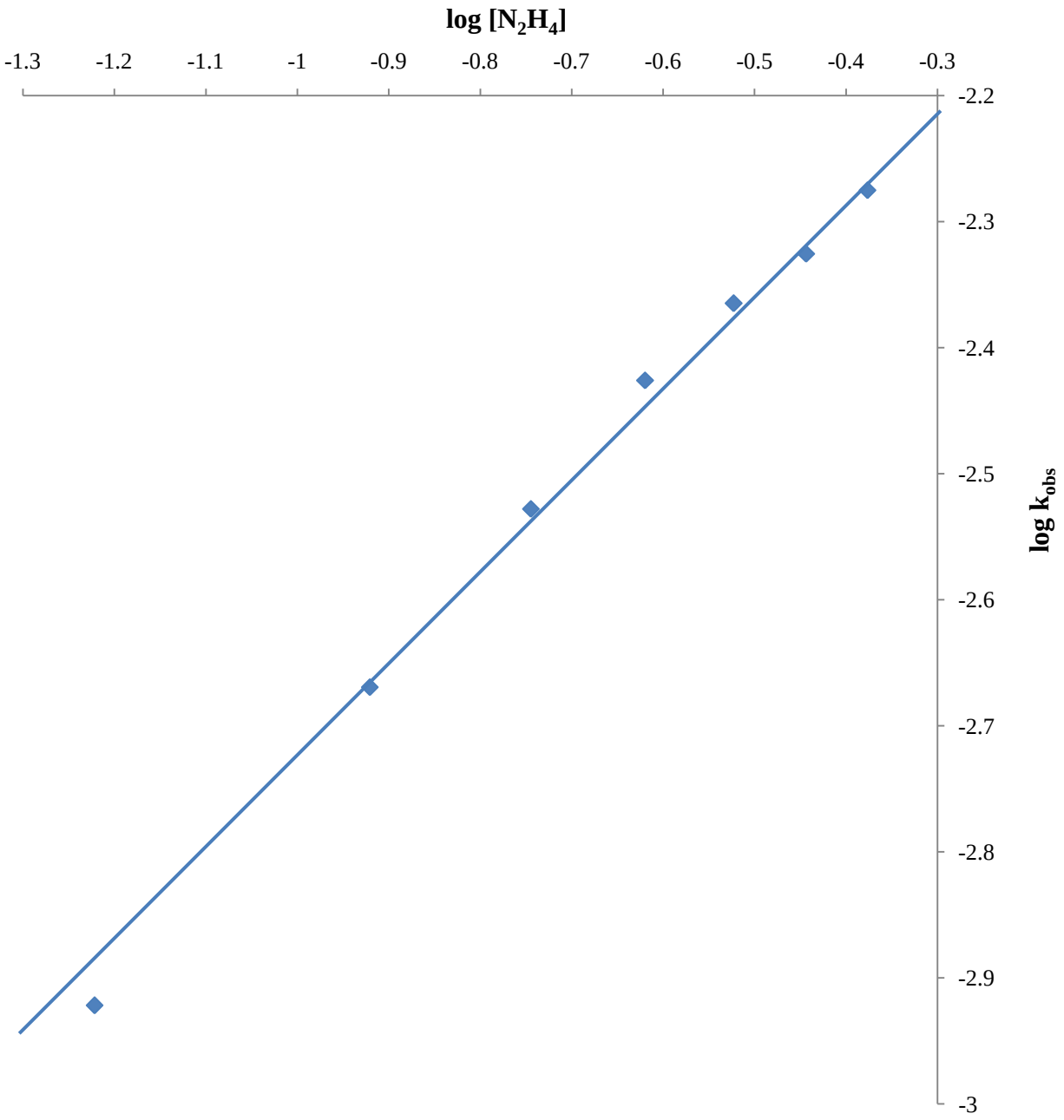

Figure 4.10: **Plot of log k_{obs} versus log $[N_2H_4]$ for the redox reaction of $[Co(EDTA)]^-$ with N_2H_4 at $[Co^{3+}] = 3.0 \times 10^{-3}$ mol dm^{-3}, $[H^+] = 1.0 \times 10^{-3}$ mol dm^{-3}, I = 0.45 mol dm^{-3} ($HClO_4$), $[Cu^{2+}] = 6.0 \times 10^{-4}$ mol dm^{-3}, λ_{max} = 535 nm and T = 298 ± 1K**

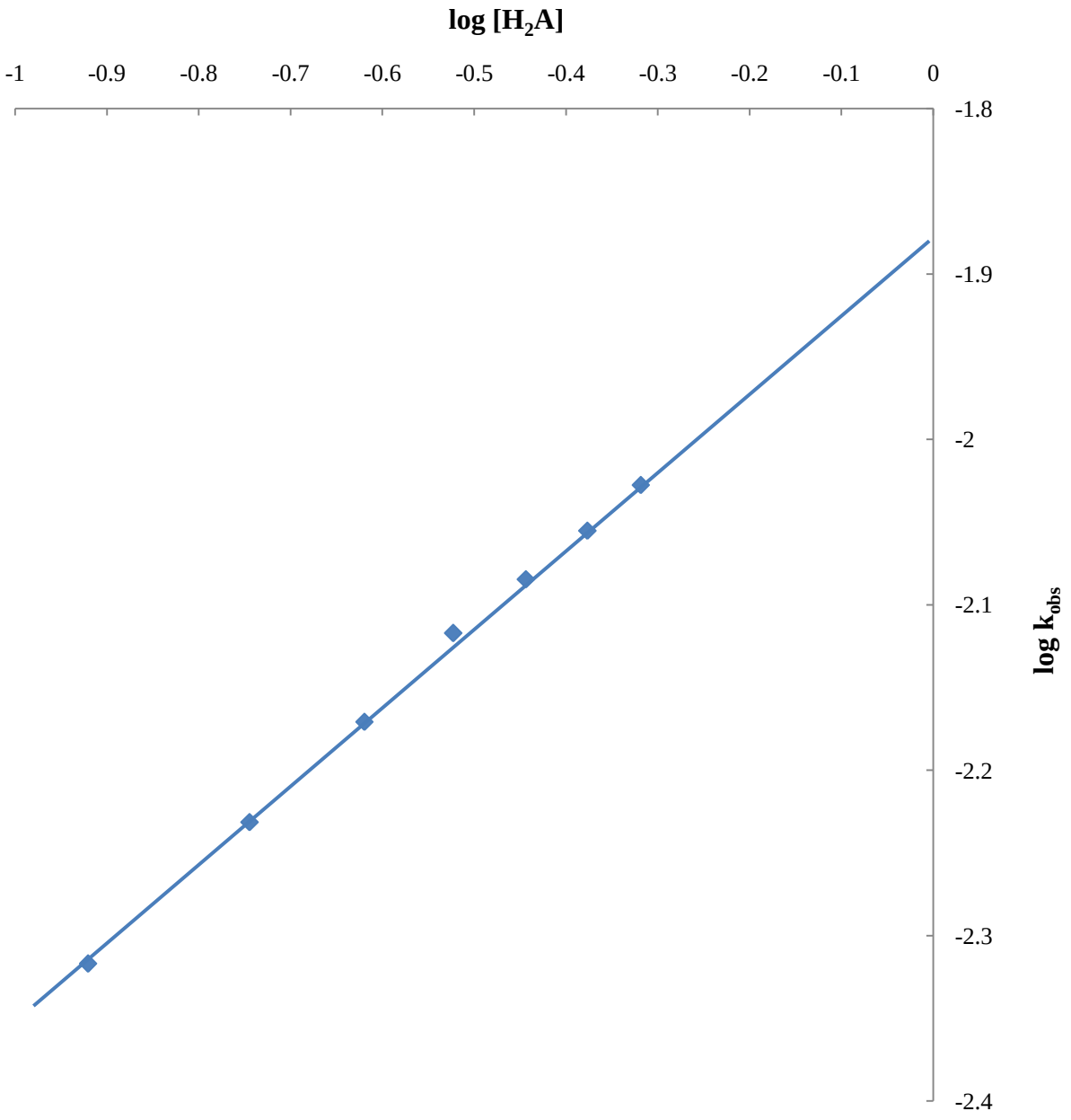

Figure 4.11: **Plot of log k_{obs} versus log [H_2A] for the redox reaction of [Co(HEDTA)OH_2] with H_2A at [Co^{3+}] = 6.0 × 10^{-3} mol dm^{-3}, [H^+] = 2.0 × 10^{-3} mol dm^{-3}, I = 0.9 mol dm^{-3} ($HClO_4$), [Cu^{2+}] = 7.0 × 10^{-3} mol dm^{-3}, λ_{max} = 550 nm and T = 299 ± 1K**

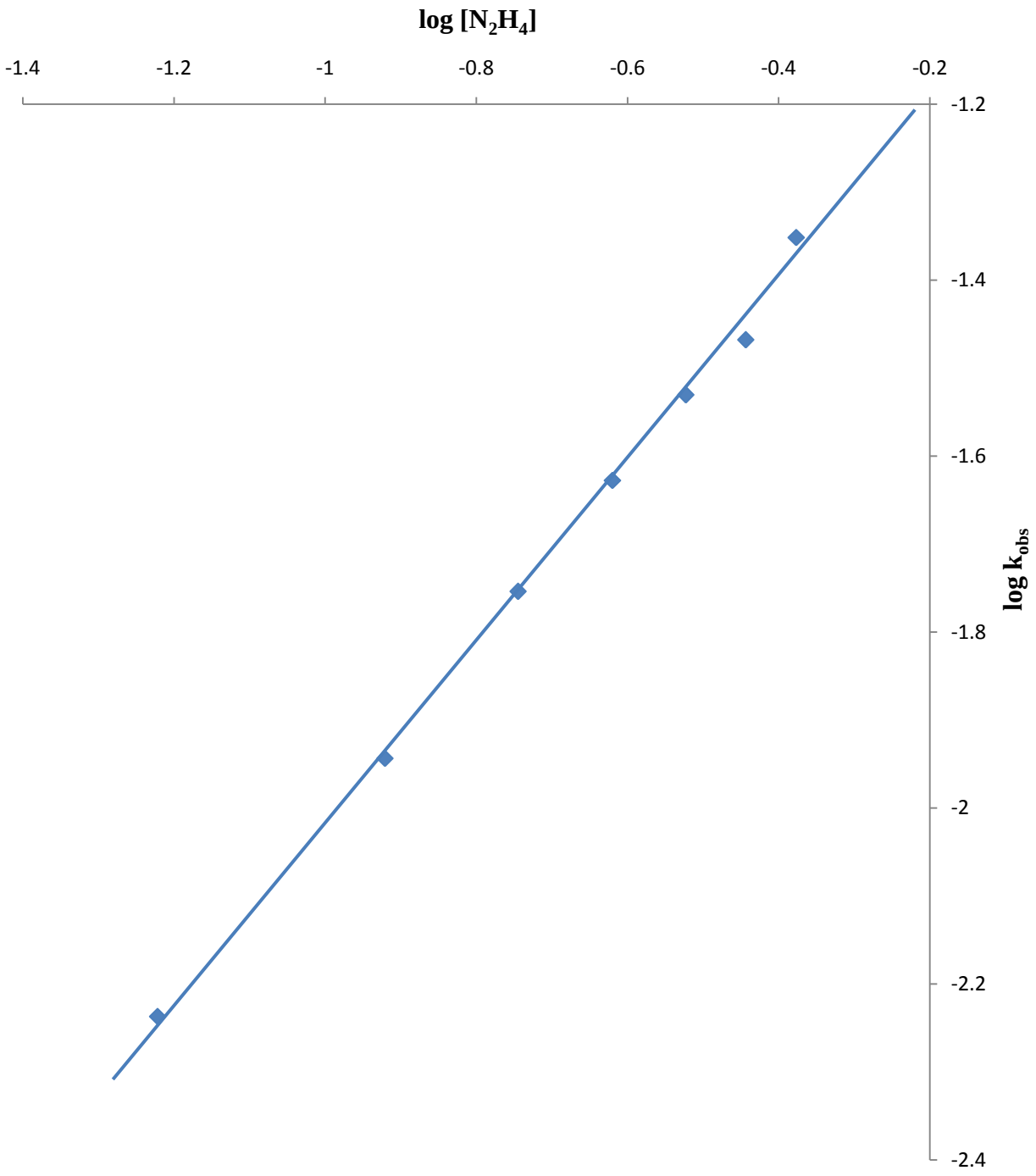

Figure 4.12: **Plot of log k_{obs} versus log $[N_2H_4]$ for the redox reaction of $[Co(HEDTA)OH_2]$ with N_2H_4 at $[Co^{3+}] = 6.0 \times 10^{-3}$ mol dm^{-3}, $[H^+] = 4.0 \times 10^{-3}$ mol dm^{-3}, I = 0.5 mol dm^{-3} ($HClO_4$), $[Cu^{2+}] = 5.0 \times 10^{-4}$ mol dm^{-3}, λ_{max} = 550 nm and T = 298 ± 1K**

$$-\frac{d[Co^{III}(HEDTA)OH_2]}{dt} = k_2[Co^{III}(HEDTA)OH_2]\,[N_2H_4]$$

(4.9)

The second order rate and three and half rate constants for the various systems are;

$[Co(EDTA)]^- - H_2A$: $k_2 = (9.88 \pm 0.065) \times 10^{-3}\ dm^3\ mol^{-1}\ s^{-1}$

$[Co(EDTA)]^- - N_2H_4$: $k_2 = (1.57 \pm 0.099) \times 10^{-2}\ dm^3\ mol^{-1}\ s^{-1}$

$[Co(HEDTA)OH_2] - H_2A$: $k_{3/2} = (1.38 \pm 0.014) \times 10^{-2}\ dm^{3/2}\ mol^{-1/2}\ s^{-1/2}$

$[Co(HEDTA)OH_2] - N_2H_4$: $k_2 = (9.81 \pm 0.144) \times 10^{-2}\ dm^3\ mol^{-1}\ s^{-1}$

4.3 Effect of Hydrogen Ion Concentration on the Rate of the Reactions

For the $[Co(EDTA)]^- - [H_2A]$, $[Co(EDTA)]^- - N_2H_4$ and $[Co(HEDTA)OH_2] - H_2A$ systems, the rate of the reaction was found to be independent on the changes in the concentration of hydrogen ion, while the rate of reaction for the $[Co(HEDTA)OH_2] - N_2H_4$ system was found to be inversely influenced by increase in the hydrogen ion concentration. These results are all contained in Tables 4.1 – 4.4. The least square plots of log k_{obs} versus log $[H^+]$ gave a straight line, with the slope of – 0.95 for the $[Co(HEDTA)OH_2] - N_2H_4$ system (Figure 4.13), this indicates an inverse first order dependence on $[H^+]$ for this reaction. The least square plots of k_2 versus $[H^+]^{-1}$ for the $[Co(HEDTA)OH_2] - N_2H_4$ system (Figure 4.14) was linear, without intercept and had a slope of $3.47 \times 10^{-4}\ s^{-1}$. The acid dependent rate constant can be represented by Equation 4.10 for the $[Co(HEDTA)OH_2] - N_2H_4$ system respectively, with "a" as the slope.

$$k_2 = a[H^+]^{-1} \qquad (4.10)$$

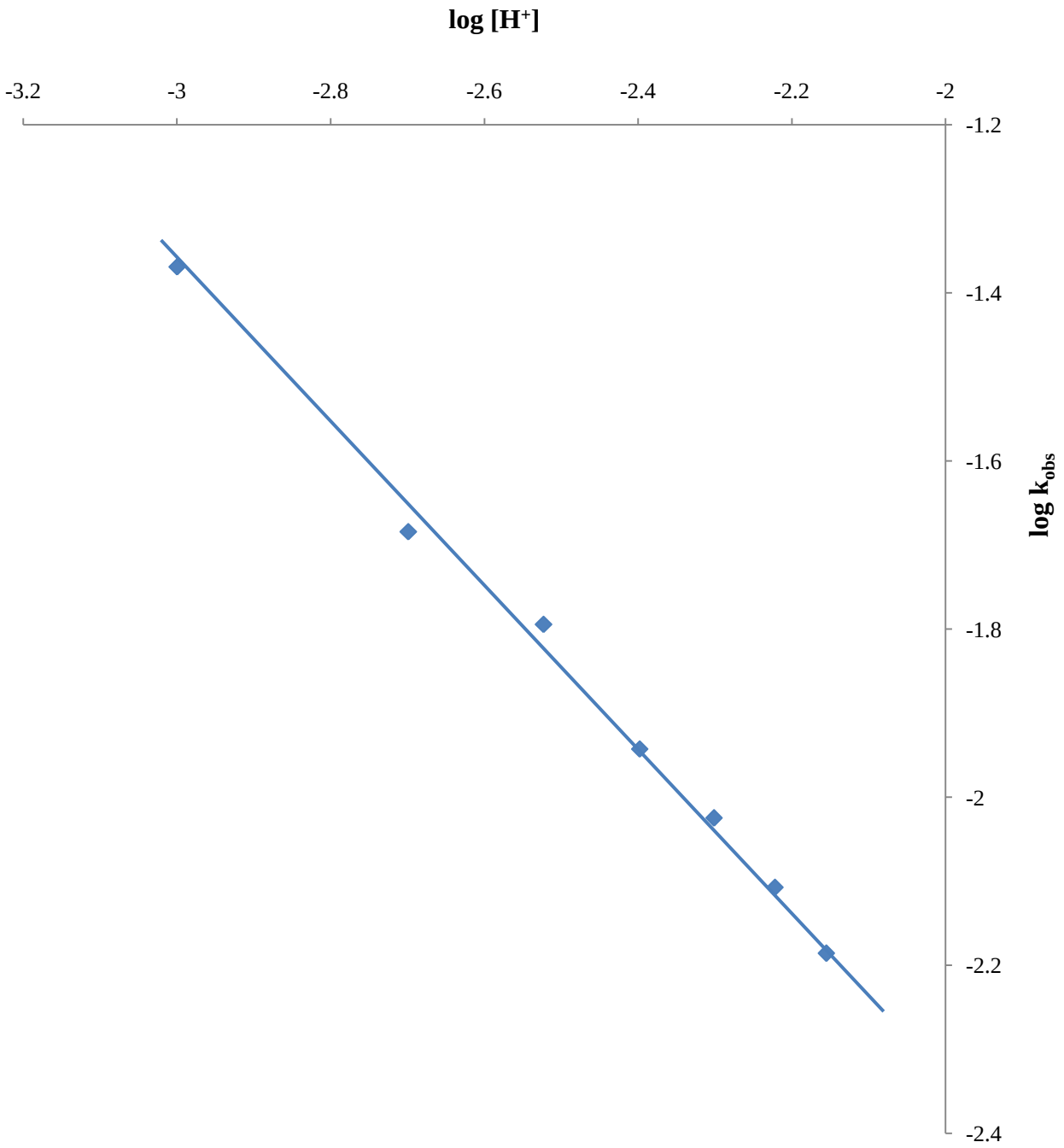
log [H+]
-3.2
-3
-2.8
-2.6
-2.4
-2.2
-2
-1.2
-1.4
-1.6
-1.8
-2
-2.2
-2.4
log kobs

Figure 4.13: Plot of log k_{obs} versus log $[H^+]$ for redox reaction of $[Co(HEDTA)OH_2]$ with N_2H_4 at $[Co^{3+}] = 6.0 \times 10^{-3}$ mol dm^{-3}, $[N_2H_4] = 0.12$ mol dm^{-3}, I = 0.5 mol dm^{-3} ($HClO_4$), $[Cu^{2+}] = 5.0 \times 10^{-4}$ mol dm^{-3}, λ_{max} = 550 nm and T = 298 ± 1K

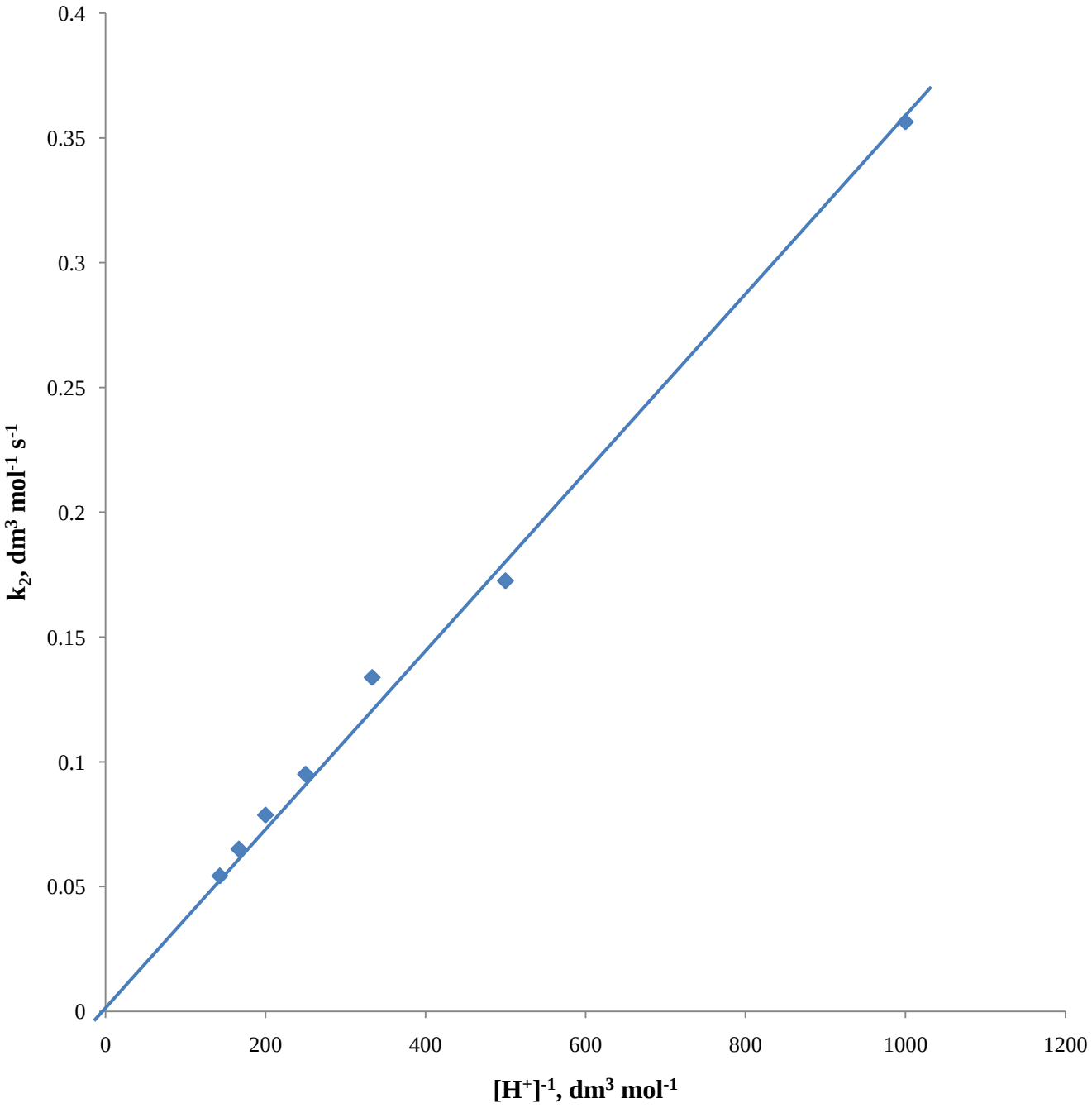

Figure 4.14: Plot k_2 versus $[H^+]^{-1}$ for the redox reaction of $[Co(HEDTA)OH_2]$ with N_2H_4 at $[Co^{3+}] = 6.0 \times 10^{-3}$ mol dm^{-3}, $[N_2H_4] = 0.12$ mol dm^{-3}, I = 0.5 mol dm^{-3} ($HClO_4$), $[Cu^{2+}] = 5.0 \times 10^{-4}$ mol dm^{-3}, λ_{max} = 550 nm and T = 298 ± 1K

4.4 Effect of Catalyst Concentration on the Rate of the Reactions

The rates of reactions for all the systems increased with increase in catalyst concentration (Tables 4.1 – 4.4). The plots of log k_{obs} versus log $[Cu^{2+}]$ gave a straight line, with the slopes of 1.24, 1.13, 2.25 and 0.84 for $[Co(EDTA)]^{-}$ – H_2A system, $[Co(EDTA)]^{-}$ – N_2H_4 system, $[Co(HEDTA)OH_2]$ – H_2A system and $[Co(HEDTA)OH_2]$ – N_2H_4 system respectively (Figures 4.15 – 4.18), this indicates a first order with respect to the $[Cu^{2+}]$ for the $[Co(EDTA)]^{-}$ – H_2A system, $[Co(EDTA)]^{-}$ – N_2H_4 system and $[Co(HEDTA)OH_2]$ – N_2H_4 system respectively, while a second order for the $[Co(HEDTA)OH_2]$ – H_2A system was obtained.

The plots of k_2 versus $[Cu^{2+}]$ for the other three systems and the plot of $k_{3/2}$ versus $[Cu^{2+}]^2$ for the $[Co(HEDTA)OH_2]$ – H_2A system were linear (Figures 4.19 – 4.22). The plot for the $[Co(EDTA)]^{-}$ – H_2A and $[Co(HEDTA)OH_2]$ – H_2A systems both had intercepts on the x – axis, while that of $[Co(EDTA)]^{-}$ – N_2H_4 and $[Co(HEDTA)OH_2]$ – N_2H_4 systems had no intercept.

The catalyst dependent rate constants can thus be represented for $[Co(EDTA)]^{-}$ – H_2A system (Equation 4.11), $[Co(EDTA)]^{-}$ – N_2H_4 system (Equation 4.12), $[Co(HEDTA)OH_2]$ – H_2A system (Equation 4.13) and $[Co(HEDTA)OH_2]$ – N_2H_4 system (Equation 4.14) respectively.

$$k_2 = b[Cu^{2+}] \quad (4.11)$$

$$k_2 = c[Cu^{2+}] \quad (4.12)$$

$$k_{3/2} = d[Cu^{2+}]^2 \quad (4.13)$$

$$k_2 = e\,[Cu^{2+}] \quad (4.14)$$

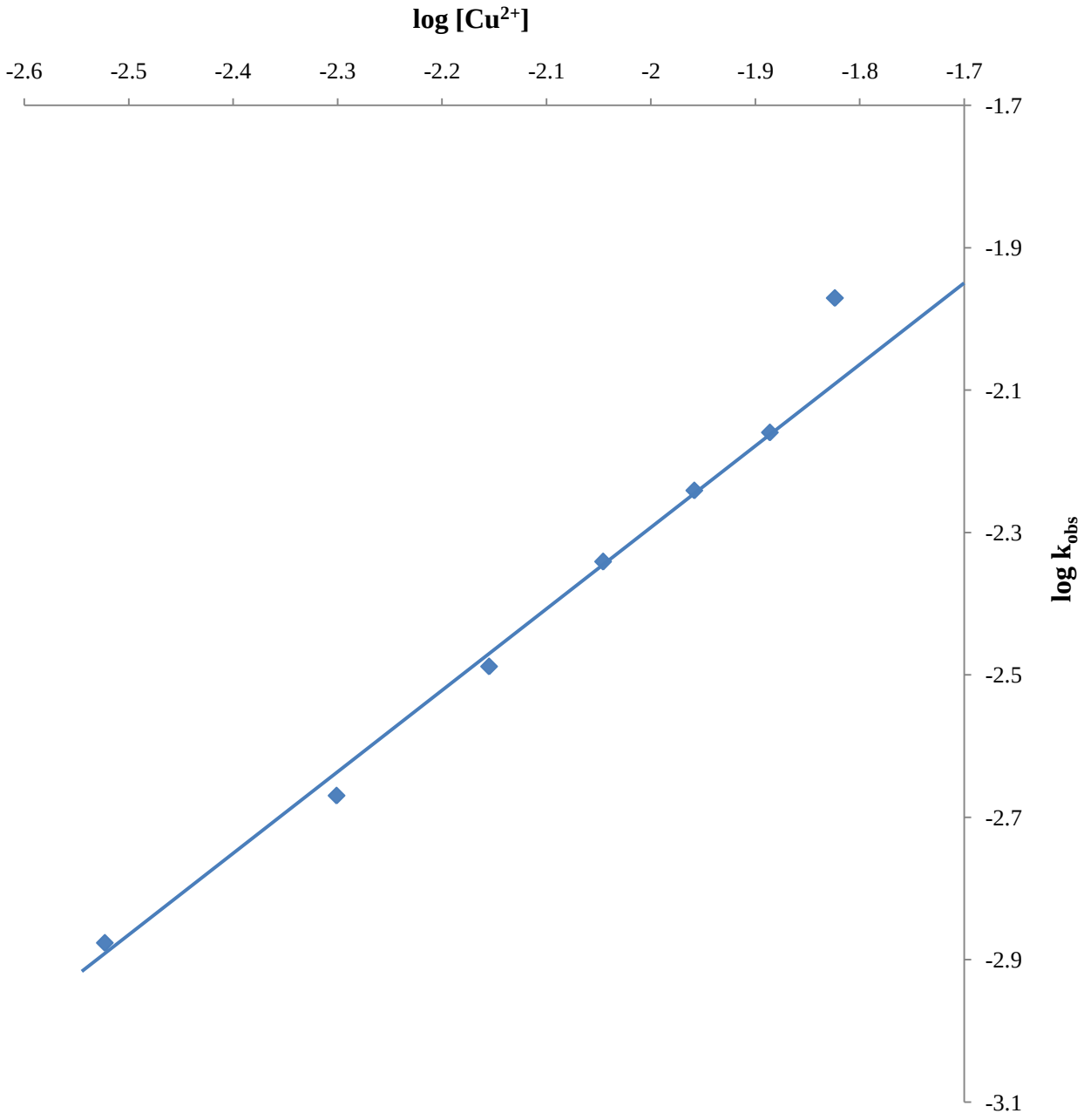

Figure 4.15: **Plot of log k_{obs} versus log $[Cu^{2+}]$ for the redox reaction of $[Co(EDTA)]^{-}$ with H_2A at $[Co^{3+}] = 3.0 \times 10^{-3}$ mol dm^{-3}, $[H_2A] = 0.21$ mol dm^{-3}, I = 0.4 mol dm^{-3} (Na_2SO_4), $[H^+] = 1.0 \times 10^{-3}$ mol dm^{-3}, $\lambda_{max} = 535$ nm and T = 299 ± 1K**

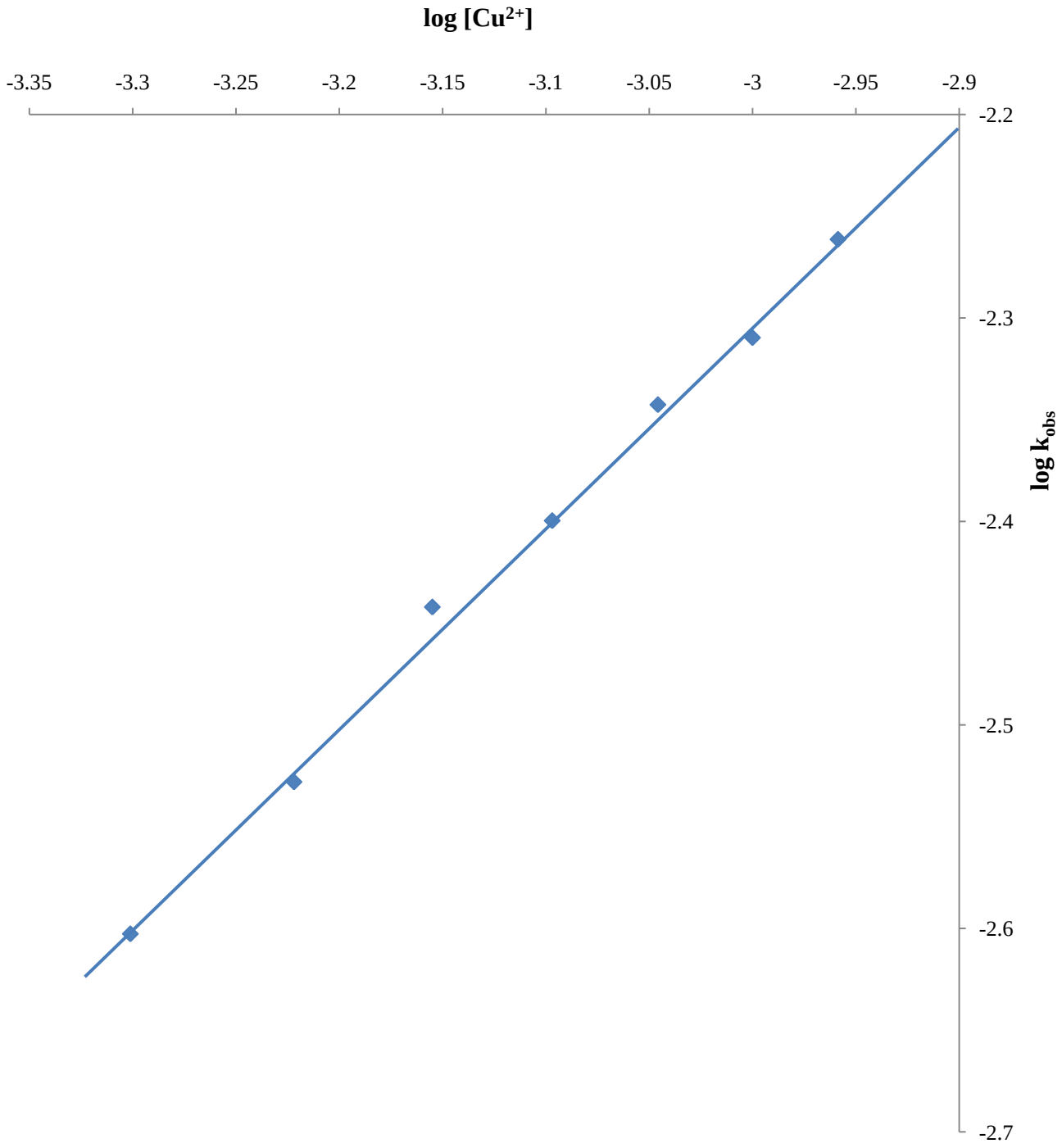

Figure 4.16: **Plot of log k_{obs} versus log $[Cu^{2+}]$ for the redox reaction of $[Co(EDTA)]^{-}$ with N_2H_4 at $[Co^{3+}] = 3.0 \times 10^{-3}$ mol dm^{-3}, $[N_2H_4] = 0.18$ mol dm^{-3}, I = 0.45 mol dm^{-3} ($HClO_4$), $[H^+] = 1.0 \times 10^{-3}$ mol dm^{-3}, $\lambda_{max} = 535$ nm and T = 298 ± 1K**

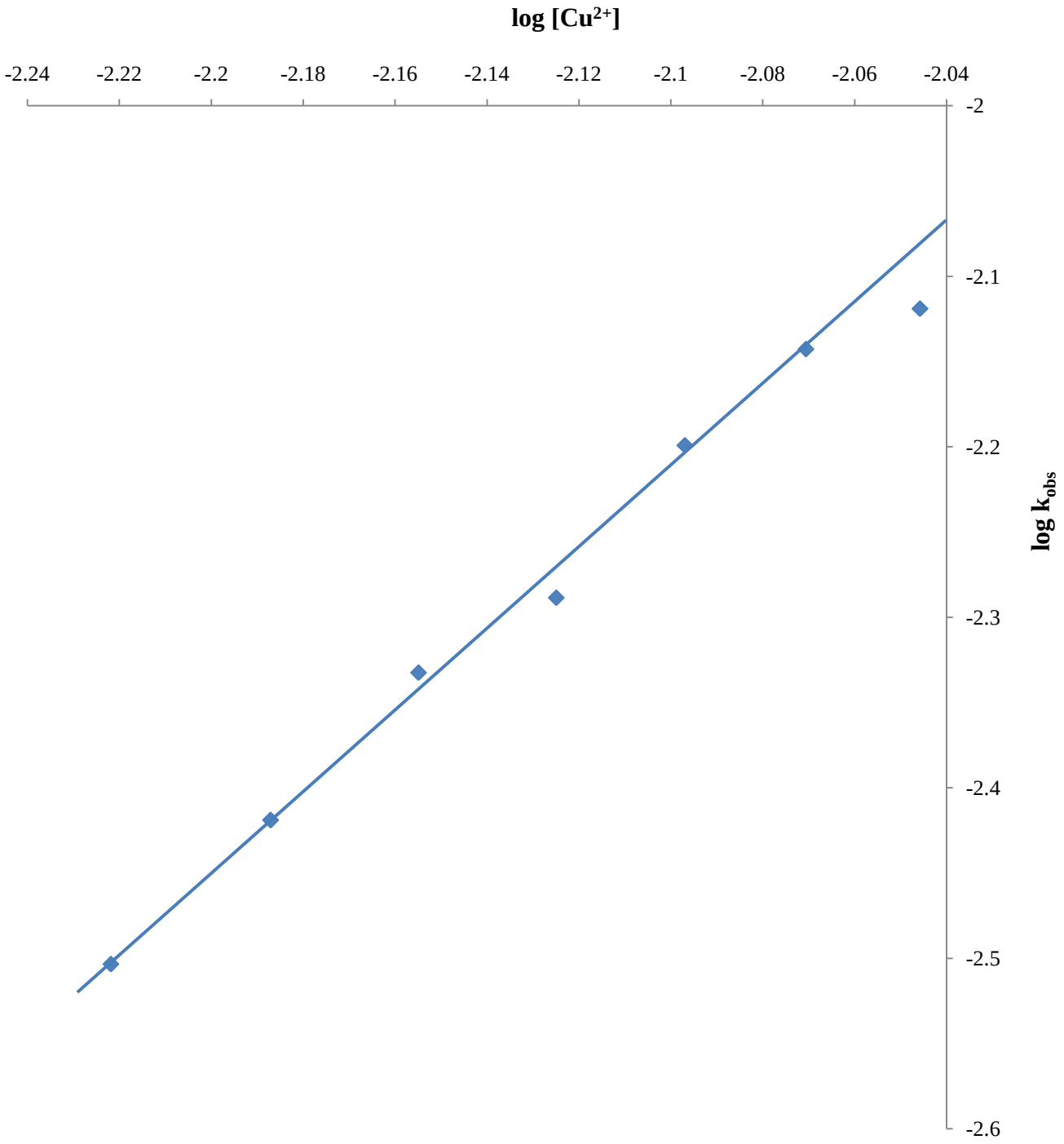

Figure 4.17: Plot of log k_{obs} versus log [Cu^{2+}] for the redox reaction of [Co(HEDTA)OH_2] with H_2A at [Co^{3+}] = 6.0 × 10^{-3} mol dm^{-3}, [H_2A] = 0.12 mol dm^{-3}, I = 0.9 mol dm^{-3} ($HClO_4$), [H^+] = 2.0 × 10^{-3} mol dm^{-3}, λ_{max} = 550 nm and T = 299 ± 1K

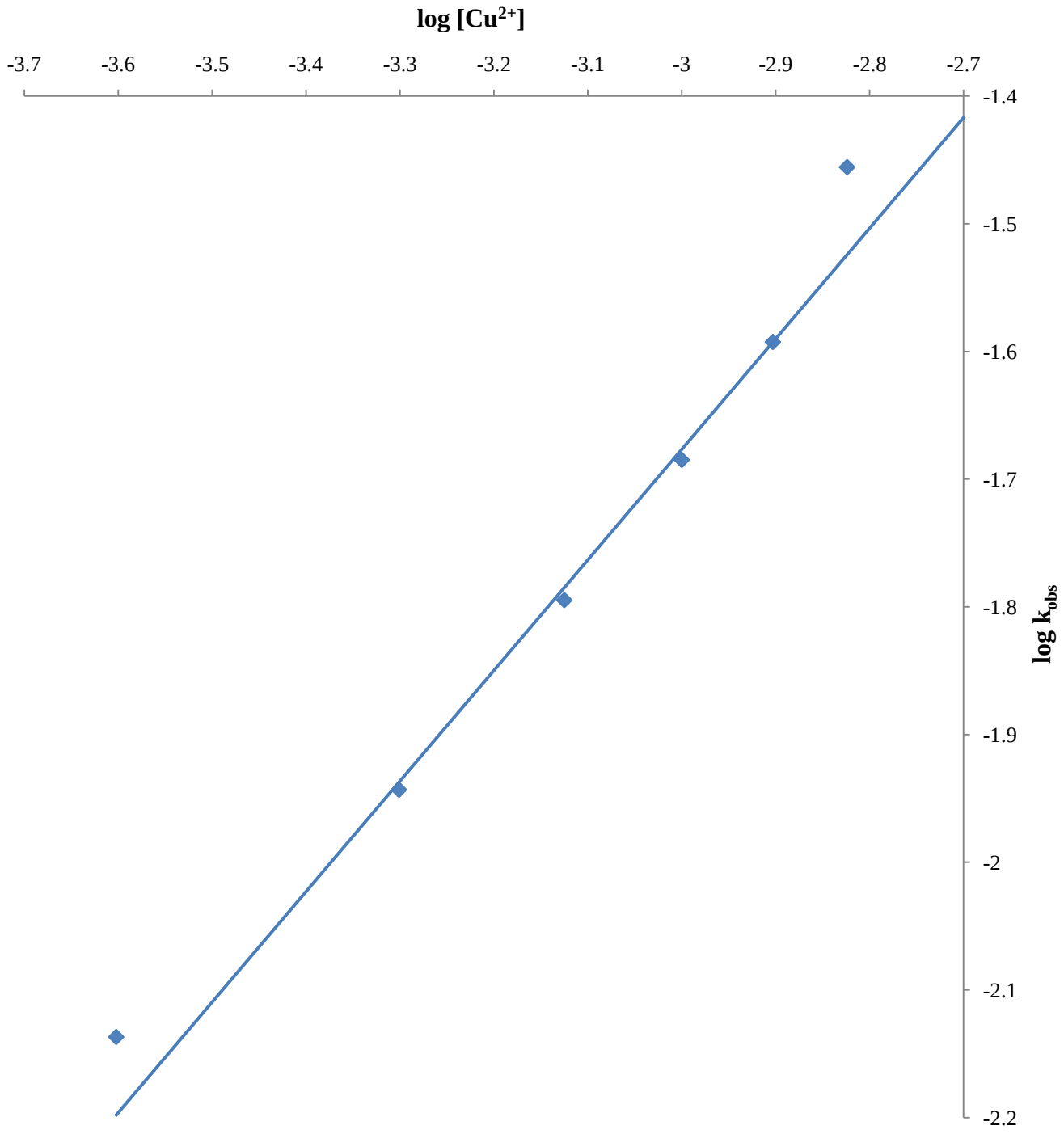

Figure 4.18: Plot of log k_{obs} versus log $[Cu^{2+}]$ for the redox reaction of $[Co(HEDTA)OH_2]$ with N_2H_4 at $[Co^{3+}] = 6.0 \times 10^{-3}$ mol dm^{-3}, $[N_2H_4] = 0.12$ mol dm^{-3}, I = 0.5 mol dm^{-3} ($HClO_4$), $[H^+] = 4.0 \times 10^{-3}$ mol dm^{-3}, λ_{max} = 550 nm and T = 298 ± 1K

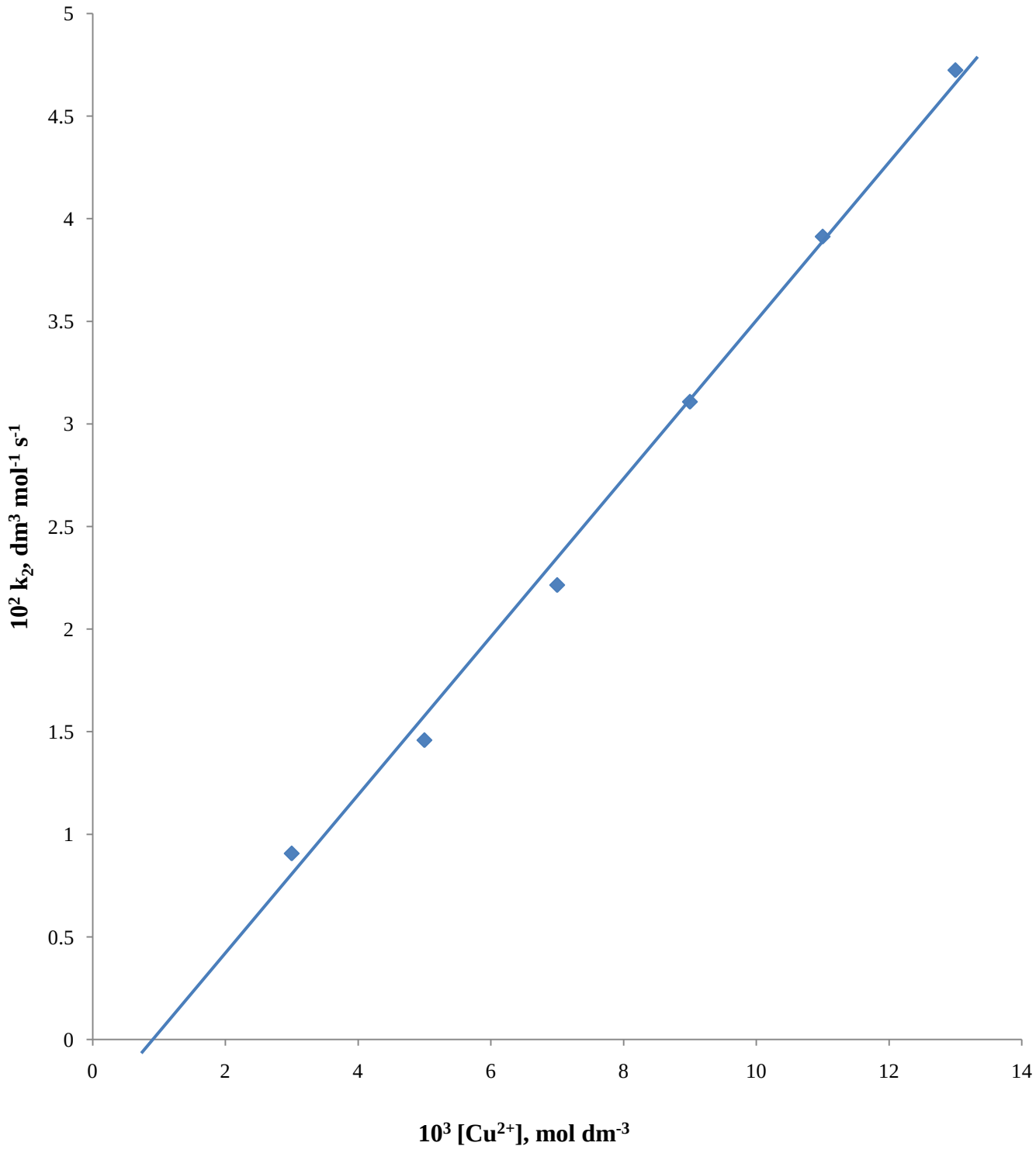

Figure 4.19: **Plot of k_2 versus $[Cu^{2+}]$ for the redox reaction of $[Co(EDTA)]^-$ with H_2A at $[Co^{3+}] = 3.0 \times 10^{-3}$ mol dm^{-3}, $[H_2A] = 0.21$ mol dm^{-3}, I = 0.4 mol dm^{-3} (Na_2SO_4), $[H^+] = 1.0 \times 10^{-3}$ mol dm^{-3}, $\lambda_{max} = 535$ nm and T = 299 ± 1K**

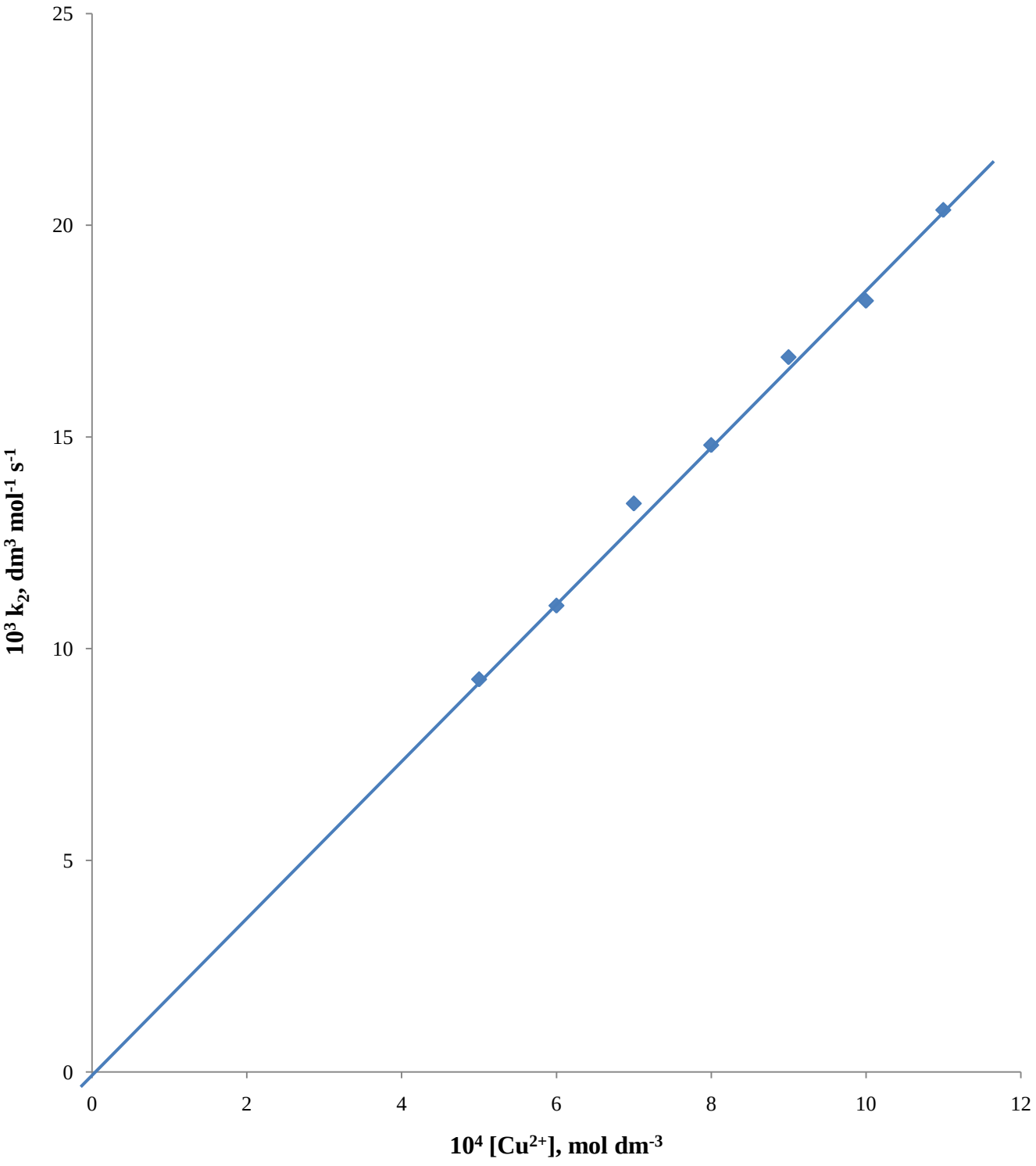

Figure 4.20: **Plot of k_2 versus $[Cu^{2+}]$ for the electron transfer reaction of $[Co(EDTA)]^-$ with N_2H_4 at $[Co^{3+}] = 3.0 \times 10^{-3}$ mol dm^{-3}, $[N_2H_4] = 0.18$ mol dm^{-3}, I = 0.45 mol dm^{-3} ($HClO_4$), $[H^+] = 1.0 \times 10^{-3}$ mol dm^{-3}, $\lambda_{max} = 535$ nm and T = 298 ± 1K**

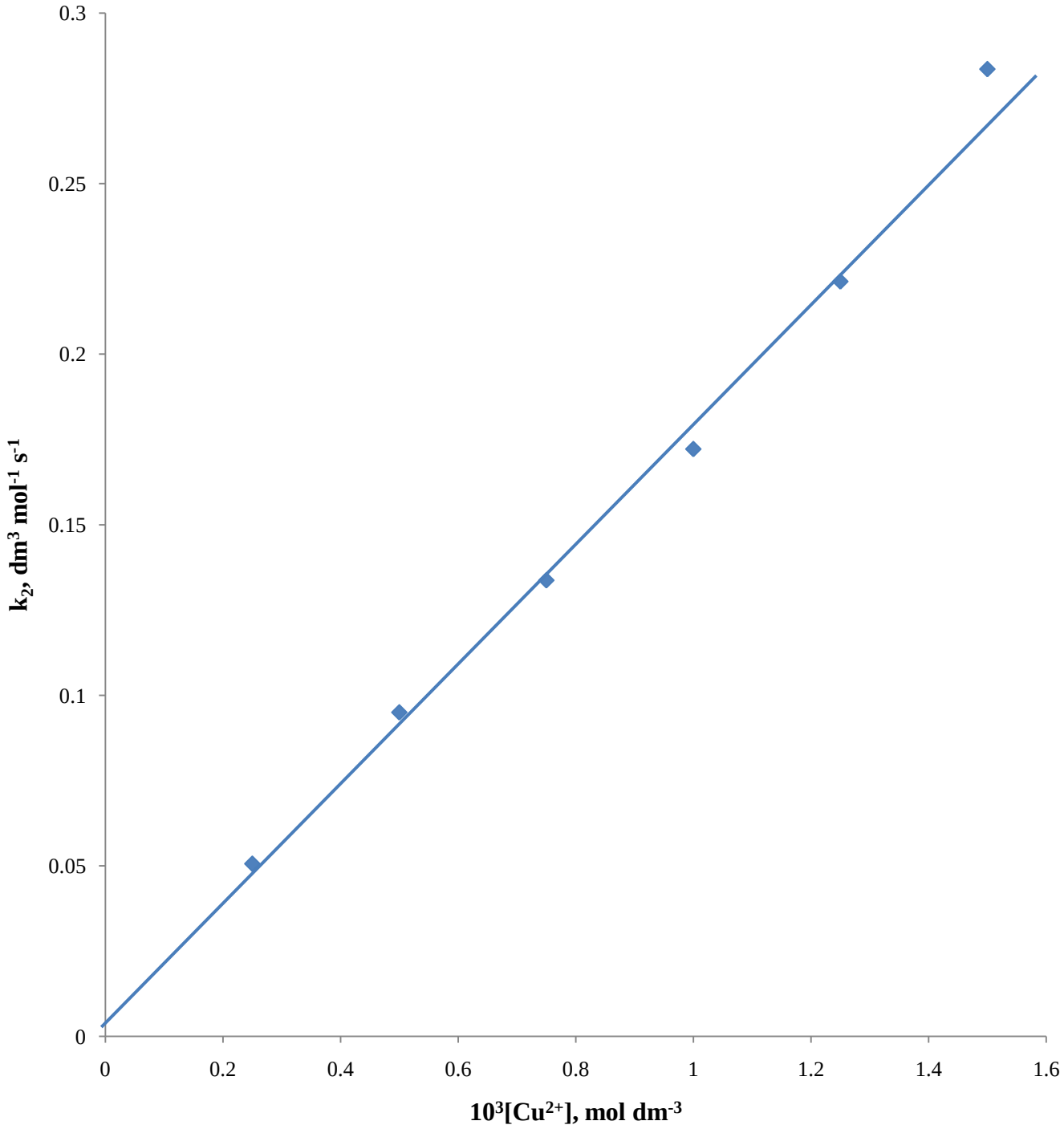

Figure 4.21: **Plot of k_2 versus $[Cu^{2+}]$ for the redox reaction of $[Co(HEDTA)OH_2]$ with N_2H_4 at $[Co^{3+}] = 6.0 \times 10^{-3}$ mol dm^{-3}, $[N_2H_4] = 0.12$ mol dm^{-3}, I = 0.5 mol dm^{-3} ($HClO_4$), $[H^+] = 4.0 \times 10^{-3}$ mol dm^{-3}, $\lambda_{max} = 550$ nm and T = 298 ± 1K**

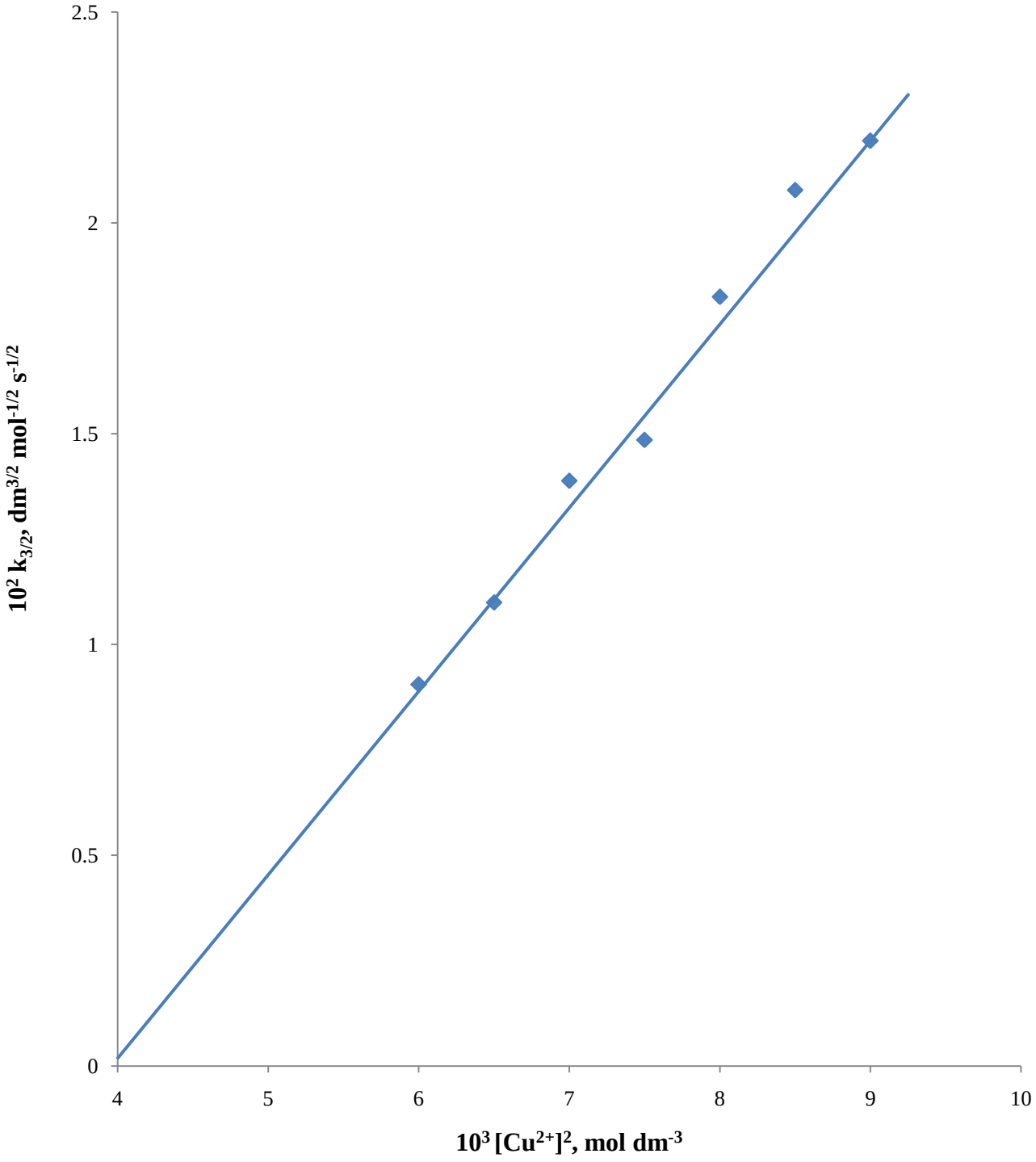

Figure 4.22: **Plot of $k_{3/2}$ versus $[Cu^{2+}]^2$ for the redox reaction of $[Co(HEDTA)OH_2]$ with H_2A at $[Co^{3+}] = 6.0 \times 10^{-3}$ mol dm^{-3}, $[H_2A] = 0.12$ mol dm^{-3}, I = 0.9 mol dm^{-3} ($HClO_4$), $[H^+] = 2.0 \times 10^{-3}$ mol dm^{-3}, $\lambda_{max} = 550$ nm and T = 299 ± 1K**

The overall rate equations for the various systems are represented in Equations 4.15 – 4.18.

$$-\frac{d[Co^{III}(EDTA)^{-}]}{dt} = b[Cu^{2+}]\,[Co^{III}(EDTA)^{-}]\,[H_2A] \quad (4.15)$$

$$-\frac{d[Co^{III}(EDTA)^{-}]}{dt} = c[Cu^{2+}]\,[Co^{III}(EDTA)^{-}]\,[N_2H_4] \quad (4.16)$$

$$-\frac{d[Co^{III}(HEDTA)OH_2]}{dt} = d[Cu^{2+}]^2\,[Co^{III}(HEDTA)OH_2]\,[H_2A]^{1/2} \quad (4.17)$$

$$-\frac{d[Co^{III}(HEDTA)OH_2]}{dt} = a[H^{+}]^{-1}\,e[Cu^{2+}]\,[Co^{III}(HEDTA)OH_2]\,[N_2H_4] \quad (4.18)$$

where a = 3.47×10^{-4} s^{-1} , b = 4.9 s^{-1}, c = 18.25 s^{-1}, d = 4.47 $s^{-1/2}$ and e = 1.8×10^{2} s^{-1}.

4.5 Effect of Ionic Strength of the Reaction Medium on the Rate of the Reaction

The effect of the change in ionic strength of the reaction medium on the reaction rate was investigated over the range of 0.30 – 0.55 mol dm^{-3} (Na_2SO_4) for $[Co(EDTA)]^{-}$ – H_2A system, 0.2 – 0.5 mol dm^{-3} ($HClO_4$) for $[Co(EDTA)]^{-}$ – N_2H_4 system, 0.3 – 0.9 mol dm^{-3} ($HClO_4$) for $[Co(HEDTA)OH_2]$ – H_2A system and 0.3 – 0.6 mol dm^{-3} ($HClO_4$) for $[Co(HEDTA)OH_2]$ – N_2H_4 system respectively, while all other conditions were kept constant. There was a marked decrease in the rate of reactions with increase in ionic strength for $[Co(EDTA)]^{-}$ – H_2A and $[Co(EDTA)]^{-}$ – N_2H_4 systems (Table 4.1 – 4.2), while an increase in ionic strength concentration had no effect on the rate of reaction for both $[Co(HEDTA)OH_2]$ – H_2A and $[Co(HEDTA)OH_2]$ – N_2H_4 systems (Table 4.3 – 4.4). The logarithmic plots of k_2 against $I^{1/2}$ are contained in Figures 4.23 – 4.24.

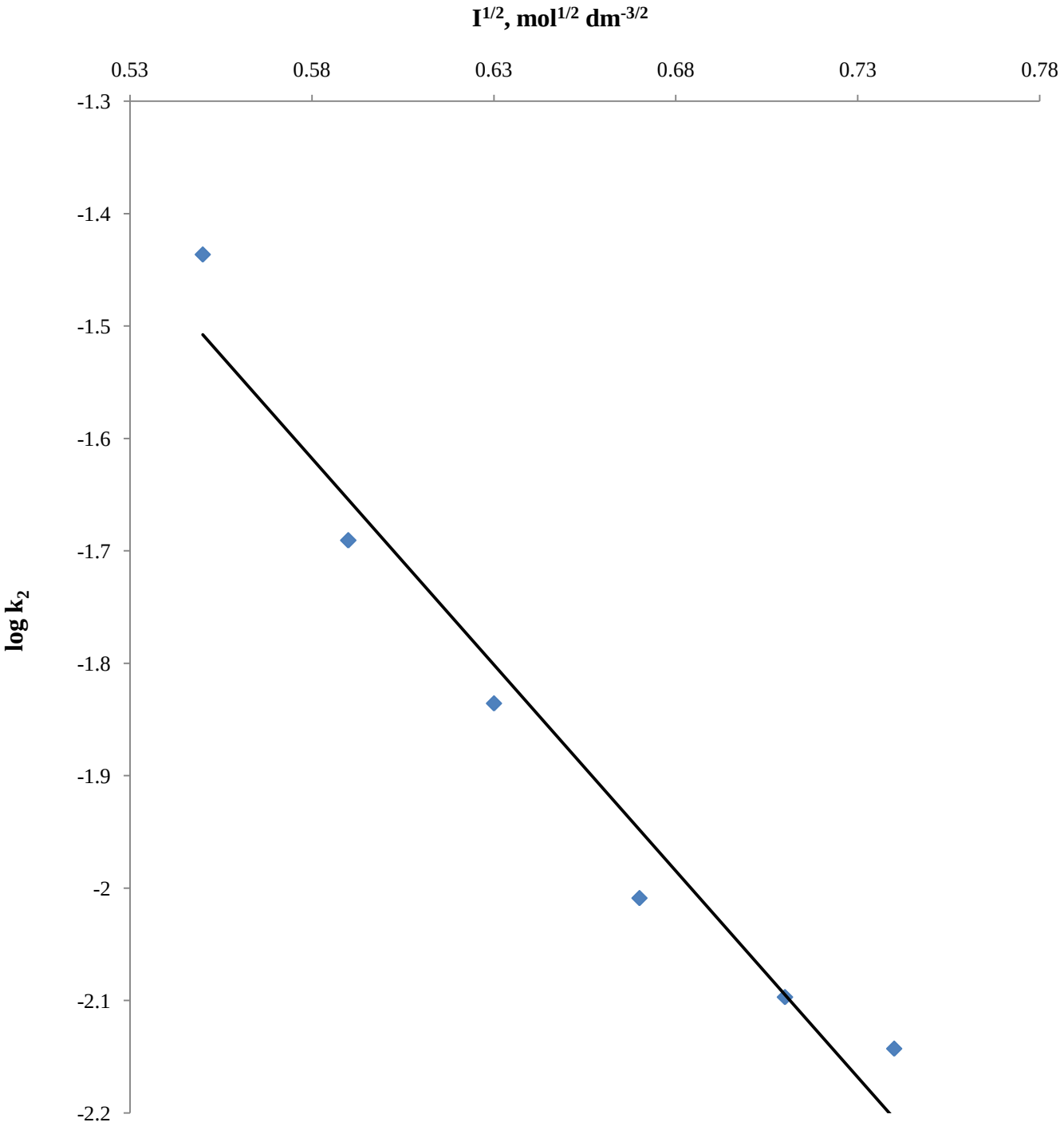

Figure 4.23: Plot of log k_2 versus $I^{1/2}$ for the redox reaction of $[Co(EDTA)]^-$ with H_2A at $[Co^{3+}] = 3.0 \times 10^{-3}$ mol dm^{-3}, $[H_2A] = 0.21$ mol dm^{-3}, $[Cu^{2+}] = 5.0 \times 10^{-3}$ mol dm^{-3}, $[H^+] = 1.0 \times 10^{-3}$ mol dm^{-3}, $\lambda_{max} = 535$ nm and T = 299 ± 1K

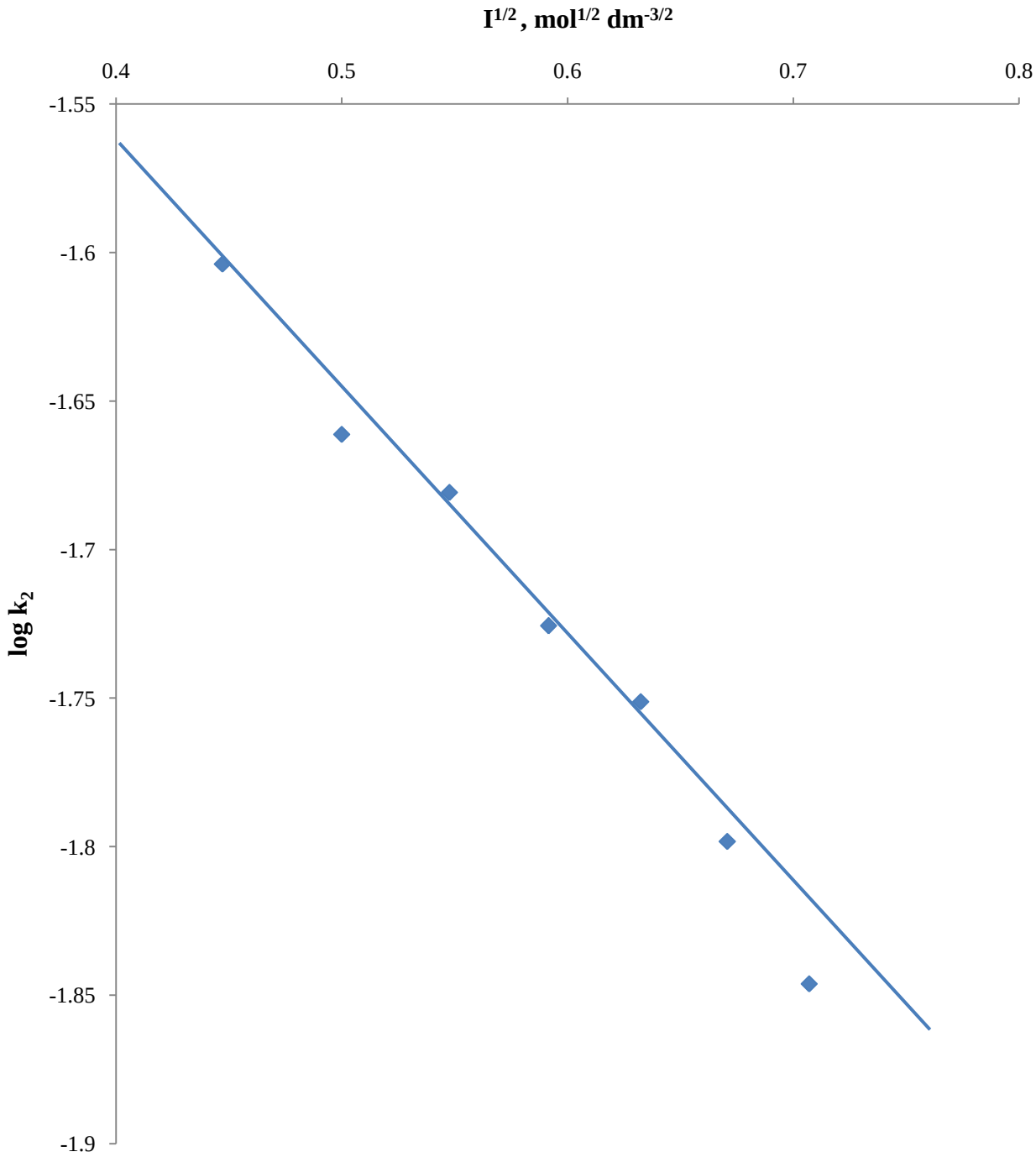

Figure 4.24: Plot of log k_2 versus $I^{1/2}$ for the redox reaction of $[Co(EDTA)]^-$ with N_2H_4 at $[Co^{3+}] = 3.0 \times 10^{-3}$ mol dm^{-3}, $[N_2H_4] = 0.18$ mol dm^{-3}, $[Cu^{2+}] = 6.0 \times 10^{-4}$ mol dm^{-3}, $[H^+] = 1.0 \times 10^{-3}$ mol dm^{-3}, $\lambda_{max} = 535$ nm and T = 298 ± 1K

4.6 Effect of Dielectric Constants of the Reaction Medium on the Rate of the Reaction

The dielectric constant (D) of the reaction medium was varied using acetone in accordance to Equation 3.2. As the dielectric constant of the reaction medium was decreasing, the rate of reaction was observed to increase for the $[Co(EDTA)]^{-}$ – H_2A system (Table 4.5), while the rate of reaction decreased for the $[Co(EDTA)]^{-}$ – N_2H_4 (Table 4.6) and $[Co(HEDTA)OH_2]$ – N_2H_4 (Table 4.7) systems respectively. Changes in the dielectric constant of the reaction medium had no effect on the rate of the reaction for the $[Co(HEDTA)OH_2]$ – H_2A system. Typical plots of log k_2 versus 1/D for the three reactions are shown in Figures 4.25 – 4.27.

4.7 Effect of Added Anions on the Rate of the Reaction

The effect of added anions on the rate of reaction was investigated using $CHOO^{-}$ and CH_3COO^{-}, within the concentration ranges of $(0.5 – 7.5) \times 10^{-2}$ mol dm^{-3} $(CHOO^{-})$ and $(0.5 – 10.0) \times 10^{-2}$ mol dm^{-3} (CH_3COO^{-}) for the $[Co(EDTA)]^{-}$ – H_2A system, $(0 – 2.5) \times 10^{-2}$ mol dm^{-3} for the $[Co(EDTA)]^{-}$ – N_2H_4 system, $(1.5 – 10.0) \times 10^{-2}$ mol dm^{-3} for the $[Co(HEDTA)OH_2]$ – H_2A system and $(0 – 2.0) \times 10^{-2}$ mol dm^{-3} for the $[Co(HEDTA)OH_2]$ – N_2H_4 system respectively. The rate of the reaction decreased with increase in anions concentration for the $[Co(EDTA)]^{-}$ – H_2A system (Table 4.8), and increased with increase in anion concentration for both $[Co(HEDTA)OH_2]$ – H_2A (Table 4.10) and $[Co(HEDTA)OH_2]$ – N_2H_4 (Table 4.11) systems. The added anions had no effect on the rate of the reaction for the $[Co(EDTA)]^{-}$ – N_2H_4 system (Table 4.9). The plots of the anion – dependent rate constants versus the anion concentrations were all linear and are contained in Figures 4.28 – 4.33.

Table 4.5: Pseudo – first order and second order rate constants for the effect of changes in dielectric constant of the medium on the reduction of $[Co(EDTA)]^-$ by H_2A, at $[Co^{3+}] = 3.0 \times 10^{-3}$ mol dm^{-3}, $[H_2A] = 0.21$ mol dm^{-3}, $[Cu^{2+}] = 5.0 \times 10^{-3}$ mol dm^{-3}, I = 0.40 mol dm^{-3} (Na_2SO_4) and T= 299 ± 1 K

D	10^2 1/D	$10^3 k_{obs}$, s^{-1}	$10^2 k_2$, $dm^3 mol^{-1} s^{-1}$
80.10	1.25	2.14	1.02
79.10	1.26	4.77	3.56
78.00	1.28	5.00	3.76
77.00	1.30	7.00	5.23
76.00	1.32	8.50	6.35
74.90	1.34	9.35	6.98

Table 4.6: **Pseudo – first order and second order rate constants for the effect of changes in dielectric constant of the medium on the reduction of $[Co(EDTA)]^-$ by N_2H_4, at $[Co^{3+}] = 3.0 \times 10^{-3}$ mol dm^{-3}, $[N_2H_4] = 0.18$ mol dm^{-3}, $[Cu^{2+}] = 6.0 \times 10^{-4}$ mol dm^{-3}, I = 0.45 mol dm^{-3} ($NaClO_4$) and T= 298 ± 1 K**

D	10^2 1/D	$10^3 k_{obs}$, s^{-1}	$10^3 k_2$, $dm^3 mol^{-1} s^{-1}$
80.100	1.248	2.970	11.020
79.680	1.255	2.700	10.040
79.260	1.262	2.300	8.550
78.850	1.268	1.750	6.510
78.430	1.275	1.320	4.910
78.000	1.282	0.900	3.360

Table 4.7: **Pseudo – first order and second order rate constants for the effect of changes in dielectric constant of the medium on the reduction of [Co(HEDTA)OH_2] by N_2H_4, at [Co^{3+}] = 6.0 × 10^{-3} mol dm^{-3}, [N_2H_4] = 0.12 mol dm^{-3}, [Cu^{2+}] = 5.0 × 10^{-4} mol dm^{-3}, I = 0.5 mol dm^{-3} ($NaClO_4$) and T = 298 ± 1K**

D	10^2 1/D	10^3 k_{obs}, s^{-1}	10^2k_2, $dm^3mol^{-1}s^1$
80.100	1.248	11.380	9.480
79.720	1.254	8.740	7.290
79.350	1.260	6.200	5.170
78.900	1.267	4.210	3.500
78.570	1.273	2.200	1.840
78.220	1.278	0.920	0.770

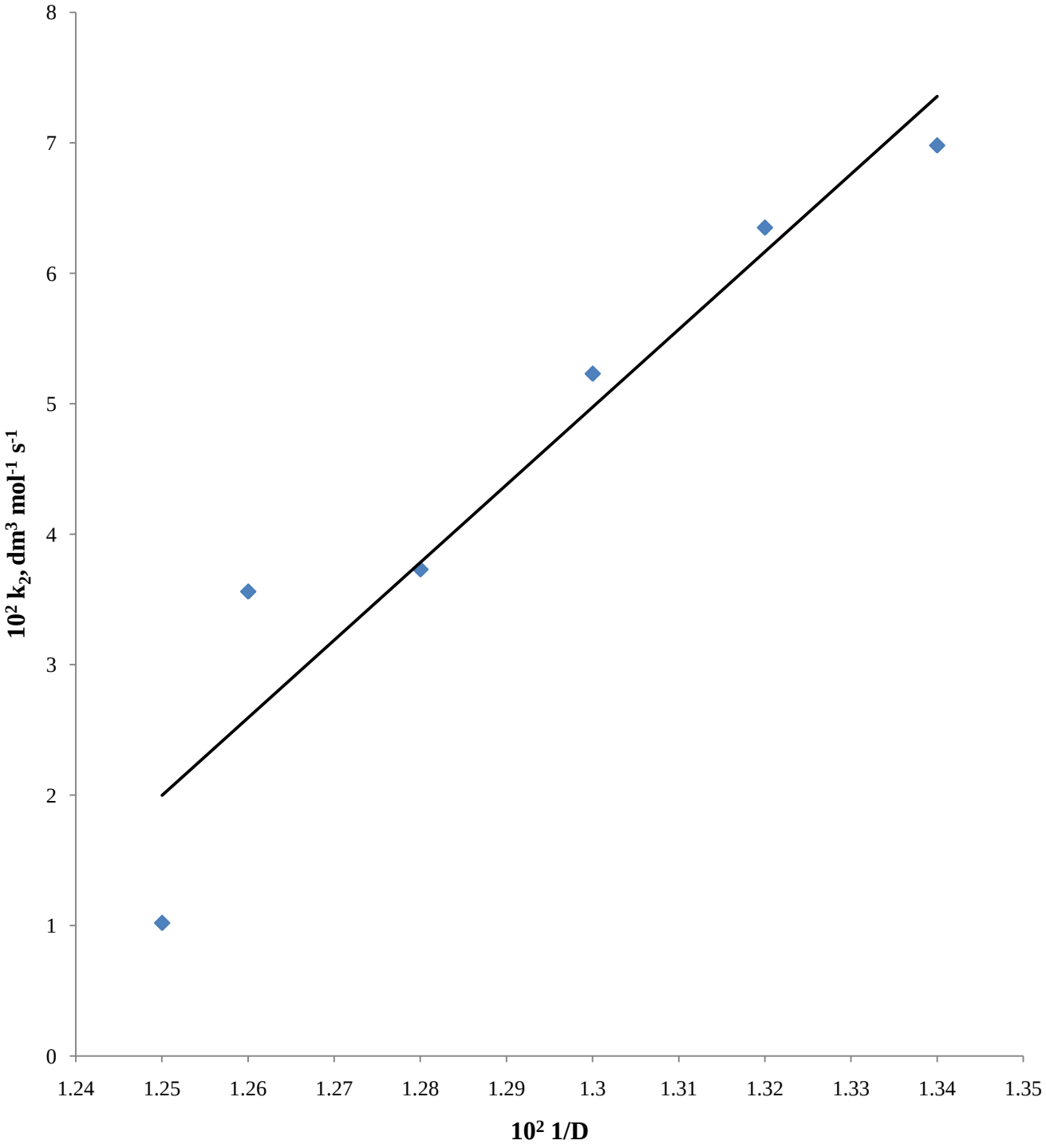

Figure 4.25: Plot of k_2 versus 1/D for the redox reaction of $[Co(EDTA)]^-$ with H_2A at $[Co^{3+}]$ = 3.0 × 10^{-3} mol dm^{-3}, $[H_2A]$ = 0.21 mol dm^{-3}, I = 0.40 mol dm^{-3} (Na_2SO_4) and T= 299 ± 1 K

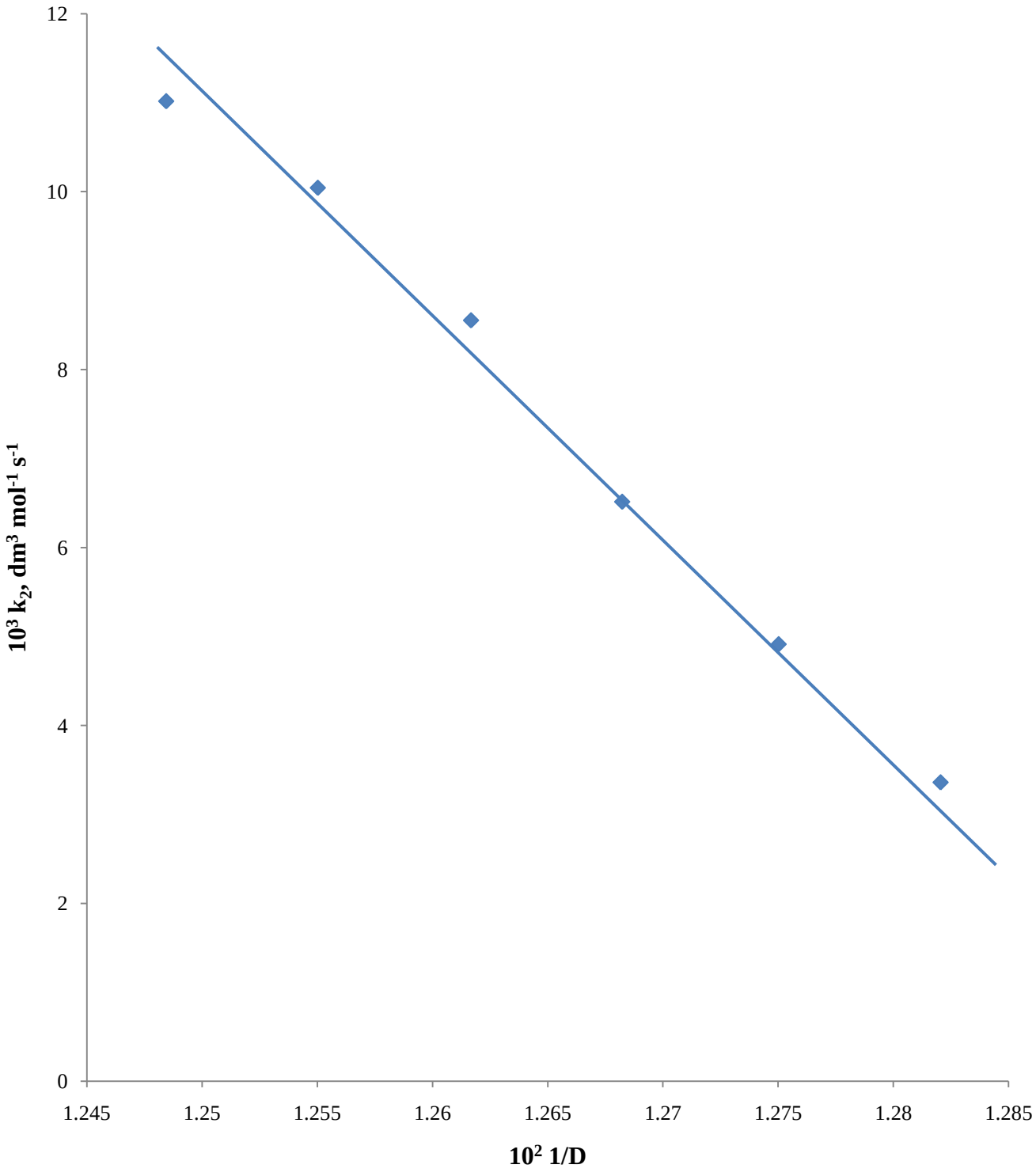

Figure 4.26: Plot of k_2 versus 1/D for the redox reaction of $[Co(EDTA)]^-$ with N_2H_4, at $[Co^{3+}]$ = 3.0 × 10^{-3} mol dm^{-3}, $[N_2H_4]$ = 0.18 mol dm^{-3}, I = 0.45 mol dm^{-3} (Na_2SO_4) and T= 298 ± 1 K

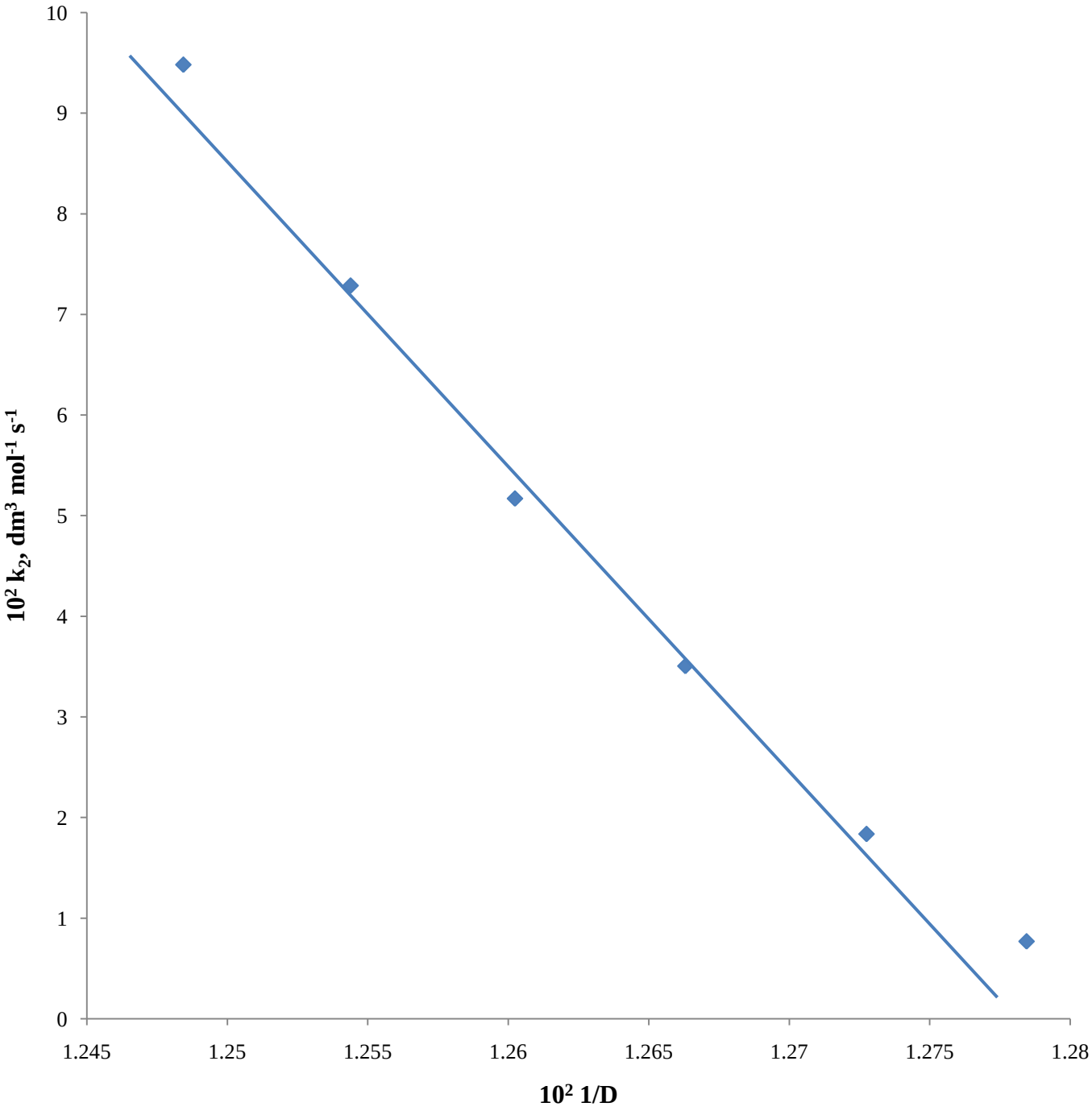

Figure 4.27: Plot of k_2 versus 1/D for the redox reaction of $[Co(HEDTA)OH_2]$ with N_2H_4, at $[Co^{3+}]$ = 6.0 × 10^{-3} mol dm^{-3}, $[N_2H_4]$ = 0.12 mol dm^{-3}, I = 0.5 mol dm^{-3} ($NaClO_4$) and T= 298 ± 1 K

Table 4.8: Pseudo – first order and second order rate constants for the effect of added ions on the reduction of $[Co(EDTA)]^-$ by H_2A in aqueous H_2SO_4 medium at $[Co^{3+}] = 3.0 \times 10^{-3}$ mol dm^{-3}, $[H_2A] = 0.21$ mol dm^{-3}, $[H^+] = 1.0 \times 10^{-3}$mol dm^{-3}, $[Cu^{2+}] = 5.0 \times 10^{-3}$ mol dm^{-3}, I = 0.4 mol dm^{-3} (Na_2SO_4), λ_{max} = 535 nm and T = 299 ± 1K

X, mol dm^{-3}	$10^4 k_{obs}$, s^{-1}	$10^3 k_2$, dm^{3}mol^{-1}s^{-1}
$10^2[HCOO^-]$		
0.5	7.9	5.4
2.5	5.1	3.5
3.5	3.9	2.7
5.0	2.2	1.5
6.0	1.3	0.9
7.5	0.7	0.5
$10^2[CH_3COO^-]$		
0.5	31.8	21.7
2.5	23.0	15.7
5.0	21.7	14.8
7.5	16.6	11.3
8.5	12.6	8.6
10.0	8.5	5.8
$10^2[Li^+]$		
0.5	7.6	5.2
1.5	8.8	6.0
2.5	9.9	6.8
3.5	18.0	12.3
5.0	22.3	15.2

7.5	31.3	21.3
8.5	35.3	24.1
$10^2[Zn^{2+}]$		
0.5	8.8	6.0
1.5	19.5	13.3
2.5	28.3	19.3
3.5	33.9	23.1
5.0	40.3	27.5
7.5	53.1	36.2
8.5	58.0	39.5

Table 4.9: Pseudo – first order and second order rate constants for the effect of added ions on the reduction of $[Co(EDTA)]^-$ by N_2H_4 in aqueous $HClO_4$ medium at $[Co^{3+}] = 3.0 \times 10^{-3}$ mol dm^{-3}, $[N_2H_4] = 0.18$ mol dm^{-3}, $[H^+] = 1.0 \times 10^{-3}$ mol dm^{-3}, $[Cu^{2+}] = 6.0 \times 10^{-4}$ mol dm^{-3}, I = 0.45 mol dm^{-3} ($NaClO_4$), λ_{max} = 535 nm and T = 298 ± 1K

X, mol dm^{-3}	$10^3 k_{obs}$, s^{-1}	$10^2 k_2$, dm^3 mol^{-1} s^{-1}
$10^2[CHOO^-]$		
0	2.97	1.10
0.50	2.98	1.10
1.00	3.06	1.14
1.50	2.83	1.05
2.00	3.01	1.12
2.50	2.86	1.06
$10^2[CH_3COO^-]$		

0	2.97	1.10
0.50	3.08	1.15
1.00	2.96	1.10
1.50	2.93	1.09
2.00	2.94	1.09
2.50	3.00	1.12
$10^2[K^+]$		
0	2.86	1.06
0.50	2.91	1.08
1.00	2.91	1.08
1.50	2.88	1.07
2.00	2.79	1.04
2.50	2.80	1.04

Table 4.10: Pseudo – first order and second order rate constants for the effect of added ions on the reduction of [Co(HEDTA)OH_2] by H_2A in aqueous $HClO_4$ medium at $[Co^{3+}] = 6.0 \times 10^{-3}$ mol dm^{-3}, $[H_2A] = 0.12$ mol dm^{-3}, $[H^+] = 2.0 \times 10^{-3}$ mol dm^{-3}, $[Cu^{2+}] = 7.0 \times 10^{-3}$ mol dm^{-3}, I = 0.9 mol dm^{-3} ($NaClO_4$), λ_{max} = 550 nm and T = 299 ± 1K

X, mol dm^{-3}	$10^2 k_{obs}$, s^{-1}	$10^2 k_{3/2}$, $dm^{3/2} mol^{-1/2} s^{-1/2}$
$10^2[HCOO^-]$		
1.50	0.87	2.52
3.00	1.49	4.31
4.50	1.79	5.18
6.00	2.20	6.36
7.50	2.84	8.20
9.00	3.28	9.46
10.00	3.77	10.89
$10^2[CH_3COO^-]$		
1.50	1.20	3.48
3.00	2.09	6.04
4.50	3.35	9.68
6.00	4.49	12.96
7.50	5.34	15.41
9.00	6.21	17.94
10.00	7.30	21.08
$10^2[K^+]$		
0.50	4.24	12.25
1.00	4.01	11.56
1.50	3.75	10.81
2.00	3.29	9.50
2.50	3.11	8.98
3.00	2.71	7.81

3.50	2.32	6.71

Table 4.11: Pseudo – first order and second order rate constants for the effect of added ions on the reduction of [Co(HEDTA)OH_2] by N_2H_4 in aqueous $HClO_4$ medium at [Co^{3+}] = 6.0 × 10^{-3} mol dm^{-3}, [N_2H_4] = 0.12 mol dm^{-3}, [H^+] = 4.0 × 10^{-3} mol dm^{-3}, [Cu^{2+}] = 5.0 × 10^{-4} mol dm^{-3}, I = 0.5 mol dm^{-3} ($NaClO_4$), λ_{max} = 550 nm and T = 298 ± 1K

X, mol dm^{-3}	10^3 k_{obs}, s^{-1}	10^2 k_2, dm^3 mol^{-1} s^{-1}
$10^2[CHOO^-]$		
0	11.38	9.48
0.50	15.83	13.19
1.00	24.08	20.07
1.50	35.40	29.50
2.00	41.04	34.20
$10^2[CH_3COO^-]$		
0	11.43	9.52
0.50	17.52	14.60
1.00	19.73	16.44
1.50	22.42	18.68
2.00	27.43	22.86
$10^2[K^+]$		

0	11.41	9.51
0.50	9.44	7.86
1.00	7.20	6.00
1.50	5.37	4.47
2.00	4.29	3.57

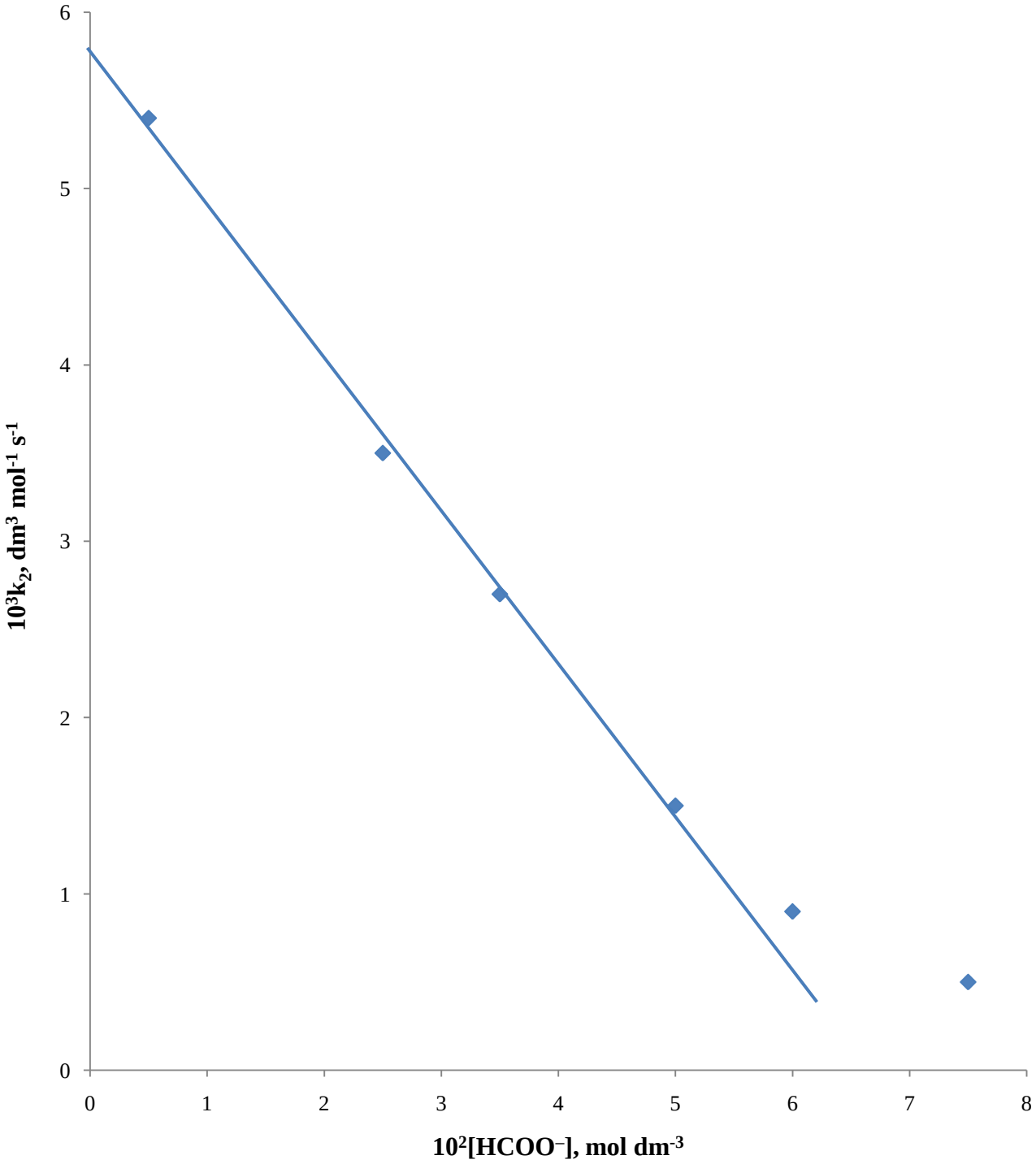

Figure 4.28: Plot of k_2 versus [HCOO$^-$] for the redox reaction of [Co(EDTA)]$^-$ with H_2A, at [Co^{3+}] = 3.0 × 10^{-3} mol dm^{-3}, [H_2A] = 0.21 mol dm^{-3}, [Cu^{2+}] = 5.0 × 10^{-3} mol dm^{-3} I = 0.40 mol dm^{-3} (Na_2SO_4) and T= 299 ± 1 K

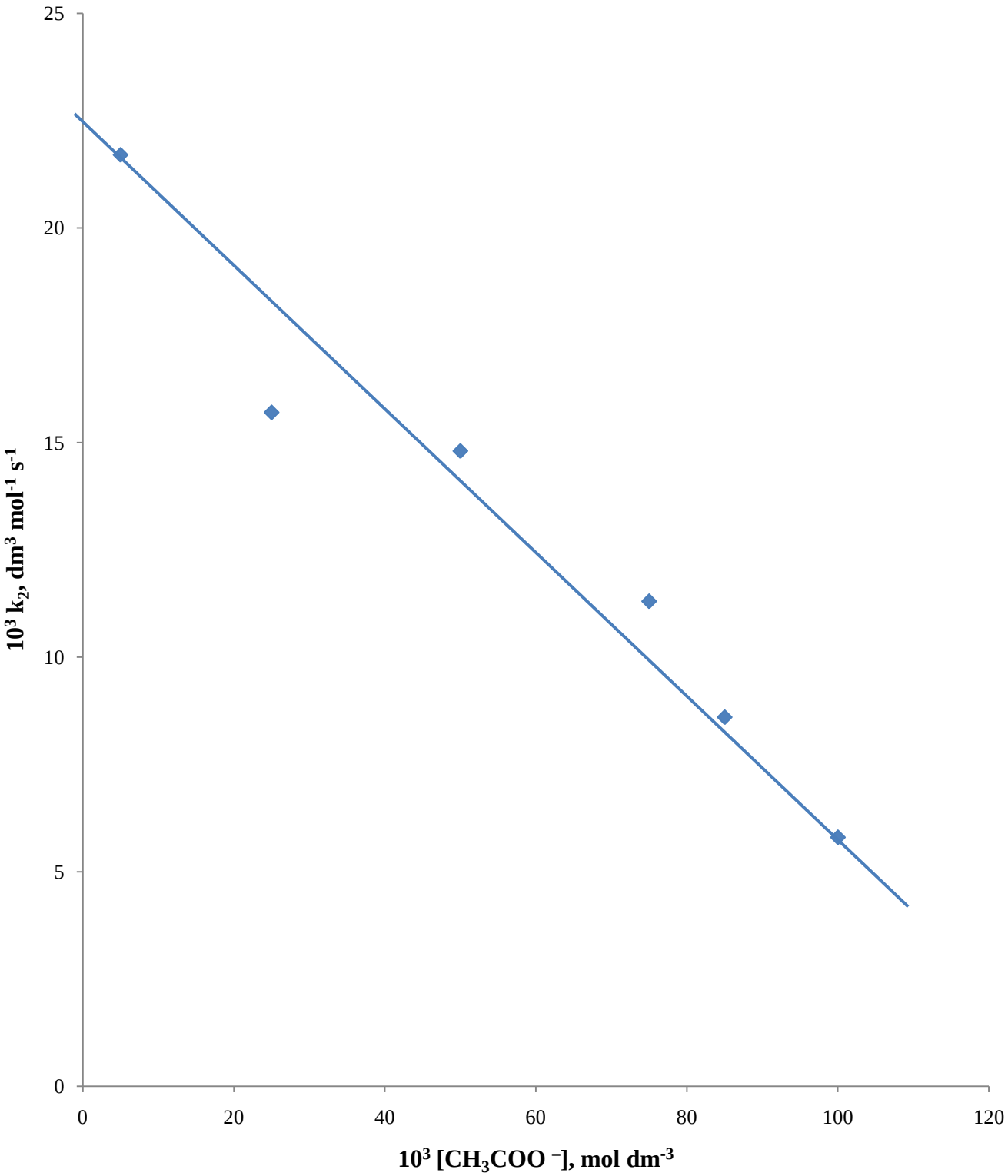

Figure 4.29: **Plot of k_2 versus $[CH_3COO^-]$ for the redox reaction of $[Co(EDTA)]^-$ with H_2A, at $[Co^{3+}] = 3.0 \times 10^{-3}$ mol dm^{-3}, $[H_2A] = 0.21$ mol dm^{-3}, $[Cu^{2+}] = 5.0 \times 10^{-3}$ mol dm^{-3}, I = 0.40 mol dm^{-3} (Na_2SO_4) and T= 299 ± 1 K**

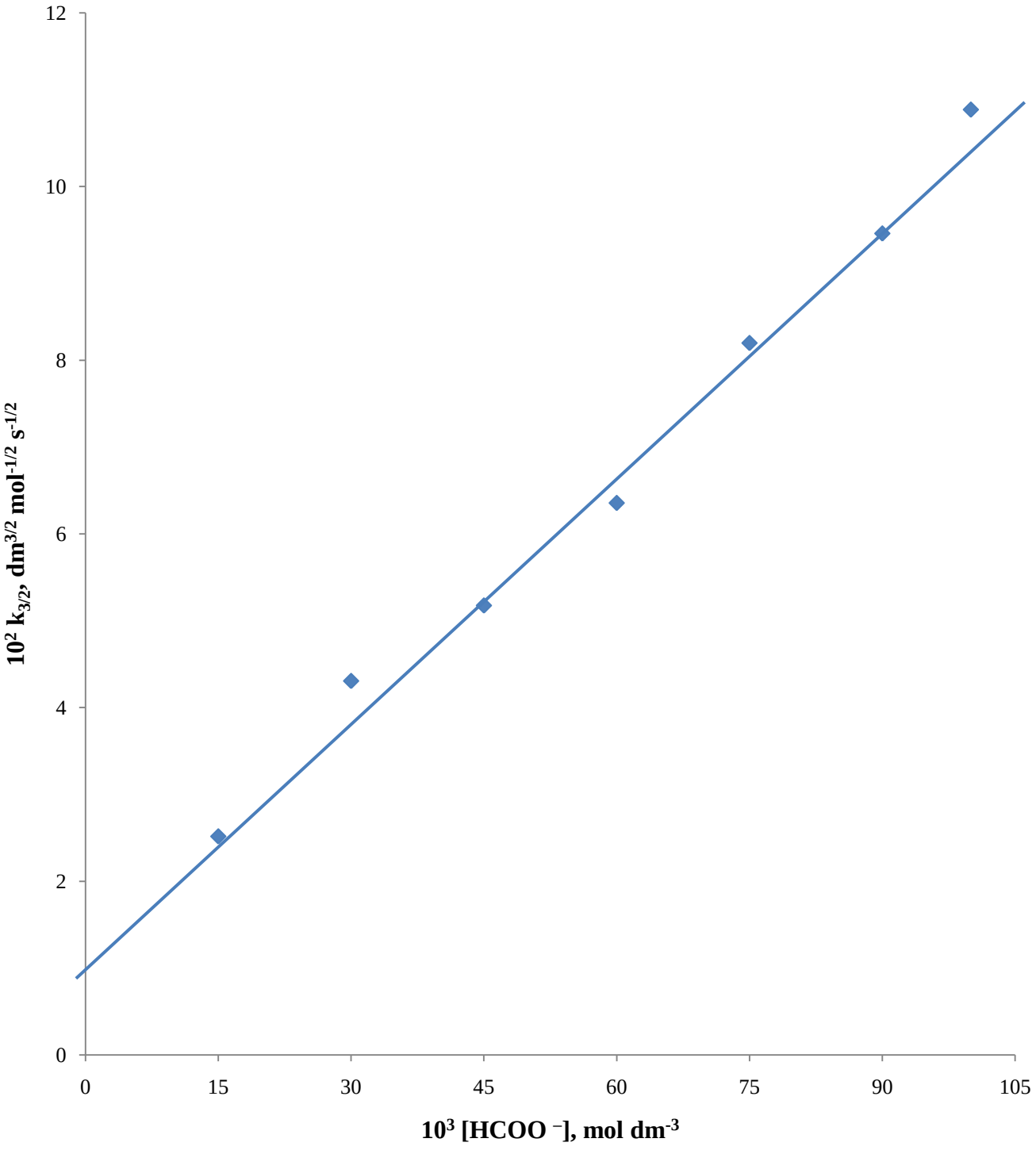

Figure 4.30: Plot of $k_{3/2}$ versus $[HCOO^-]$ for the redox reaction of $[Co(HEDTA)OH_2]$ with H_2A, at $[Co^{3+}] = 6.0 \times 10^{-3}$ mol dm^{-3}, $[H_2A] = 0.12$ mol dm^{-3}, $[Cu^{2+}] = 7.0 \times 10^{-3}$ mol dm^{-3}, I = 0.9 mol dm^{-3} ($NaClO_4$) and T= 299 ± 1 K

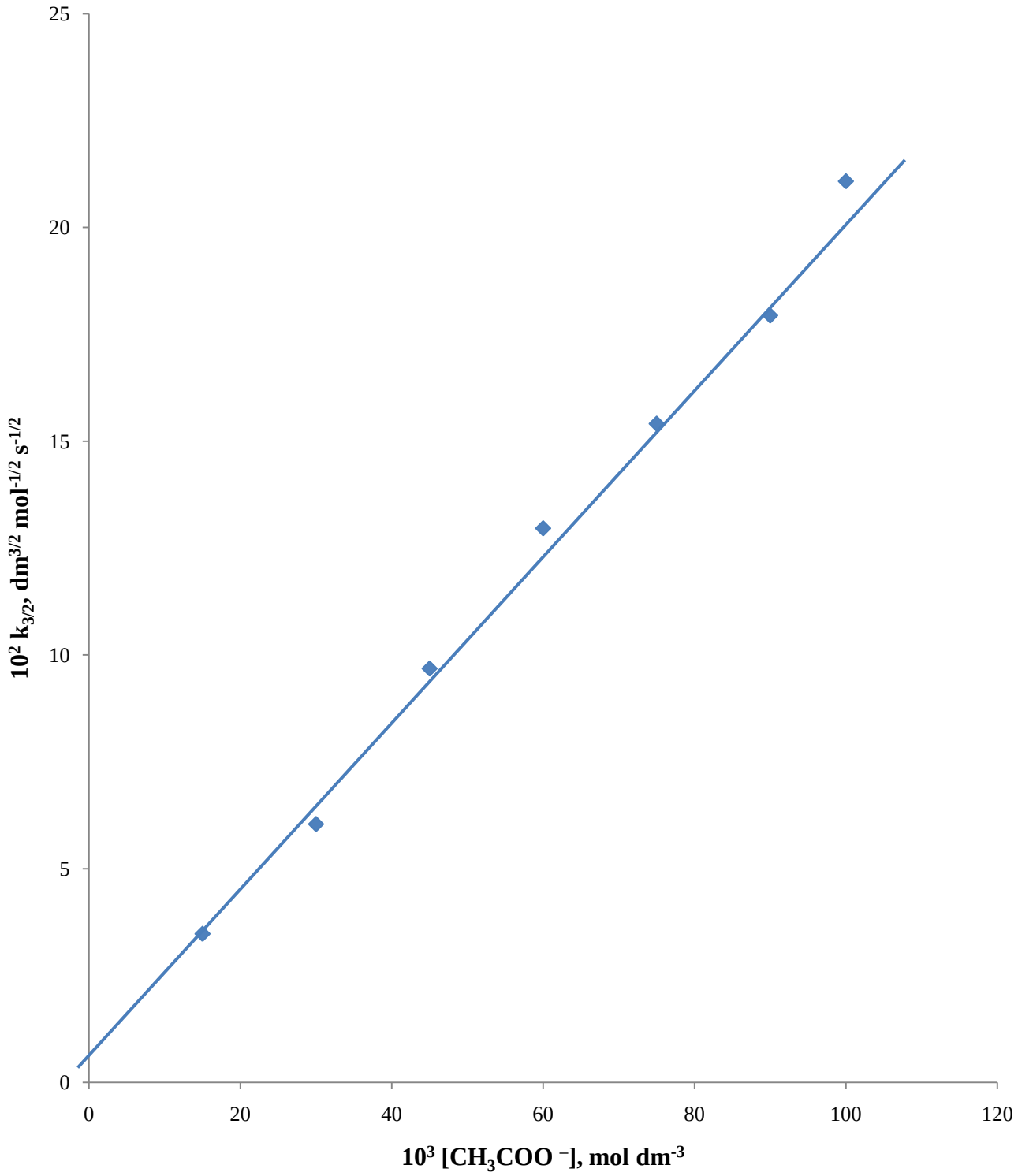

Figure 4.31: Plot of $k_{3/2}$ versus $[CH_3COO^-]$ for the redox reaction of $[Co(HEDTA)OH_2]$ with H_2A, at $[Co^{3+}] = 6.0 \times 10^{-3}$ mol dm^{-3}, $[H_2A] = 0.12$ mol dm^{-3}, $[Cu^{2+}] = 7.0 \times 10^{-3}$ mol dm^{-3}, I = 0.9 mol dm^{-3} ($NaClO_4$) and T= 299 ± 1 K

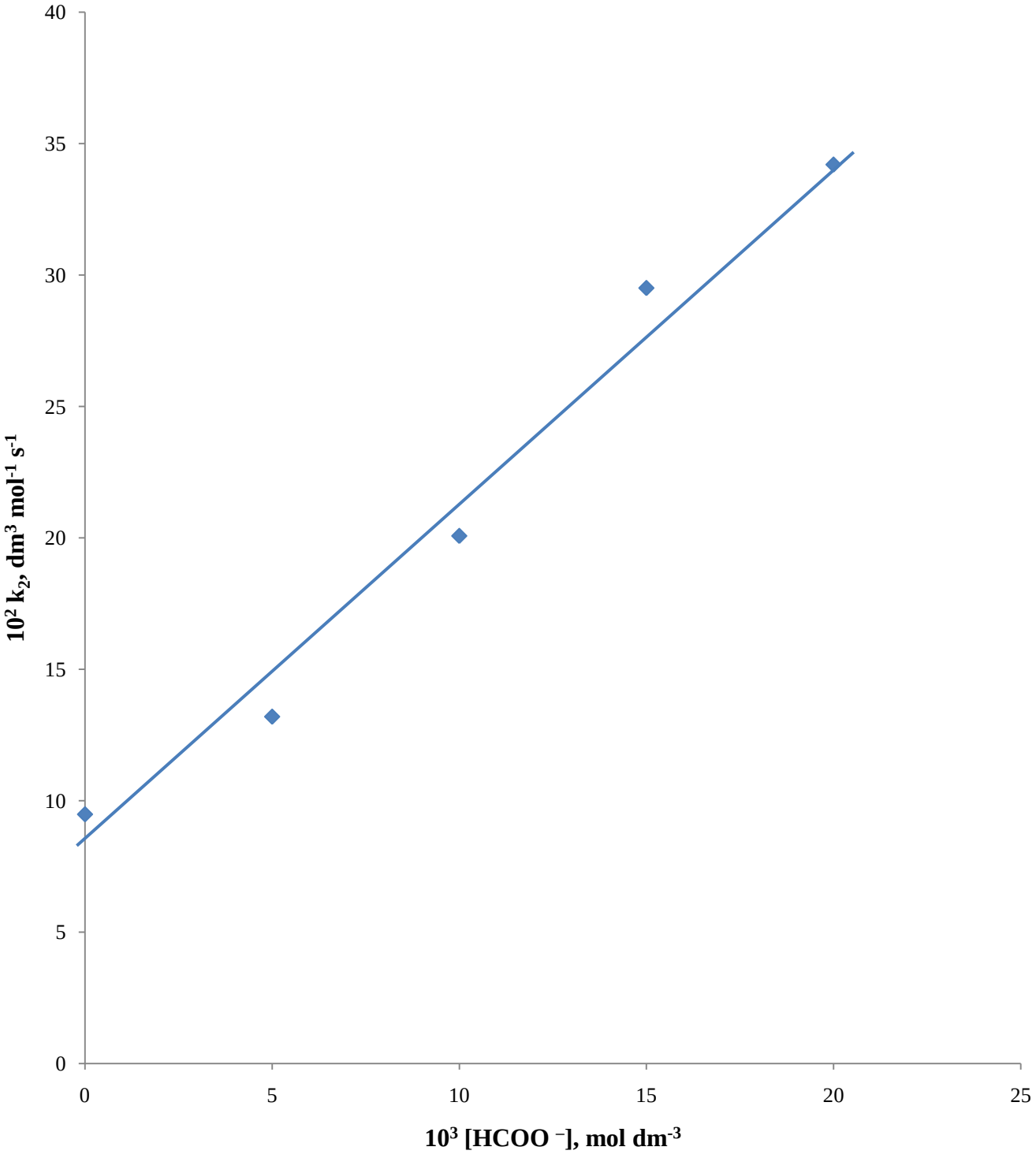

Figure 4.32: Plot of k_2 versus $[HCOO^-]$ for the redox reaction of $[Co(HEDTA)OH_2]$ with N_2H_4, at $[Co^{3+}] = 6.0 \times 10^{-3}$ mol dm^{-3}, $[N_2H_4] = 0.12$ mol dm^{-3}, $[Cu^{2+}] = 5.0 \times 10^{-4}$ mol dm^{-3}, I = 0.5 mol dm^{-3} ($NaClO_4$) and T= 298 ± 1 K

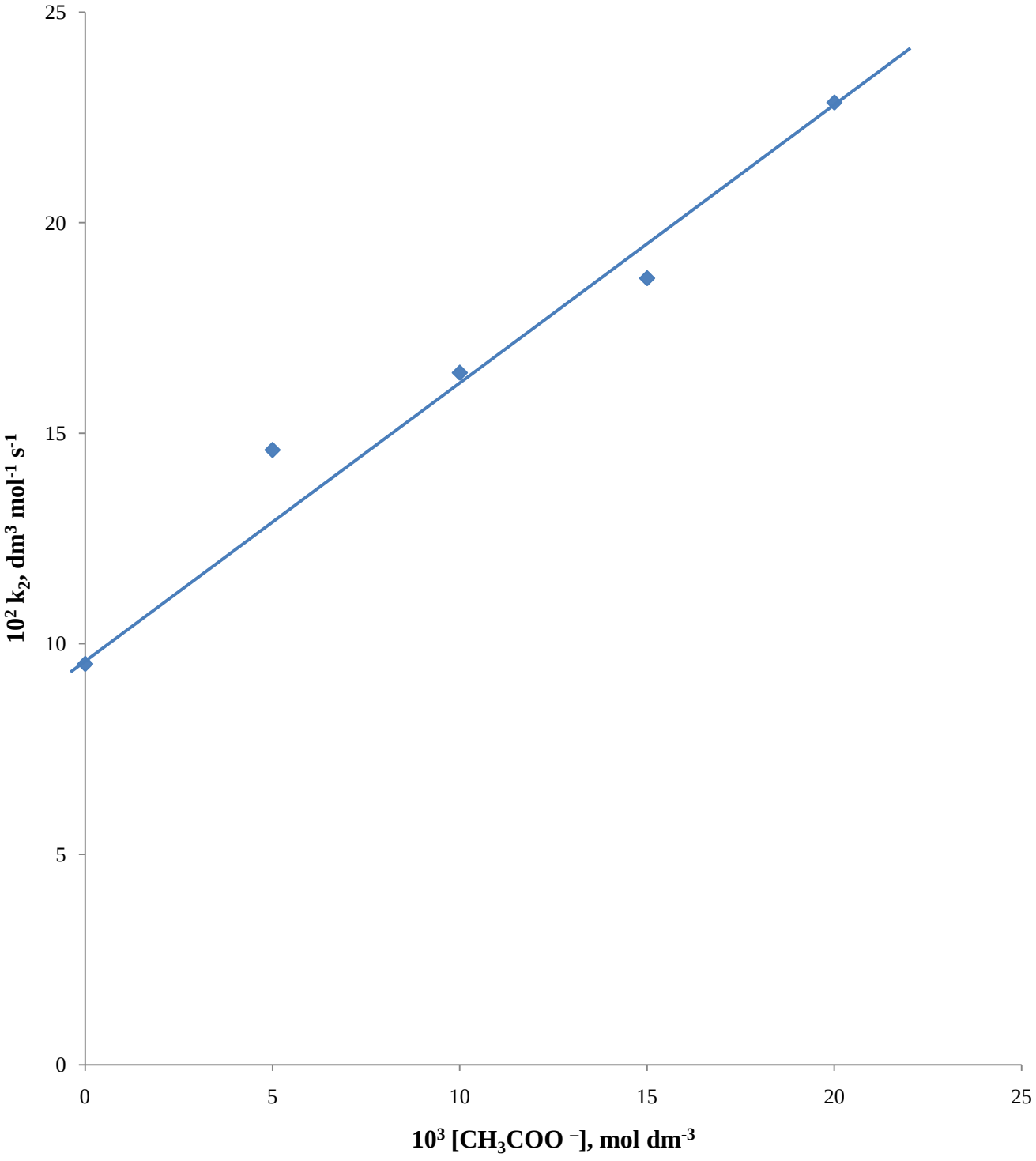

Figure 4.33: Plot of k_2 versus [CH_3COO^-] for the redox reaction of [Co(HEDTA)OH_2] with N_2H_4, at [Co^{3+}] = 6.0 × 10^{-3} mol dm^{-3}, [N_2H_4] = 0.12 mol dm^{-3}, [Cu^{2+}] = 5.0 × 10^{-4} mol dm^{-3}, I = 0.5 mol dm^{-3} ($NaClO_4$) and T= 298 ± 1 K

4.8 Effect of Added Cations on the Rate of the Reaction

Li^+ and Zn^{2+} were used to carry out the investigation of the parametre for $[Co(EDTA)]^-$ – H_2A system, an increase in the concentration of both cations led to increase in the reaction rate (Table 4.8). K^+ was used for $[Co(EDTA)]^-$ – N_2H_4, $[Co(HEDTA)OH_2]$ – H_2A and $[Co(HEDTA)OH_2]$ – N_2H_4 systems. Increase in the $[K^+]$ had no effect on the rate for the $[Co(EDTA)]^-$ – N_2H_4 system (Table 4.9), while a marked decrease in the rates of the reactions for both $[Co(HEDTA)OH_2]$ – H_2A (Table 4.10) and $[Co(HEDTA)OH_2]$ – N_2H_4 (Table 4.11) systems were observed. The plots of the cation – dependent rate constants versus the cation concentrations were linear and are contained in Figures 4.34 – 4.37.

4.9 Effect of Change in Temperature on the Rate of Reaction

The results obtained for the effect of the change in temperature on the reaction rate showed an increase in the rate of the reaction as the temperature rises for all the four (4) systems. These results are contained in Tables 4.12 – 4.15.

Figures 4.38 – 4.41 show plots of $ln\ k/T$ versus *1/T*, which are linear, with $-\Delta H^{\ddagger}/R$ and $ln(k_b/h) + \Delta S^{\ddagger}/R$ as the gradient and intercept respectively. The slope of 8750 with an intercept of 18.51 was recorded for the $[Co(EDTA)]^-$ – H_2A system, a slope of –3783.88 and an intercept of 2.98 for the $[Co(EDTA)]^-$ – N_2H_4 system, a slope of 10248.5 with an intercept of 24.604 for the $[Co(HEDTA)OH_2]$ – H_2A system and a slope of –9961.76 and an intercept of 25.80 for the $[Co(HEDTA)OH_2]$ – N_2H_4 system respectively.

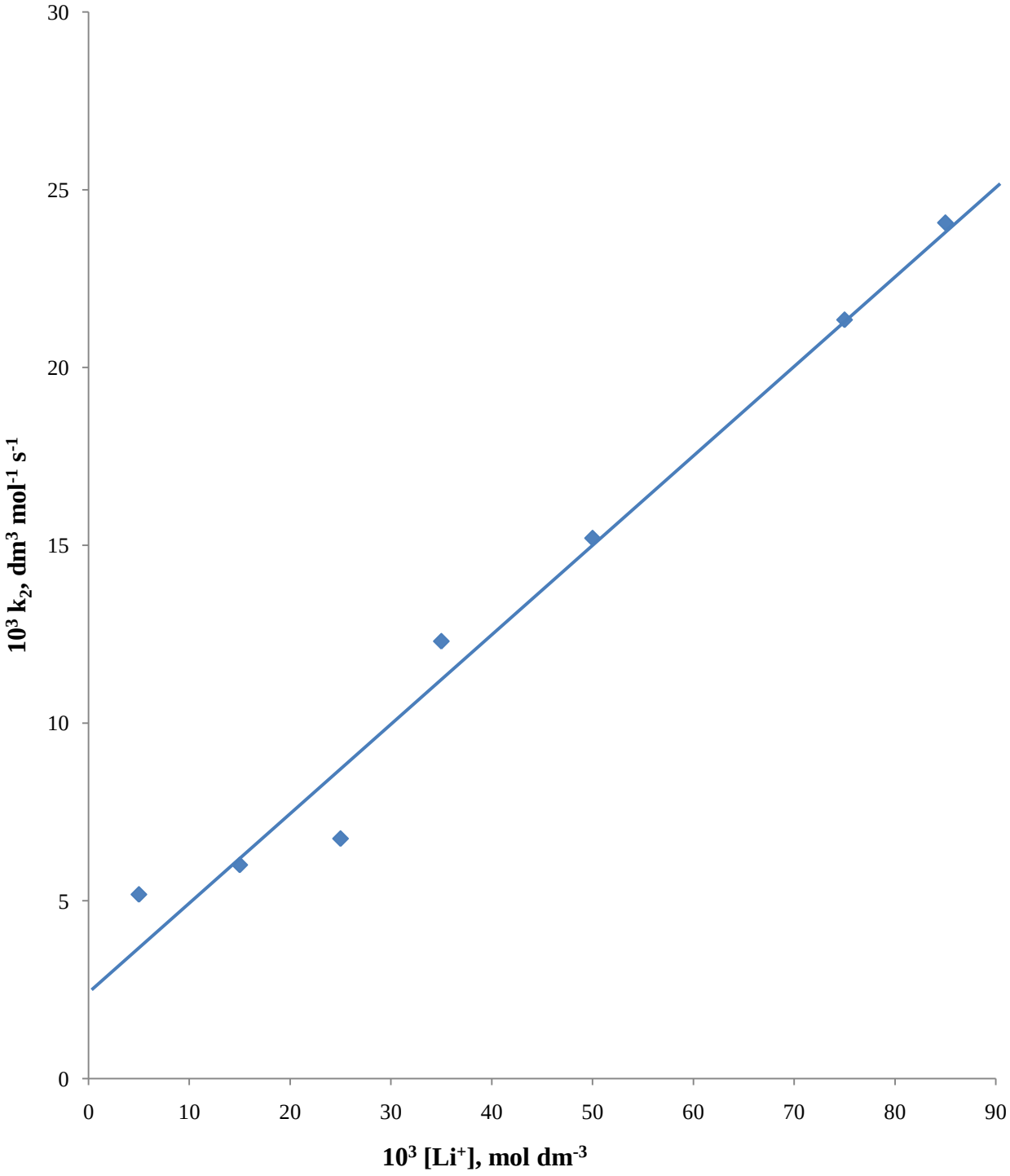

Figure 4.34: **Plot of k_2 versus $[Li^+]$ for the redox reaction of $[Co(EDTA)]^-$ with H_2A, at $[Co^{3+}] = 3.0 \times 10^{-3}$ mol dm^{-3}, $[H_2A] = 0.21$ mol dm^{-3}, $[Cu^{2+}] = 5.0 \times 10^{-3}$ mol dm^{-3}, I = 0.40 mol dm^{-3} (Na_2SO_4) and T= 299 ± 1 K**

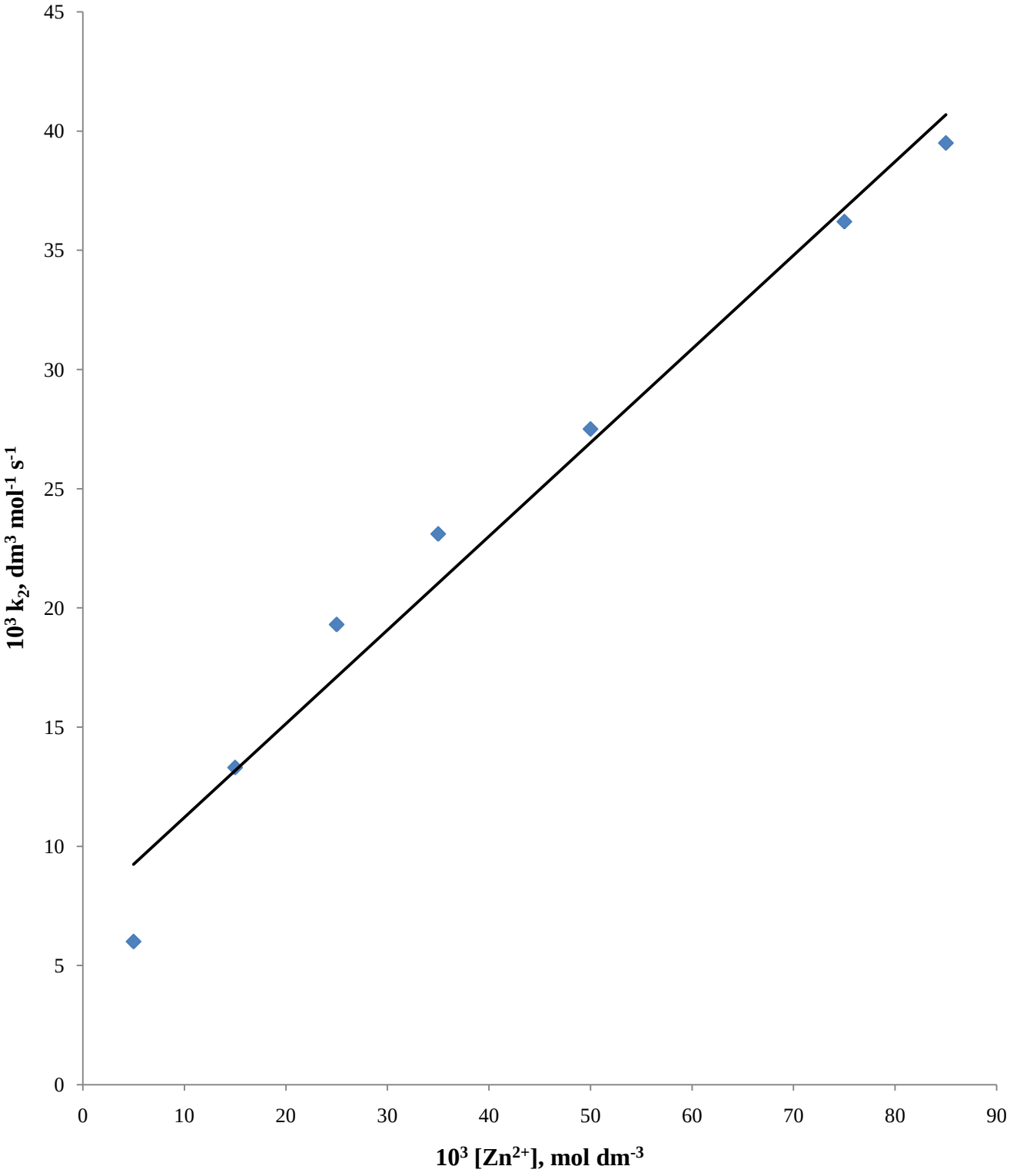

Figure 4.35: Plot of k_2 versus $[Zn^{2+}]$ for the redox reaction of $[Co(EDTA)]^-$ with H_2A, at $[Co^{3+}] = 3.0 \times 10^{-3}$ mol dm^{-3}, $[H_2A] = 0.21$ mol dm^{-3}, $[Cu^{2+}] = 5.0 \times 10^{-3}$ mol dm^{-3}, I = 0.40 mol dm^{-3} (Na_2SO_4) and T= 299 ± 1 K

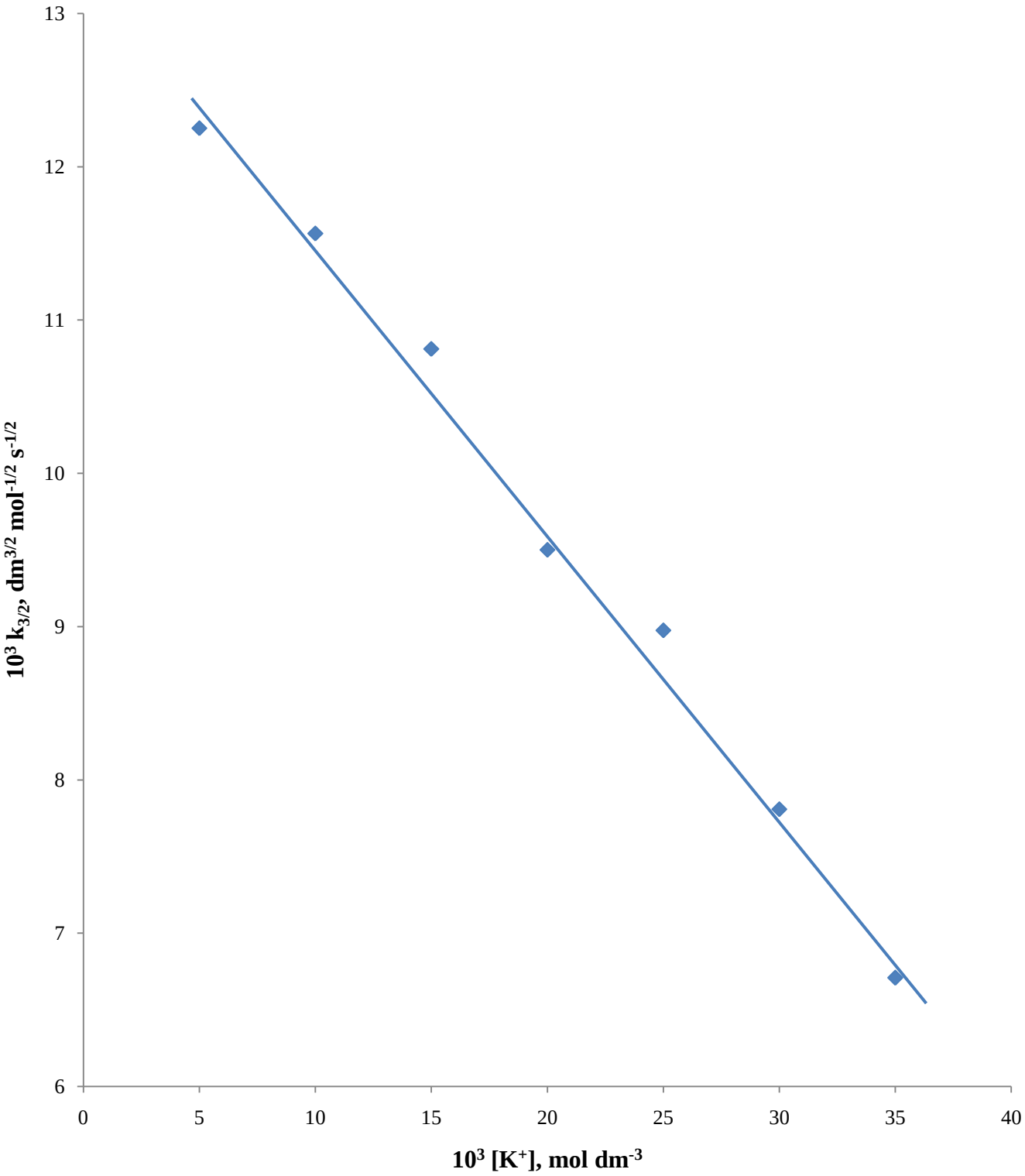

Figure 4.36: **Plot of $k_{3/2}$ versus $[K^+]$ for the redox reaction of $[Co(HEDTA)OH_2]$ with H_2A, at $[Co^{3+}] = 6.0 \times 10^{-3}$ mol dm^{-3}, $[H_2A] = 0.12$ mol dm^{-3}, $[Cu^{2+}] = 7.0 \times 10^{-3}$ mol dm^{-3}, I = 0.9 mol dm^{-3} ($NaClO_4$) and T= 299 ± 1 K**

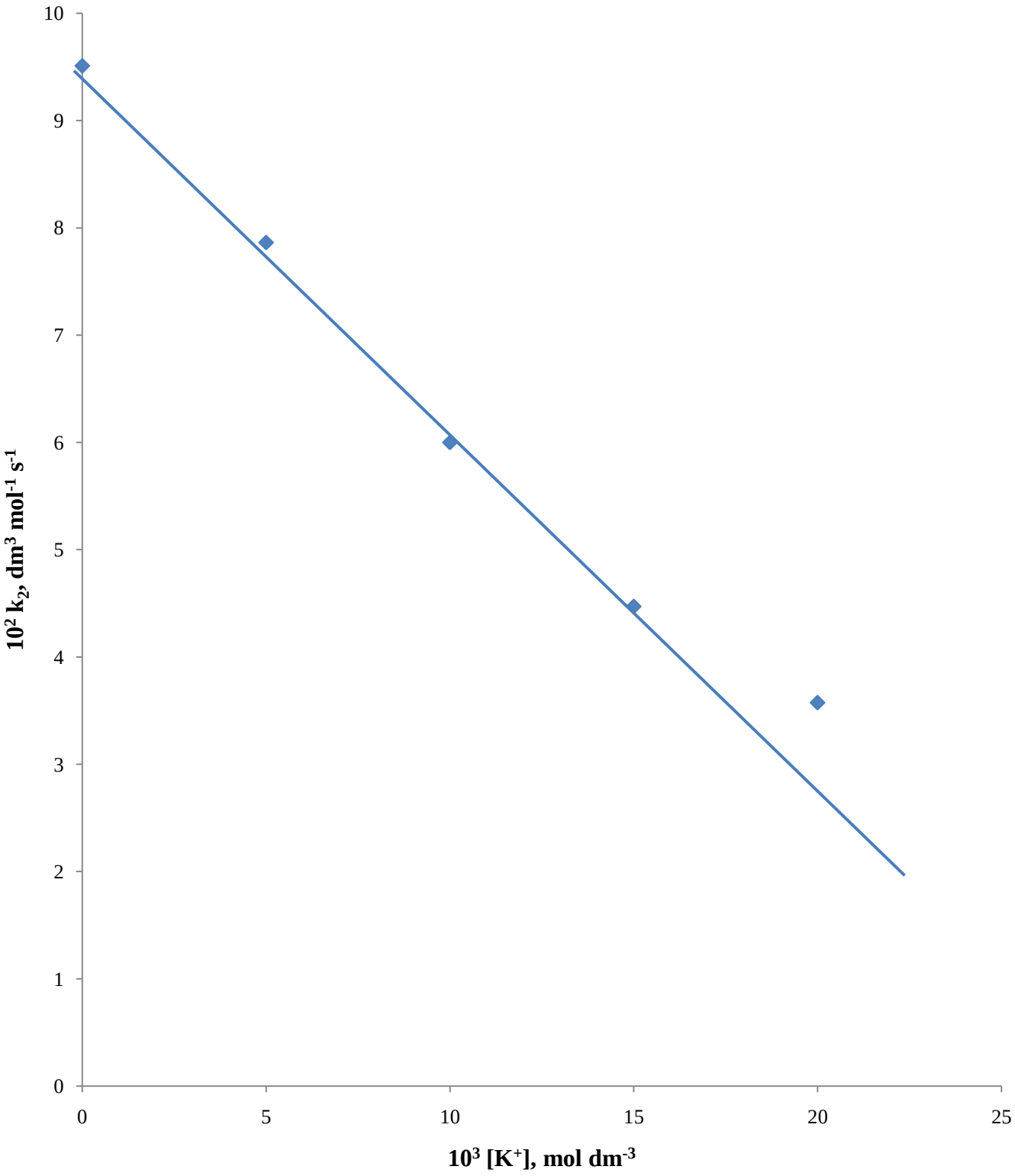

Figure 4.37: Plot of k_2 versus $[K^+]$ for the redox reaction of $[Co(HEDTA)OH_2]$ with N_2H_4, at $[Co^{3+}] = 6.0 \times 10^{-3}$ mol dm^{-3}, $[N_2H_4] = 0.12$ mol dm^{-3}, $[Cu^{2+}] = 5.0 \times 10^{-4}$ mol dm^{-3}, I = 0.5 mol dm^{-3} ($NaClO_4$) and T= 298 ± 1 K

Table 4.12: Pseudo – first order and second order rate constants for the effect of change in temperature on the reduction of $[Co(EDTA)]^-$ by H_2A at $[Co^{3+}] = 3.0 \times 10^{-3}$ mol dm^{-3} and $\lambda_{max} = 535$ nm

Temperature, K	$10[H_2A]$, mol dm^{-3}	$10^3[H^+]$, mol dm^{-3}	$10^3[Cu^{2+}]$, mol dm^{-3}	$10[I]$, mol dm^{-3}	$10^3\ k_{obs}$, s^{-1}	$10^2 k_2$, $dm^3mol^{-1}s^1$
299	2.10	1.00	5.00	4.00	2.14	1.02
313	2.10	1.00	5.00	4.00	3.69	2.52
323	2.10	1.00	5.00	4.00	7.74	5.28
333	2.10	1.00	5.00	4.00	22.52	15.36

Table 4.13: Pseudo – first order and second order rate constants for the effect of change in temperature on the reduction of $[Co(EDTA)]^-$ by N_2H_4 at $[Co^{3+}] = 3.0 \times 10^{-3}$ mol dm^{-3} and $\lambda_{max} = 535$ nm

Temperature, K	$10[N_2H_4]$, mol dm^{-3}	$10^3[H^+]$, mol dm^{-3}	$10^4[Cu^{2+}]$, mol dm^{-3}	$10[I]$, mol dm^{-3}	$10^3\ k_{obs}$, s^{-1}	$10^2 k_2$, dm^{3}mol^{-1}s^1
293	2.40	1.00	6.00	4.50	3.31	0.99
298	2.40	1.00	6.00	4.50	3.75	1.12
303	2.40	1.00	6.00	4.50	5.67	1.69
313	2.40	1.00	6.00	4.50	8.06	2.40

Table 4.14: Pseudo – first order and second order rate constants for the effect of change in temperature on the reduction of [Co(HEDTA)OH_2] by H_2A, at [Co^{3+}] = 6.0×10^{-3} mol dm^{-3} and λ_{max} = 550 nm

Temperature, K	$10[H_2A]$, mol dm^{-3}	$10^3[H^+]$, mol dm^{-3}	$10^3[Cu^{2+}]$, mol dm^{-3}	$10[I]$, mol dm^{-3}	$10^2\ k_{obs}$, s^{-1}	$10^2 k_{3/2}$, $dm^{3/2}\ mol^{-1/2}\ s^{-1/2}$
299	0.12	2.00	7.00	2.00	0.49	1.40
303	0.12	2.00	7.00	2.00	1.03	2.97
313	0.12	2.00	7.00	2.00	3.23	9.33
323	0.12	2.00	7.00	2.00	8.91	25.72

Table 4.15: Pseudo-first order and second order rate constants for the effect of change in temperature on the reduction of $[Co(HEDTA)OH_2]$ with N_2H_4, at $[Co^{3+}] = 6.0 \times 10^{-3}$ mol dm^{-3} and $\lambda_{max} = 550$ nm

Temperature, K	$10[N_2H_4]$, mol dm^{-3}	$10^3[H^+]$, mol dm^{-3}	$10^4[Cu^{2+}]$, mol dm^{-3}	$10[I]$, mol dm^{-3}	$10^2\ k_{obs}$, s^{-1}	$10^2 k_2$, dm^3 mol^{-1}s^1
293	1.20	4.00	5.00	5.00	0.87	7.27
298	1.20	4.00	5.00	5.00	1.14	9.49
303	1.20	4.00	5.00	5.00	3.75	31.21
313	1.20	4.00	5.00	5.00	8.12	67.70

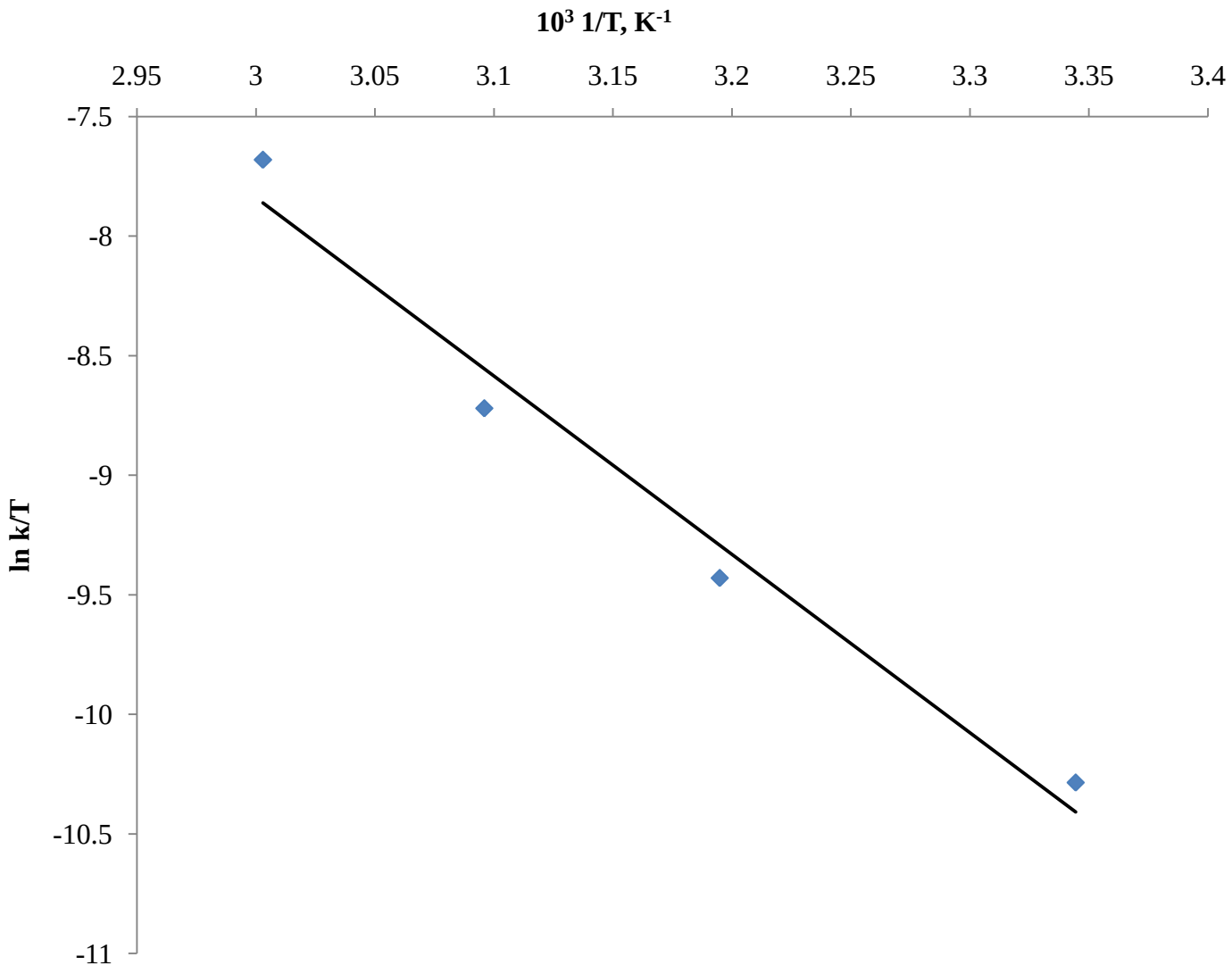

Figure 4.38: **Plot of ln $\left(\frac{k}{T}\right)$ versus $\frac{1}{T}$ for the redox reaction of $[Co(EDTA)]^-$ with H_2A, at $[Co^{3+}] = 3.0 \times 10^{-3}$ mol dm^{-3}, $[H_2A] = 0.21$ mol dm^{-3}, $[Cu^{2+}] = 5.0 \times 10^{-3}$ mol dm^{-3}, I = 0.40 mol dm^{-3} (Na_2SO_4)**

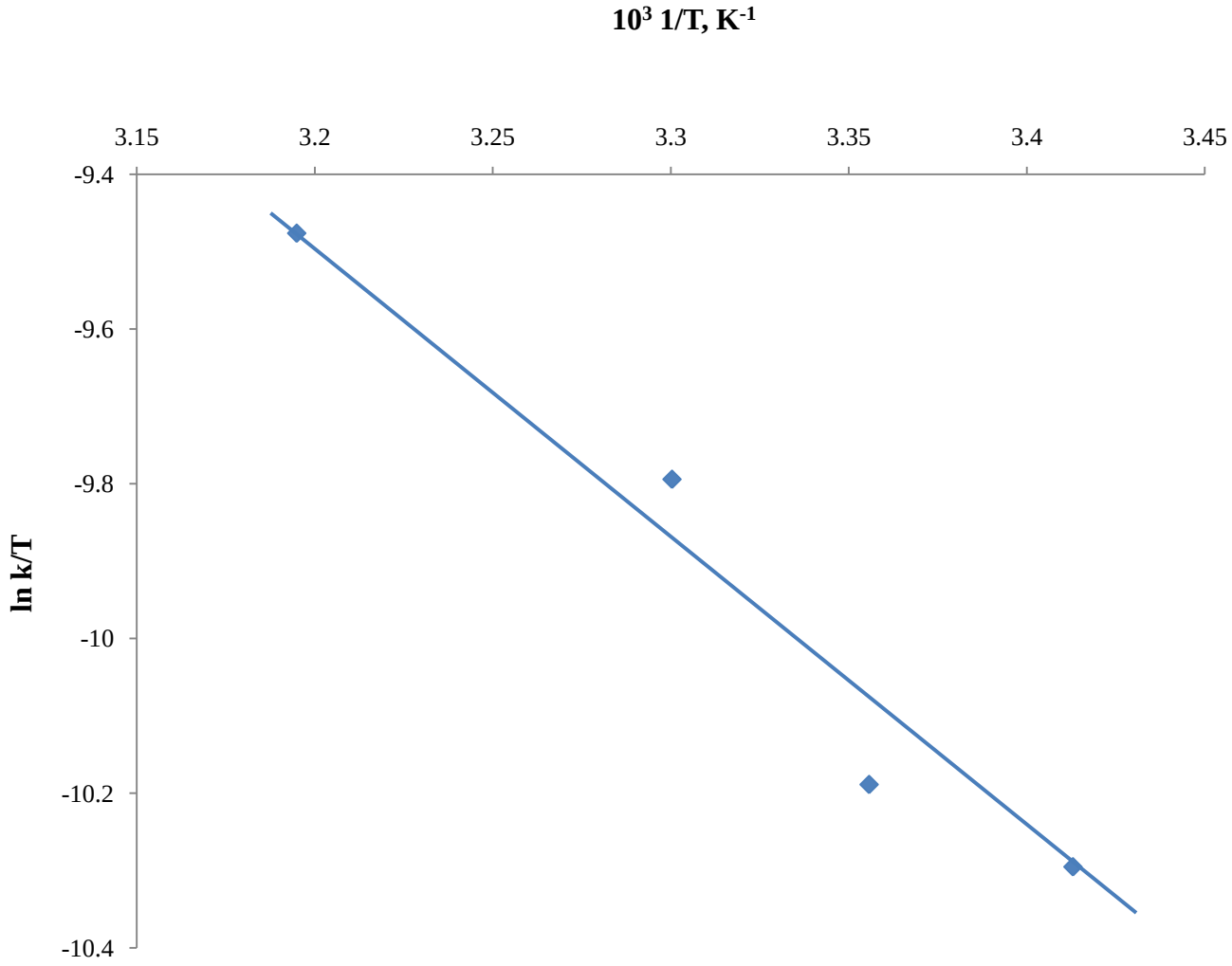

Figure 4.39: **Plot of ln $\left(\frac{k}{T}\right)$ versus $\frac{1}{T}$ for the redox reaction of $[Co(EDTA)]^-$ with N_2H_4, at $[Co^{3+}] = 3.0 \times 10^{-3}$ mol dm^{-3}, $[N_2H_4] = 0.24$ mol dm^{-3}, $[Cu^{2+}] = 6.0 \times 10^{-4}$ mol dm^{-3}, I = 0.45 mol dm^{-3} ($NaClO_4$)**

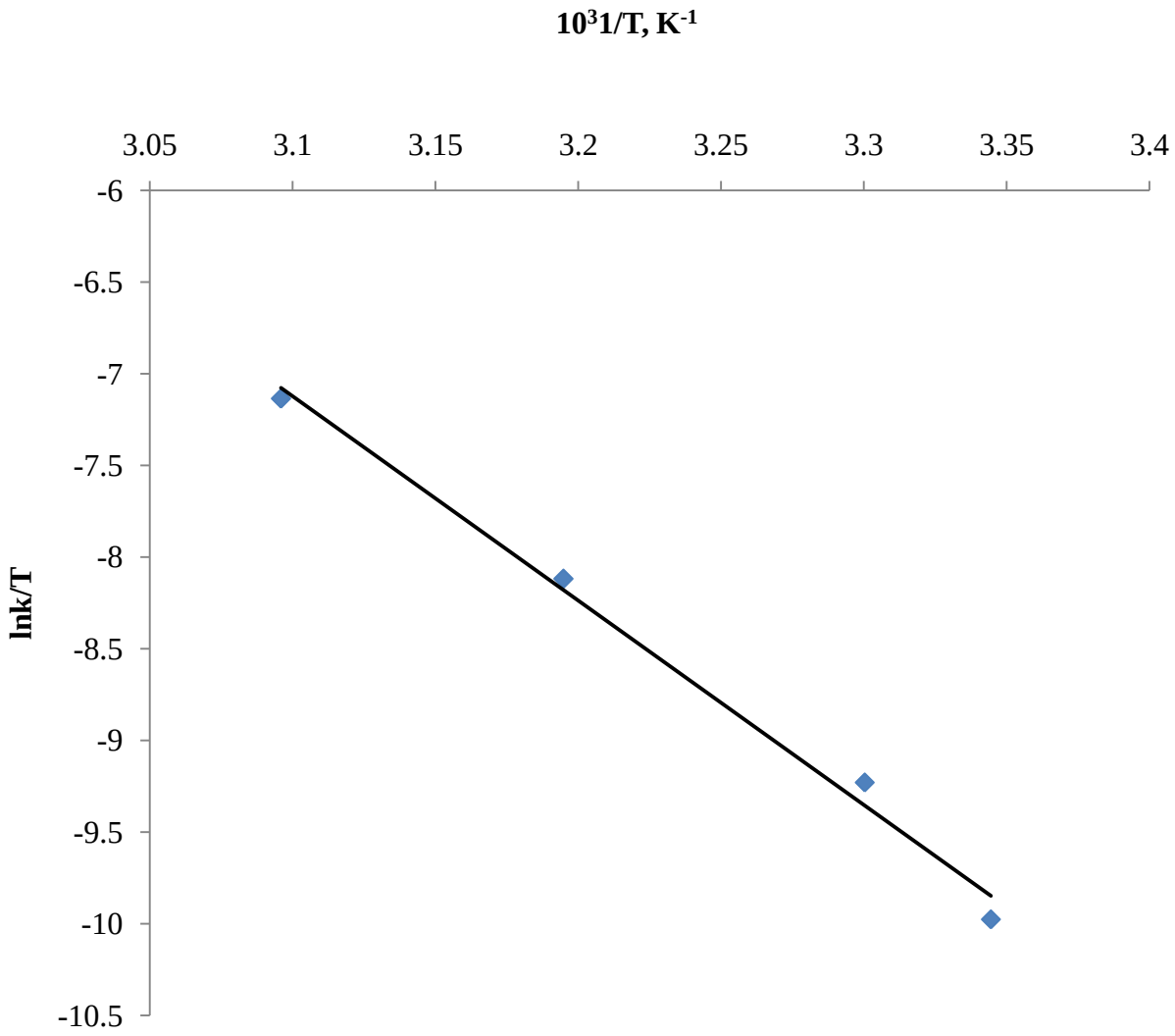

Figure 4.40: **Plot of ln $\left(\frac{k}{T}\right)$ versus $\frac{1}{T}$ for the redox reaction of [Co(HEDTA)OH_2] with H_2A, at [Co^{3+}] = 6.0 × 10^{-3} mol dm^{-3}, [H_2A] = 0.12 mol dm^{-3}, [Cu^{2+}] = 7.0 × 10^{-3} mol dm^{-3}, I = 0.2 mol dm^{-3} ($NaClO_4$)**

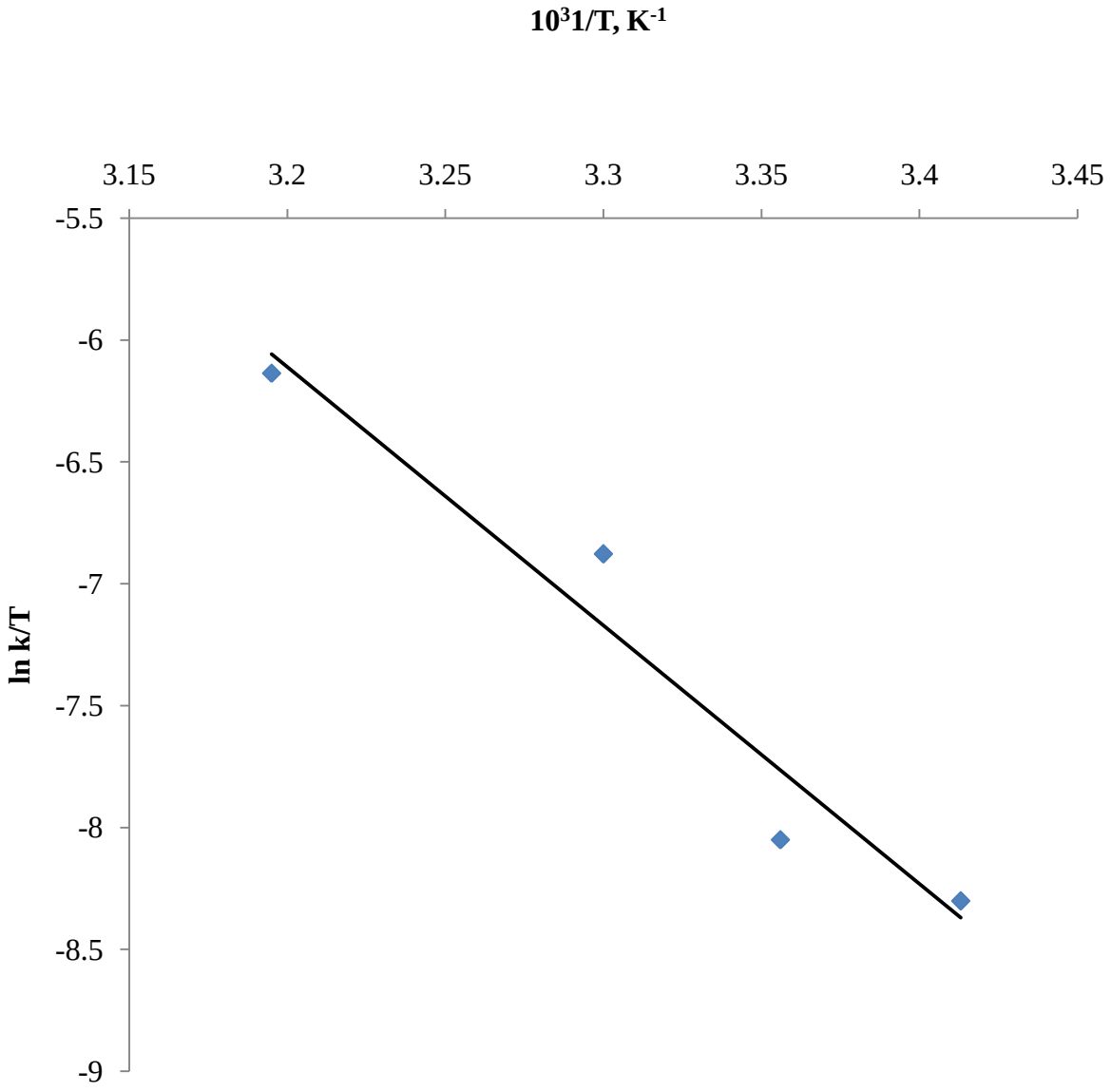

Figure 4.41: **Plot of ln $\left(\frac{k}{T}\right)$ versus $\frac{1}{T}$ for the redox reaction of [Co(HEDTA)OH_2] with N_2H_4, at [Co^{3+}] = 6.0 × 10^{-3} mol dm^{-3}, [N_2H_4] = 0.12 mol dm^{-3}, [Cu^{2+}] = 5.0 × 10^{-4} mol dm^{-3}, I = 0.5 mol dm^{-3} ($NaClO_4$)**

The activation enthalpies and entropies evaluated for the systems using the Eyring equation are presented below:

$[Co(EDTA)]^{-} - H_2A$: $\Delta H^{\ddagger} = 72.75$ kJ mol^{-1}. $\Delta S^{\ddagger} =$ □ 43.65 JK^{-1} mol^{-1}

$[Co(EDTA)]^{-} - N_2H_4$: $\Delta H^{\ddagger} = 31.46$ kJ mol^{-1}. $\Delta S^{\ddagger} = -175.58$ JK^{-1} mol^{-1}

$[Co(HEDTA)OH_2] - H_2A$: $\Delta H^{\ddagger} = 85.21$ kJ mol^{-1}. $\Delta S^{\ddagger} = 7.02$ JK^{-1} mol^{-1}

$[Co(HEDTA)OH_2] - N_2H_4$: $\Delta H^{\ddagger} = 82.89$ kJ mol^{-1}. $\Delta S^{\ddagger} = 17.13$ JK^{-1} mol^{-1}.

4.10 Test for Intermediate

4.10.1 Test for free radicals

On addition of acrylamide solution followed by excess methanol to the partially reduced reaction mixture, a gelatinous polymeric layer was formed for the $[Co(EDTA)]^{-} - H_2A$ system, indicating the presence of free radical. No precipitate was observed in the other three systems.

4.10.2 Michaelis – Menten plot

The Michaelis – Menten plot of $1/k_{obs}$ versus 1/[reductant] were all linear, with zero intercept for $[Co(EDTA)]^{-} - H_2A$ and $[Co(HEDTA)OH_2] - N_2H_4$ systems and non – zero intercept for $[Co(EDTA)]^{-} - N_2H_4$ and $[Co(HEDTA)OH_2] - H_2A$ systems (Figures 4.42 – 4.45).

4.10.3 Spectrophotometric test

From the results obtained from this test, there was an observed shift in the λ_{max} from 535 nm to 520 nm for the $[Co(EDTA)]^{-} - N_2H_4$ system (Figure 4.47), while no new peak or shift was observed for the rest of the three (3) systems (Figures 4.46, 4.48 – 4.49).

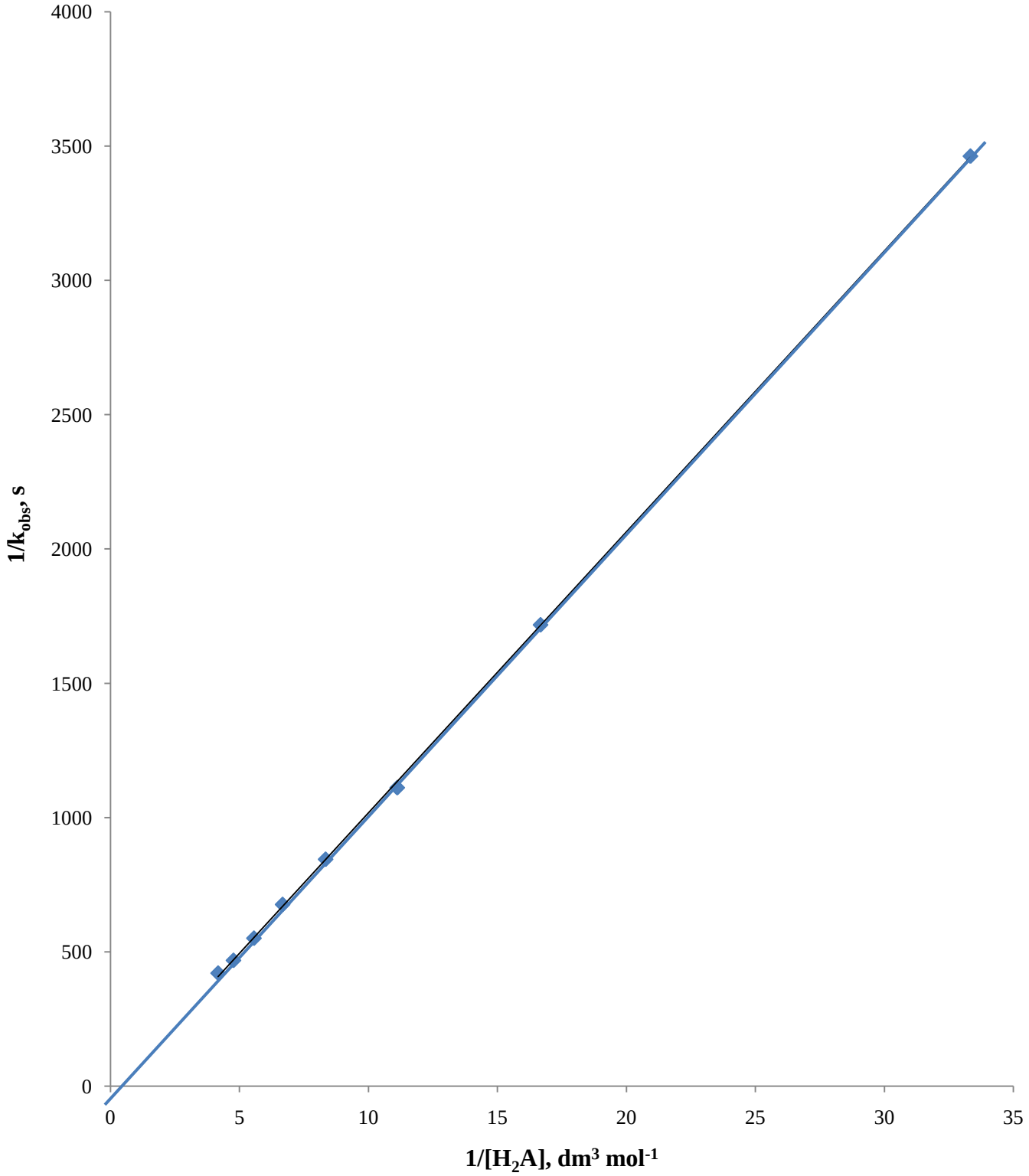

Figure 4.42: Michaelis – Menten plot of $1/k_{obs}$ versus $1/[H_2A]$ for the redox reaction of $[Co(EDTA)]^-$ with H_2A, at $[Co^{3+}] = 3.0 \times 10^{-3}$ mol dm^{-3}, $[Cu^{2+}] = 5.0 \times 10^{-3}$ mol dm^{-3}, I = 0.40 mol dm^{-3} (Na_2SO_4)

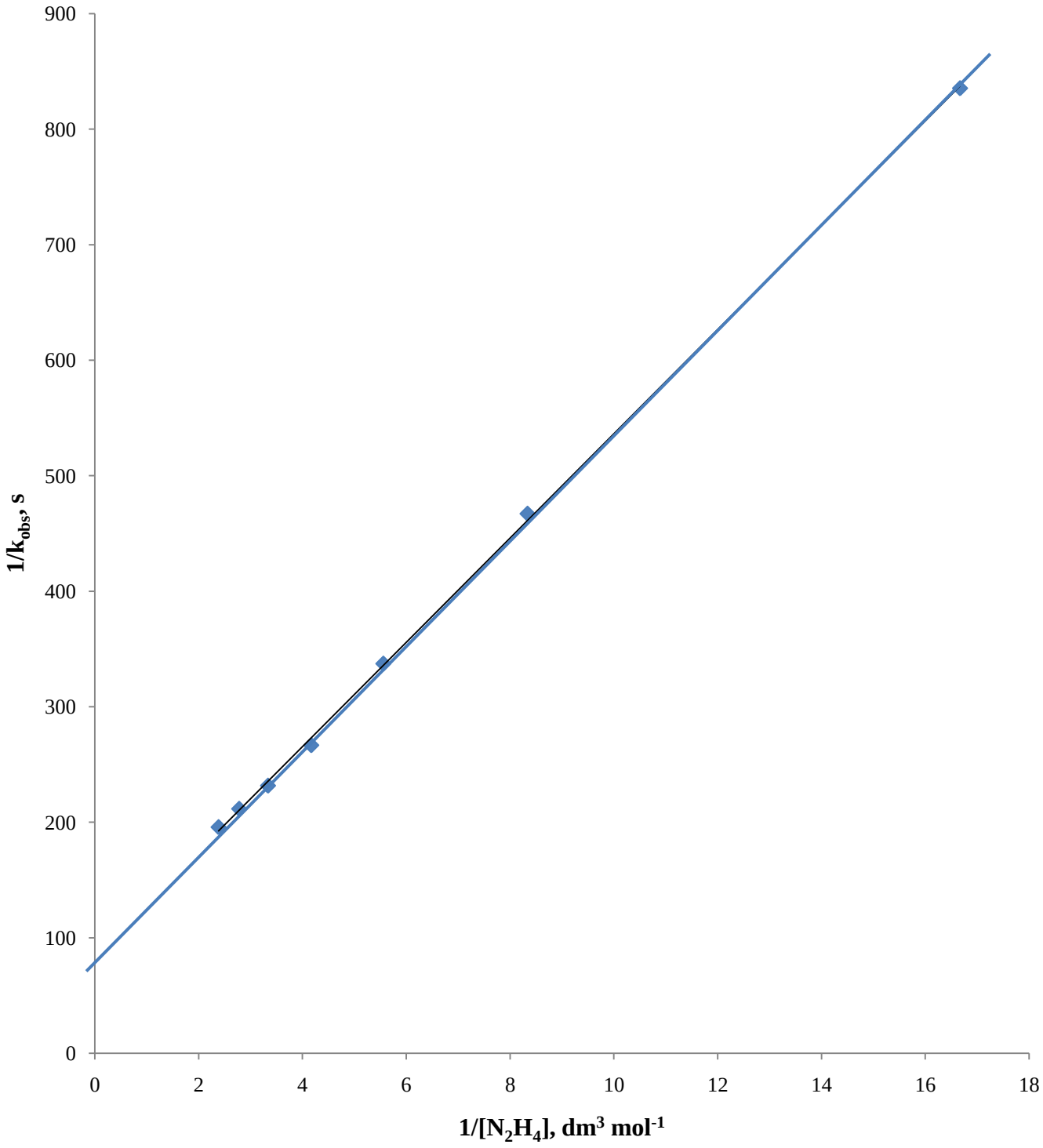

Figure 4.43: Michaelis – Menten Plot of $1/k_{obs}$ versus $1/[N_2H_4]$ for the redox reaction of $[Co(EDTA)]^-$ with N_2H_4 at $[Co^{3+}] = 3.0 \times 10^{-3}$ mol dm^{-3}, $[Cu^{2+}] = 6.0 \times 10^{-4}$ mol dm^{-3}, I = 0.45 mol dm^{-3} ($NaClO_4$)

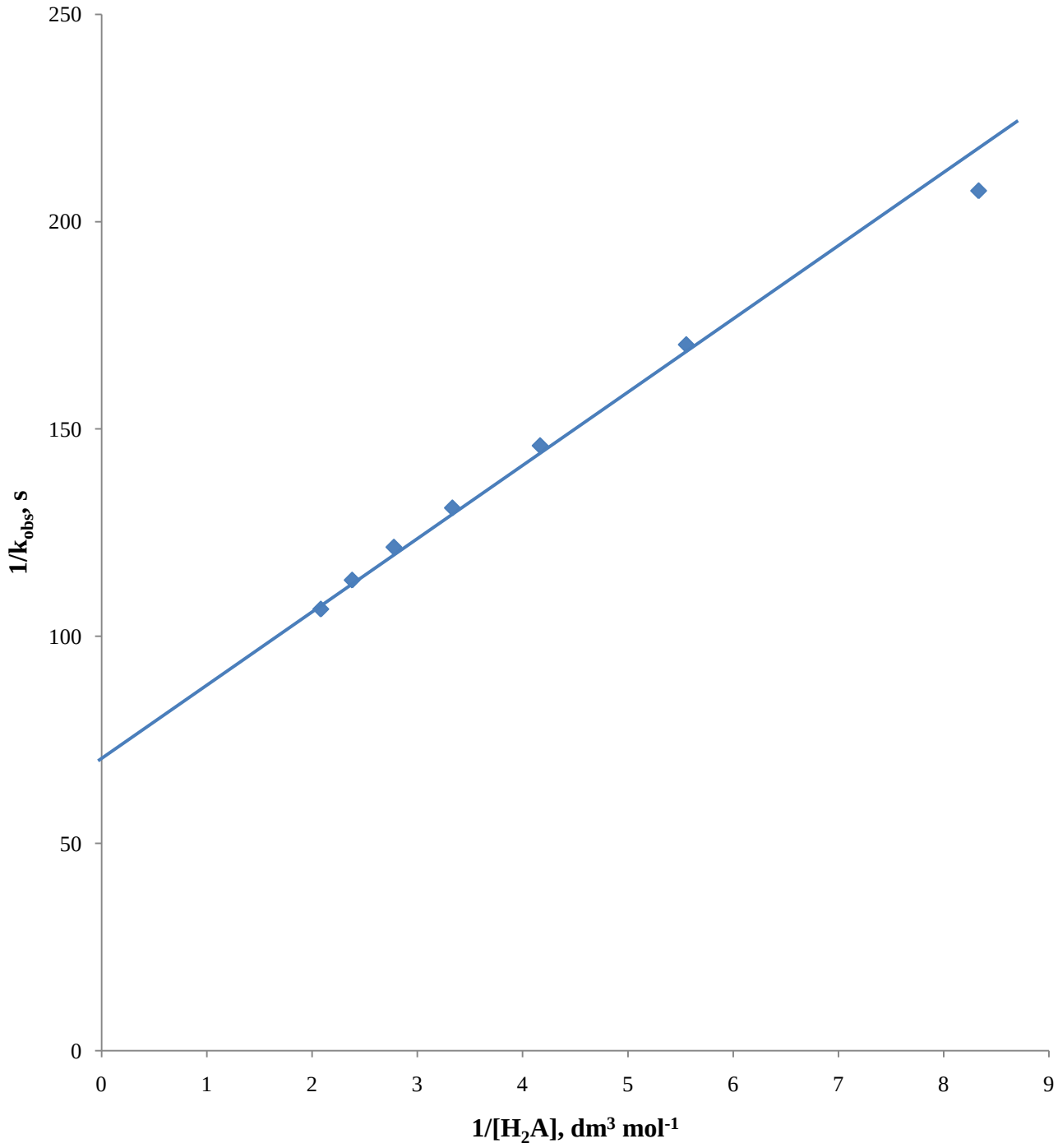

Figure 4.44: Michaelis – Menten Plot of $1/k_{obs}$ versus $1/[H_2A]$ for the redox reaction of $[Co(HEDTA)OH_2]$ with H_2A, at $[Co^{3+}] = 6.0 \times 10^{-3}$ mol dm^{-3}, $[Cu^{2+}] = 7.0 \times 10^{-3}$ mol dm^{-3}, I = 0.2 mol dm^{-3} ($NaClO_4$)

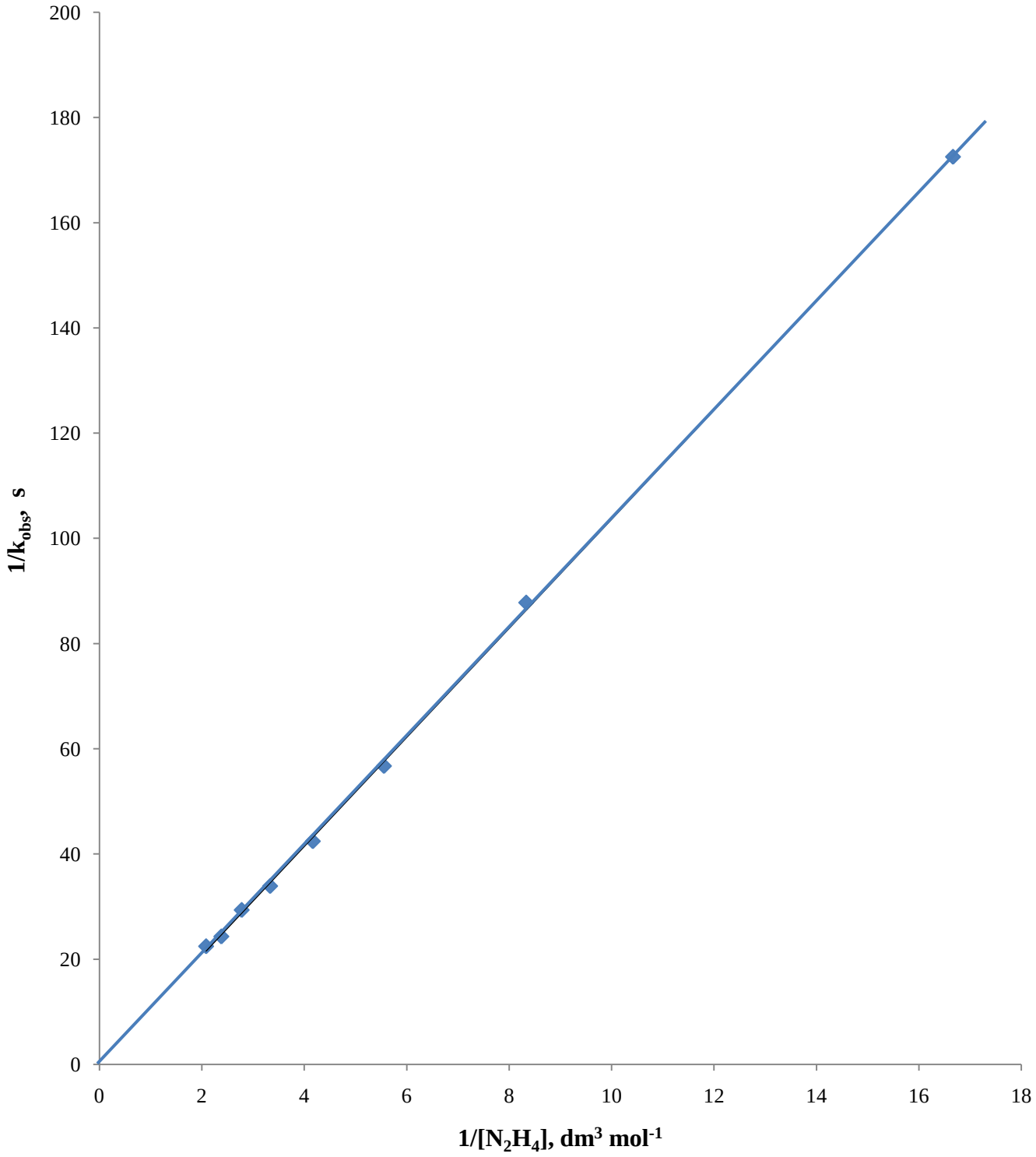

Figure 4.45: Michaelis – Menten plot of $1/k_{obs}$ versus $1/[N_2H_4]$ for the redox reaction of $[Co(HEDTA)OH_2]$ with N_2H_4, at $[Co^{3+}] = 6.0 \times 10^{-3}$ mol dm^{-3}, $[Cu^{2+}] = 5.0 \times 10^{-4}$ mol dm^{-3}, I = 0.5 mol dm^{-3} ($NaClO_4$)

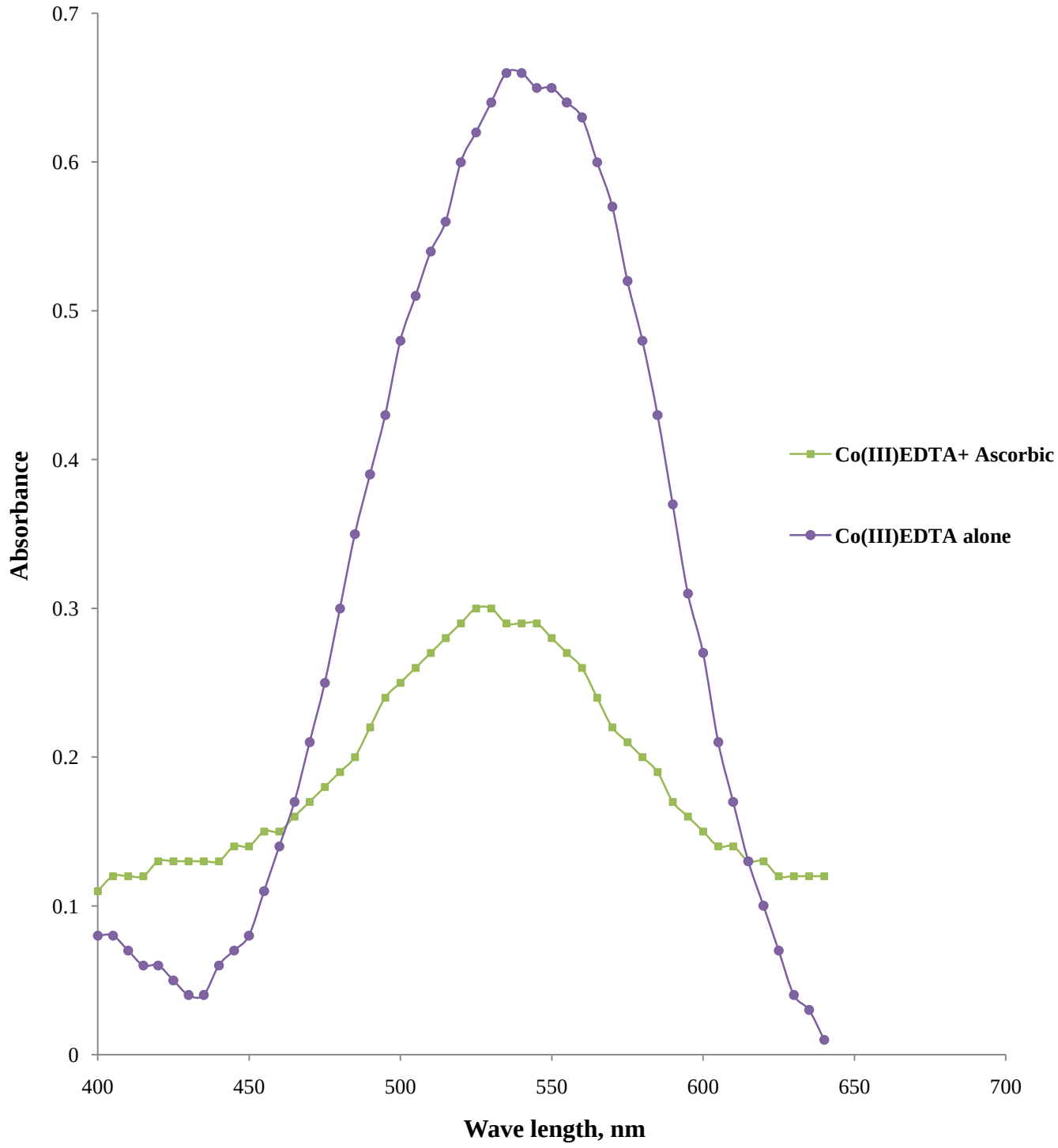

Figure 4.46: Spectrum of the redox reaction mixture of $[Co(EDTA)]^-$ and H_2A after four minutes of reaction

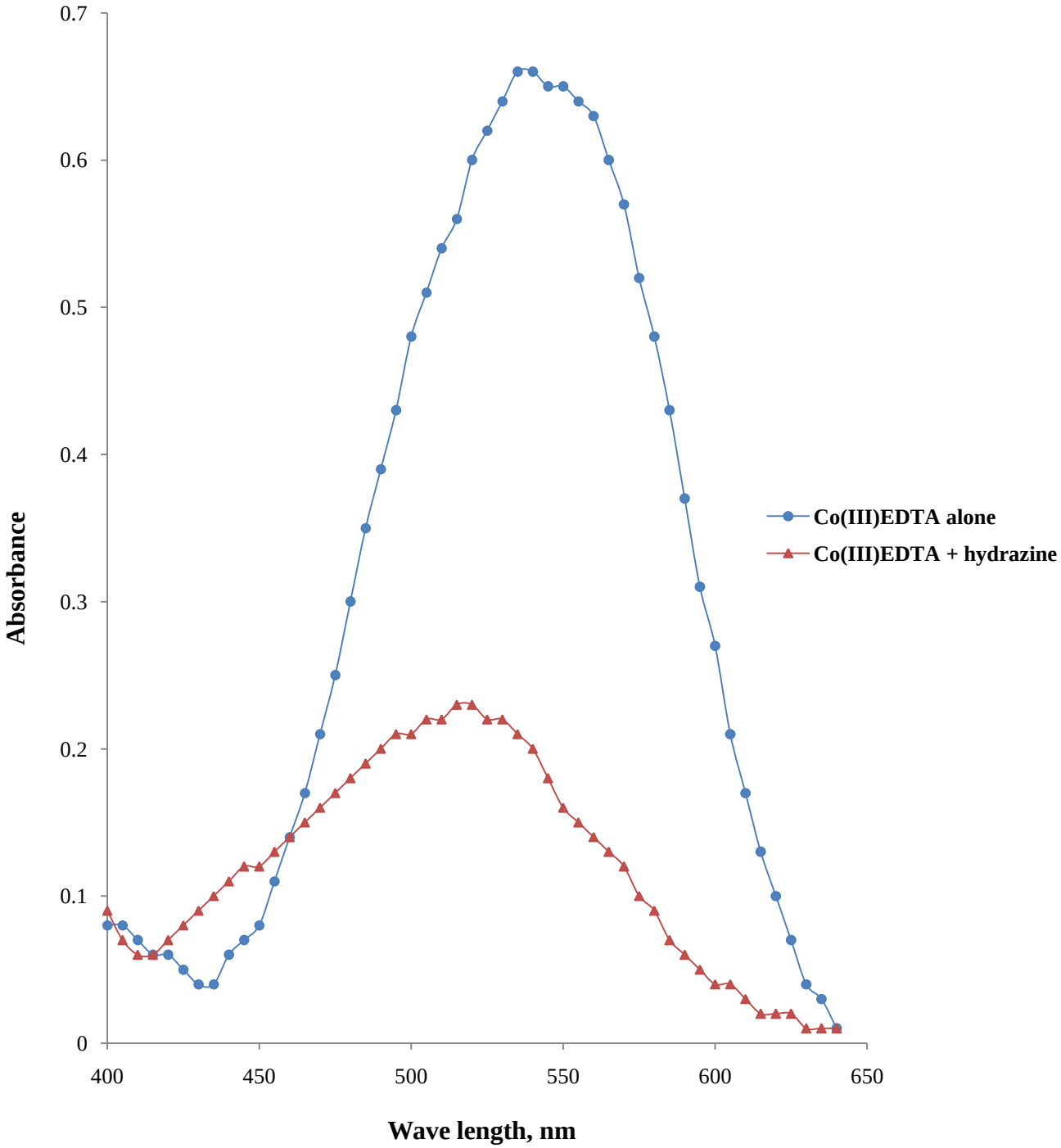

Figure 4.47: Spectrum of the redox reaction mixture of $[Co(EDTA)]^-$ and N_2H_4 after two minutes of reaction

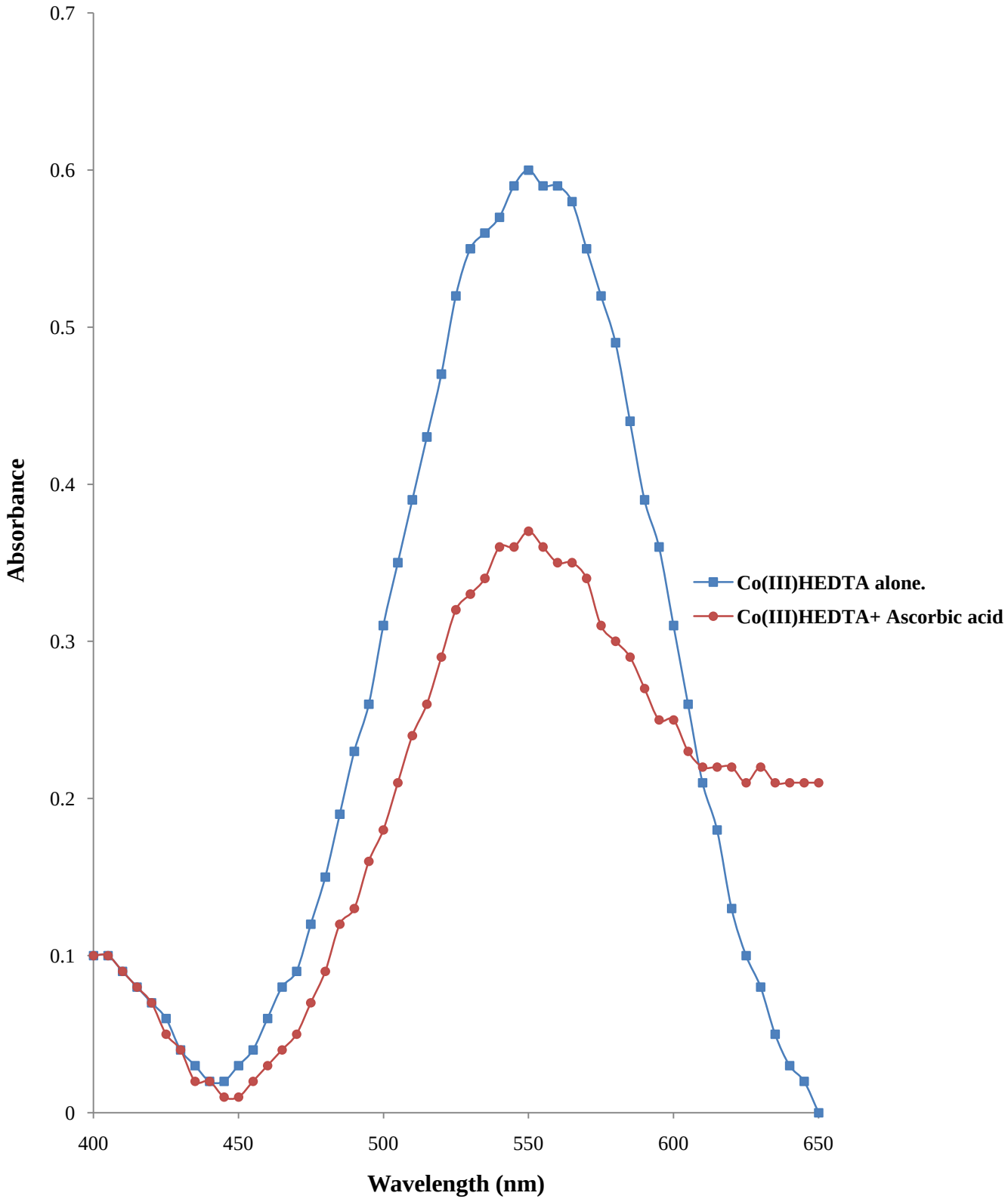

Figure 4.48: Spectrum of the redox reaction mixture of [Co(HEDTA)OH_2] and H_2A after four minutes of reaction

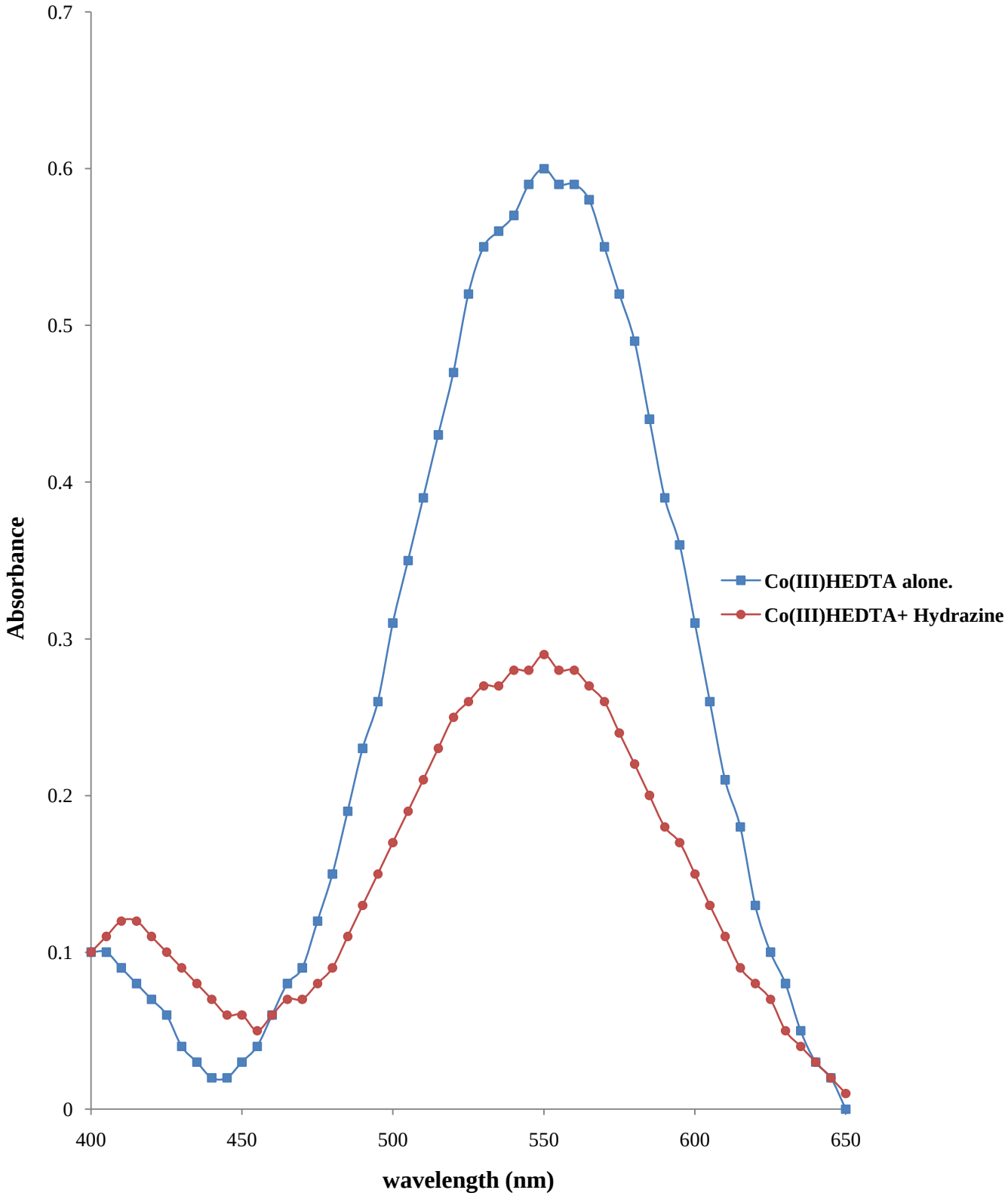

Figure 4.49: Spectrum of the redox reaction mixture of [Co(HEDTA)OH_2] and N_2H_4 after four minutes of reaction

4.11 Product Analysis

4.11.1 Qualitative methods

The Co^{2+} product detected by the addition of excess KSCN to the reaction mixture led to a colour change from faint pink to blue. This was noticed in all four (4) systems, signifying the existence of Co^{2+} (Hahn and Welcher, 1963). The reaction product of the H_2A systems reacted with pyrrole in excess trichloroacetic acid to give a blue – green colour, which signifies the presence of dehydroascorbic acid (Tipson, 1945).

In the test carried out for the presence of NH_3 for both N_2H_4 systems, a black precipitate was not noticed upon introduction of iodine to the reaction mixture at the end of the reaction. This signifies the absence of NH_3 as a possible product and as such, suggests the formation of N_2 gas (Richard and Renfrow, 1952).

4.11.2 Spectrophotometric methods

Spectrophotometric result showed a change in λ_{max} from the characteristics Co(III) complexes to that for Co(II) in all the systems investigated. The spectra of the product of reaction gave λ_{max} of 507 nm for the $[Co(EDTA)]^-$ – H_2A system, 504 nm for the $[Co(EDTA)]^-$ – N_2H_4 system, 509 nm for the $[Co(HEDTA)OH_2]$ – H_2A system and 510 nm for the $[Co(HEDTA)OH_2]$ – N_2H_4 system respectively. The values of λ_{max} obtained for the reaction product agreed with literature values of 490 nm – 510 nm for Co^{2+} complexes (Onu, 2010; Arunachalam *et al*., 2015).

CHAPTER FIVE

5.0 DISCUSSION

5.1 $[Co(EDTA)]^-$ – L-ascorbic Acid System

The observed result from the stoichiometric study ($2[Co(EDTA)]^-$: H_2A) showed that H_2A is undergoing a two electron transfer oxidation. A similar stiochiometry has been reported in the reduction of oxovanadium(V) complexes by as ascorbic acid (Maity *et al*., 2007), the reduction of tri-nuclear iron(III)/chromium(III) cations by ascorbic acid (Lawrence *et al*., 2012), the oxidation of ascorbic acid by hexacynoferrate(III) (Laxmi *et al*., 2013) and the oxidation of ascorbic acid by silver(I) (Narendra *et al*., 2014).This form of stoichiometry involving a two – electron oxidation will often produce a dehydroascorbic acid product (Davis, 1992; Mondal *et al*., 2009; Bitziou *et al*., 2013). However, the stoichiometry of 1:1 for Ru^{VI} : H_2A and Ru^{IV} : H_2A have been reported in the reduction of *trans*-$[Ru^{VI}(tmc)(O)_2]^{2+}$ and *trans*-$[Ru^{IV}(tmc)(OH_2)_2]^{2+}$ by ascorbic acid respectively (Wang *et al*., 2009). The change in colour observed from faint pink to blue upon the qualitative test for Co(II) indicates the formation of $[Co^{II}(SCN)_4]^{2-}$ (Hahn and Welcher, 1963). Also, the blue – green colour observed upon treating the reaction mixture with pyrrole in excess trichloroacetic acid confirms the presence of dehydroascorbic acid product in the reaction mixture (Tipson, 1945). The product analysis of the metal complex indicates the reduction of Co(III) to Co(II) from both spectroscopic and qualitative analyses.

Kinetic study shows that the reaction is first-order in $[Co(EDTA)^-]$ and $[H_2A]$ respectively, and second order overall with the second order rate constant k_2 to be $(9.88 \pm 0.065) \times 10^{-3}$ dm^3 mol^{-1} s^{-1}. Similar orders have been documented for H_2A and other forms of Co(III) complexes in earlier works (Tsukahara *et* al., 1982; Hamzeh, 2001; Sadhana *et al*., 2014; 2015)

From the study of the effect of acid on the reaction, it was found that the reaction was independent of $[H^+]$, indicating a zero order with respect to the $[H^+]$. The independence of the $[H^+]$ on the rate of this reaction suggests that the reactants were neither protonated nor deprotonated in solution prior to or during electron transfer process. Hence, the protonation or otherwise of H_2A was not important in this reaction (Davis, 1992). Similar results have been obtained from the oxidation of ascorbic acid by hexachloroplatinate(IV) ion (Mehrota *et al.*, 1970) and tris(1,10-phenanthroline)iron(III) complexes in aqueous solution (Kimura *et al.*, 1982).

The rate of reaction was first order with respect to [catalyst], which is similar to result obtained by earlier workers (Luty-Blocho *et al*., 2013; Sadhana *et al*., 2014; Singh *et al*., 2014). The plot of k_2 versus $[Cu^{2+}]$ was linear (Figure 4.19), signifying an increase in reaction rate due to increase in catalyst concentration.

Investigation on the effect of ionic strength on the reaction species showed a decrease in the rate of the reaction with increase in concentration of inert salt (Table 4.1). The plot of log k_2 versus $I^{1/2}$ gave a negative slope of –3.66, indicating a negative kinetic salt. This result suggests the presence of oppositely charged species at the rate determining step. Similar results were obtained from previous studies (Iyun and Tinuoye, 1998; Onu and Iyun, 2000; Mandal *et al*., 2013; Singh *et al*., 2014; Idris *et al.*, 2015). The magnitude of the slope of − 3.66, translated into the linear equation $log\ k = log\ k_0 + 1.04\ z_a z_b I^{1/2}$ would suggest that the oppositely charged species at the rate determining step are a dianion and dication respectively. However this magnitude is not reflected in Equation 5.3, the higher magnitude of this slope could be attributed to interactions from other ionic components that may be present in the solution.

The rate of reaction increased with decrease in the dielectric constant of the reaction medium (Table 4.5), and the plot of k_2 versus 1/D gave a slope of 59.53. The explanation for this marked increase in rate with a decrease in dielectric constant could be due to the negatively charged $[Co(EDTA)]^{\square}$ present in the solution. Reactants that are negatively charged or polar, have a greater tendency of forming hydrogen bond of the form $[R\text{-}O\text{-}H^{\delta+}\text{----}X^{\delta\square}\text{----}H^{\delta+}\text{-}O\text{-}R]$ with polar protic solvents like water unlike acetone that is aprotic and lacks the –OH group. This hydrogen bonded species are bulky and slow towards electron transfer reactions, thus decrease in the dielectric constant (increase in the volume of acetone) of the reaction medium means decrease in the formation of bulky hydrogen bonded species and hence increase in the rate of reaction (Asperger, 2003).

The inhibition by added anions is in order, as the added anions would further increase the distance between the reactants species at the activated complex by repelling the $[Co(EDTA)]^{-}$ specie and hence, reduce the rate of electron transfer. The observed effect of added ions shows that the reactant ions maintain their coordination integrity in the activated complex prior to and during electron transfer (Anweting, 2012). This fact is however not supported by the negative value of activation entropy ($\Delta S^{\ddagger} = \square$ 43.65 JK^{-1} mol^{-1}) obtained for the reaction. The negative value of entropy of activation suggests a more ordered activated complex occasioned by possible bridging of the reactant partners.

The addition of acrylamide to the reaction mixture followed by excess methanol resulted in the formation of a gelatinous precipitate; this indicates that a free radical was present in the reaction mixture to have initiated polymerisation of the acrylamide, while the methanol was responsible in converting this polymer into precipitate (Gromov *et al.,* 1966). Ascorbic acid has been reported to give such radicals (Snehalatha *et al*., 1997; Wang *et al*., 2009; Sailani *et al*.,

2011; Khan *et al*., 2013). Also, spectroscopic study indicated no shift from the absorption maxima of 535 nm (Figure 4.46). This also suggests the probable absence of an intermediate complex of significant stability during the reactions. In addition, the Michaelis – Menten plot of $1/k_{obs}$ versus $1/[H_2A]$ (Figure 4.42) was linear with zero intercept, further supporting the absence of intermediate complex.

Evidences in this study confirms that the reaction is occurring by the outer – sphere mechanism. The choice of the mechanism is guided by the following:

a. The zero intercept obtained from the plot of k_1^{-1} versus $[H_2A]^{-1}$ (Michaelis-Menten plot).

b. The catalytic and inhibitory effect of added ions on the rate of the reaction.

c. The absence of spectroscopically determinable intermediate.

On the basis of the above findings, the following mechanistic steps are proposed for the Cu^{2+} catalysed reaction of $[Co(EDTA)]^-$ with H_2A.

Where $Co^{III}L^-$ and $Co^{II}L^{2-}$ represents $[Co(EDTA)]^-$ and $[Co(EDTA)]^{2-}$, then from Equation 5.2 which is the rate determining step, gives;

$$\text{Rate} = k_1[CuH_2A^{2+}][Co(EDTA)^-] \quad (5.5)$$

$[CuH_2A^{2+}]$ is an intermediate that is produced in an equilibrium step (Equation 5.1), hence;

$$[CuH_2A^{2+}] = K_{eq}[H_2A][Cu^{2+}] \quad (5.6)$$

substituting Equation 5.6 into Equation 5.5, gives;

$$\text{Rate} = K_{eq}k_1[Cu^{2+}][H_2A][Co(EDTA)^{-}] \quad (5.7)$$

The rate law in Equation 5.7 can thus be written as;

$$\text{Rate} = a[Cu^{2+}][H_2A][Co(EDTA)^{-}] \quad (5.8)$$

Equation 5.8 corresponds to the experimental rate law in Equation 4.15, where $a = K_{eq}k_1 = 4.9$ $dm^3\ mol^{-1}\ s^{-1}$.

5.2 $[Co(EDTA)]^{-}$ – N_2H_4 System

The stoichiometric study gave a result of N_2H_4 : $2[Co(EDTA)]^{-}$, this is similar to the results obtained from other reactions of N_2H_4 (Thakuria and Gupta, 1975; Al-Subu *et* al., 1990; Peter *et al.,* 1991; Jhimli *et* al., 2004; Mshelia *et al.,* 2010; Gain *et al*., 2011), the N_2H_4 underwent a two electron transfer giving an electron each to the two cobalt(III) complexes. The stoichiometry obtained is associated with N_2 product of N_2H_4 oxidation, especially where a two electron transfer process is involved to give diazine (Patapati *et al.,* 1986), followed by oxidation by atmospheric oxygen to give N_2 and H_2O (Wagnerova *et al.,* 1973; Cookson *et al.,* 1977). This stoichiometry is further supported by the product analysis as spectroscopic test obtained for the Co(II) product and further qualitative test confirms that the reduction of Co(III) into Co(II) as earlier mentioned was obtained. In addition, the qualitative test for ammonia was negative, indicating the absence of NH_3 as one of the reaction product. The absence of NH_3 in the product further confirms the fact that a two electron transfer process was involved, with Co(II) as the evident product.

From the kinetic study, the pseudo – first order plot of log (A_t - A_∞) against time was linear up to 70 % of the reaction time. This linearity signifies a first order with respect to

$[Co^{III}(EDTA)]^-$. The plots of log k_{obs} versus log $[N_2H_4]$ gave a slope of 0.76544, this signifies a first order with respect to the $[N_2H_4]$ and thus a second order overall. Such orders have been recorded for reactions of N_2H_4 (Sadagopa *et al*., 1975; Sultan *et al*., 1985; Zagal *et al*., 1986; Al-Subu *et* al., 1990; Gain *et al*., 2011; Das *et al*., 2015).

Results obtained from the acid dependent study showed that changes in acid concentration had an independent effect on the reaction rate. There was a marked increase in the rate of the reaction with increase in $[Cu^{2+}]$ as seen in Table 4.3. Cu^{2+} has been documented to be a potent catalyst for the reactions of hydrazine and its derivatives, since it binds with the hydrazine to form a highly reactive Cu(II) – hydrazine complex (Carl *et al.*, 1975; Micheal *et al*., 1978; Lim and Zhong, 1989; Mondal and Banerjee, 2009). The plot of k_2 versus $[Cu^{2+}]$ was linear with zero intercept (Figure 4.20) suggesting a one term rate law.

The rate of the reaction was observed to decrease with increase in ionic strength (Table 4.3) and the plot of log k_2 versus $I^{1/2}$ gave a negative slope of –0.88, indicating a negative kinetic salt effect. This shows that the activated complex is made up of two oppositely charged species (Asperger, 2003). The magnitude of the slope of –0.88 implies that the two charged species at the activated complex compose of ions of +1 and –1 charge respectively. Although the negative salt effect is observed in Equation 5.10, there is reason to believe that interference by other ions that might be in solutions could be responsible for the different value obtained. The decrease in dielectric constant led to a marked decrease on the observed rate (Table 4.6), an evidence which is in support of nature of salt effect obtained from the ionic strength study.

The added anions and cations had no effect on the rate of this reaction (Table 4.9). The non – catalysis by these ions suggests that the reaction occur by the inner – sphere mechanism, as

the reactant species at the activated complex are linked together thereby making the effect of added ions negligible. Non – catalysis of the reaction rate by added ions has been reported as characteristic of inner – sphere pathway (Adegite et al., 1977; Abdulsalam, 2015).

Result obtained from the free radical test was negative, indicating that free radical formation is not important in this reaction. The test of spectroscopically determinable intermediate (Figure 4.47), showed a shift in the λ_{max} from 550 nm to 520nm, this suggests the presence of a spectroscopically detectable intermediate (Anweting, 2012).

Michaelis – Menten plot of $1/k_1$ versus $1/[N_2H_4]$ gave an intercept of ~ 85 s, implying the presence of intermediate complex, which is characteristics of reactions occurring by the inner – sphere mechanism. This is further supported by the entropy ($\Delta S^{\ddagger} = -175.58$ JK^{-1} mol^{-1}) and enthalpy ($\Delta H^{\ddagger} = 31.46$ kJ mol^{-1}) of activation obtained from the temperature dependent study as negative value of $\Delta S^{\ddagger}$ suggests loss of freedom at the activated complex. This observation can be attributed to the reactant centres being held by a bridging ligand at the activated complex, which is a characteristic in favour of inner – sphere mechanism (James, 2002).

The inner – sphere mechanism is therefore proposed for this reaction based on the following criteria:

a. The intercept obtained from the plot of k_1^{-1} versus $[H_2A]^{-1}$ (Michaelis-Menten plot).

b. The non catalysis of the reaction by added ions.

c. The presence of spectroscopically determinable intermediate.

d. The negative value of the change in activation entropy.

Based on the above findings, the following mechanism is proposed for the reaction:

Equation 5.10 is the rate determining step, given that $Co^{III}L^{-}$ and $Co^{II}L^{2-}$ are $[Co^{III}(EDTA)]^{-}$ and $[Co^{II}(EDTA)]^{2-}$ respectively, then the rate is expressed as;

$$\text{Rate} = k_1[CuN_2H_4^{2+}][Co^{III}(EDTA)^{-}] \quad (5.14)$$

$CuN_2H_4^{2+}$ is transients specie produced in Equation 5.9, thus;

$$K_{eq} = \frac{[CuN_2H_4^{2+}]}{[N_2H_4]\,[Cu^{2+}]} \quad (5.15)$$

$$[CuN_2H_4^{2+}] = K_{eq}[N_2H_4][Cu^{2+}] \quad (5.16)$$

Substituting Equation 5.16 into 5.14 gives;

$$\text{Rate} = k_1 K_{eq}\,[Cu^{2+}][N_2H_4][Co^{III}(EDTA)^{-}] \quad (5.17)$$

Therefore;

$$\text{Rate} = a[Cu^{2+}][N_2H_4][Co^{III}(EDTA)^{-}] \quad (5.18)$$

Equation 5.18 conforms with the experimental rate law (Equation 4.16), where $a = k_1 K_{eq} = 18.25\ dm^3\ mol^{-1}\ s^{-1}$.

5.3 $[Co^{III}(HEDTA)OH_2]$ – H_2A System

The stiochiometry of $[Co(HEDTA)OH_2]$: H_2A obtained showed that H_2A is donating an electron to reduce Co(III) to Co(II). A similar stiochiometry has been reported in the reduction of Au(III) chloride complex (Luty-Blocho *et al*., 2013), and binuclear Co(III) complexes (Sadhana *et al.,* 2014; Sadhana *et al.,* 2015) by ascorbic acid. The stoichiometry is further supported by the result of product analysis. The spectroscopic test of the reaction product gave a λ_{max} of 509 nm which is in agreement with literature value of 490 nm – 510 nm for Co(II) product (Arunachalam *et al*., 2015; Onu *et al.,* 2015). The reduction of Co(III) to Co(II) product is further confirmed by the formation of $[Co(SCN)_4]^{2-}$ upon treatment with KSCN. Furthermore, the presence of dehydroascorbic acid in the reaction product is an indication that the complex was reduced by ascorbic acid to give Co(II) and dehydroascorbic acid respectively.

The pseudo – first order plot for the reaction was linear as shown in Figure 4.7, suggesting a first order dependence with respect to the $[Co(HEDTA)OH_2]$ complex. The logarithmic plot of k_{obs} versus $[H_2A]$ was also linear, with a gradient of 0.48. This shows that the reaction is half – order with respect to $[H_2A]$, and three over two – order overall. The $k_{3/2}$ was obtained as $k_{3/2} = (1.40 \pm 0.023) \times 10^{-2}$ $dm^{3/2}$ $mol^{-1/2}$ $s^{-1/2}$. Monomer – polymer equilibria can be the basis for a half order reaction, with the monomer as the reactive species (Wilkins, 2002). Another basis for a half order reaction has been attributed to molecular dissociation (Berry *et al*., 1980; Onu *et al*., 2016) and this is the basis adopted in this study. Similar order has been documented for reactions of H_2A (Pap *et al*., 2011; Rehana *et al.*,2012) and Co(III) complexes (Bamford and Tipper, 1972; Scott and Chester, 1972).

From the study of the effect of acid on the reaction, it was found that the reaction was independent of acid concentration (Table 4.3). Similar results have been documented for the

reduction of hexachloroplatinate(IV) ion (Mehrota *et al.,* 1970) and tris(1,10-phenanthroline)iron(III) (Kimura *et al.,* 1982) complexes in aqueous solution by ascorbic acid.

The rate of reaction was second order with respect to [catalyst]. The plot of $k_{3/2}$ versus $[Cu^{2+}]^2$ was linear (Figure 4.21), signifying an increase in reaction rate due to increase in catalyst concentration. The Cu^{2+} ion has been known to catalyse the reactions of ascorbic acid by forming a more reactive complex with the reductant (Jones and Hughes, 1976; Sadhanna *et al*., 2014).

Investigation on the effect of ionic strength on the reaction species showed that the rate of reaction was independent of ionic strength concentration, as changes in ionic strength concentration had no effect on the rate of the reaction (Table 4.3). The results imply that either one or both reactant species is/are neutral (Asperger, 2003). Similar results were obtained from the reduction of other forms of Co(III) complexes (Srinivas *et al.,* 2007).

Added anion however catalysed the reaction. The catalytic effect on the rate of the reaction by the added ions is possibly due to the absence of a bridged intermediate at the activated complex, such that the closeness of approach of the reactant ions in the activated complex is such as to allow the intervention of added ion. In view of this fact, influence of reaction rate by added ions is a characteristic of an outer – sphere mechanism, were most of the reactant ions maintain their coordination integrity in the activated complex prior to and during electron transfer (Sharpe, 1981; Babatunde and Ajayi, 2013).

The result for free radical test was negative, suggesting the that presence of free radicals is not an important factor in the reaction (Davis, 1992), the work of Osunlaja *et al.,* (2013) on binuclear Co(III) complex gave similar result. From Figure 4.48, there is no shift in the wavelength of the two spectra from the λ_{max} of 550 nm characteristics of $[Co(HEDTA)OH_2]$ complex. This suggests the absence of any spectroscopically determinable intermediate. Kinetic

evidence for the presence of intermediate via the Michaelis–Menten plot of $1/k_1$ versus $1/[H_2A]$ (Figure 4.44) however, indicated the presence of intermediate complex. This is illustrated by the intercept of 76.32 mol dm^{-3} s^{-1} obtained from the plot. The nature of this intermediate complex could be transient species that were not stable enough to be monitored spectroscopically (Lohdip, 1989). The change in activation enthalpy ($\Delta H^{\ddagger}$ = 85.21 kJ mol^{-1}) and entropy of activation ($\Delta S^{\ddagger}$ = 7.02 JK^{-1} mol^{-1}) were however positive. Such change in activation entropy suggests that the species at the activated complex are loosely held together, which infers that the reactant partners are not bridged. This is a supportive evidence in favour of an outer – sphere mechanism. Similar activation parameters have been obtained from related studies involving Co(III) complexes (Olayinka *et al.,* 2006; Asemave *et al.,*2012) and ascorbic acid (Khan and Sarwar, 1999).

Evidences in this study confirms that the reaction is occurring through both the inner – sphere and outer – sphere mechanism, this type of mechanism has been reported for the redox reaction of $Cr(H_2O)_6^{2+}$ with $IrCl_6^{2-}$ (Haim, 1983) and $Ru(NH_3)_5pz^{3+}$ with $Co(edta)^{2-}$ (Wilkins, 2002). The choice of the mechanism was guided by the following:

a. The intercept obtained from the plot of $1/k_1$ versus $1/[H_2A]$ (Michaelis-Menten plot) suggesting an inner – sphere mechanism.

b. The effect of catalysis and inhibition by added anions and cations respectively on the rate of the reaction suggesting an outer – sphere mechaninsm.

c. The positive value of the change in activation entropy ($\Delta S^{\ddagger}$ = 7.02 JK^{-1} mol^{-1}) supporting the outer – sphere mechanism.

On the basis of the above findings, the following mechanistic steps are proposed for the Cu^{2+} catalysed reduction of $[Co(HEDTA)OH_2]$ by H_2A;

Given that $Co^{III}L$ and $Co^{II}L^{-}$ are $[Co^{III}(HEDTA)OH_2]$ and $[Co^{II}(HEDTA)OH_2]^{-}$ respectively,

$$\text{Rate} = k_3\,[Cu_2\text{-}Co^{III}L^{4+}][HA] \qquad (5.23)$$

But Equations 5.20 gives;

$$[Cu_2\text{-}Co^{III}L^{4+}] = K_2[Cu^{2+}]^2\,[HA] \qquad (5.24)$$

Substituting Equations 5.24 into 5.23, gives;

$$\text{Rate} = K_2\,k_3\,[Cu^{2+}]^2\,[Co^{III}L][HA] \qquad (5.25)$$

If [HA] = [H], hence from Equation 5.19;

$$[HA]^2 = K_1[H_2A];\;\; [HA] \;= K_1^{1/2}\,[H_2A]^{1/2} \qquad (5.26)$$

Substituting this into Equation 5.25 gives;

$$\text{Rate} = K_1^{1/2}K_2k_3[Cu^{2+}]^2[Co(HEDTA)OH_2][H_2A]^{1/2} \qquad (5.27)$$

Equation 5.27 conforms with the experimental rate law in Equation 4.17, where $d = K_1^{1/2}K_2k_3$.

5.4 $[Co^{III}(HEDTA)OH_2]$ – N_2H_4 System

The stoichiometry of 2 : 1 ($2[Co(HEDTA)OH_2] : N_2H_4$) obtained in this reaction suggests that two moles of Co(III) complex were reduced by a mole of hydrazine. This stoichiometry agrees with other reactions of N_2H_4 (Thakuria and Gupta, 1975; Peter *et al.,* 1991; Jhimli *et* al., 2004; Mshelia *et al.,* 2010; Gain *et al*., 2011). The stoichiometry obtained is associated with N_2 product of N_2H_4 oxidation, especially where a two electron transfer process is involved to give diazene (Patapati *et al.,* 1986), followed by oxidation by atmospheric oxygen to give N_2 and H_2O (Wagnerova *et al.,* 1973; Cookson *et al.,* 1977). Further evidence from products analysis of the reaction mixture showed a decrease in the λ_{max} from 550 nm, characteristics of $[Co(HEDTA)OH_2]$ to 510 nm for the Co(II) product, this is in support of the reduction of Co(III) to Co(II) (Onu, 2010; Arunachalam *et al*., 2015). Moreover, absence of NH_3 from the reaction mixture supports the formation of N_2 product (Dhas *et al*., 1991).

The linearity of the pseudo – first order plot of log $(A_t - A_\infty)$ against time suggests a first order with respect $[Co(HEDTA)OH_2]$. The gradient of the logarithmic plots of log k_{obs} vs log $[N_2H_4]$ was 1.03, signifying a first order with respect to the $[N_2H_4]$ and thus a second order overall. Such order has been known for reactions of N_2H_4 (Sultan *et al*., 1985; Zagal *et al*., 1986; Sadagopa *et al*., 1975; Gain *et al*., 2011).

The plot of log k_1 versus log $[H^+]$ (Figure 4.12) showed an inverse acid dependence on the reaction rate. Similar results has been obtained for the reactions of N_2H_4 (Thakuria and Gupta, 1975; Al-Subu *et al.,*1990; Mondal and Banerjee, 2009; Mshelia *et al.,* 2010), the plot of k_2 versus $[H^+]^{-1}$ had no intercept (Figure 4.14) and therefore suggests that the reaction occurs via

a single pathway of inverse acid dependence (Mshelia *et al.,* 2010; Das *et al*., 2015; Onu *et al.,* 2015). N_2H_4 could be responsible for such deprotonation as reported by Mshelia *et al,* (2010).

The result obtained from Table 4.4 showed an increase in the rate of reaction with an increase in $[Cu^{2+}]$. The ability of Cu^{2+} to bind with the reductants forming a more reactive complex has made it a potent catalyst for the reactions of hydrazine and its derivatives (Carl *et al.,* 1975; Micheal *et al*., 1978; Mondal and Banerjee, 2009).

Changes in the ionic strength of the reaction medium had no significant effect on the k_{obs} values (Table 4), the non – dependence of rate of reaction on ionic strength is known to occur when one or both of the reactants are neutral (Asperger, 2003; Mondal and Benerjee, 2009). Since one of the reactant specie in the reaction is neutral, the zero salt effect in this study is not unexpected.

The increase in the reaction rate with increase in added anions ($CHCOO^-$ and CH_3COO^-) implies absence of bridge linked reactants at the activated complex, making the intervention of anions and cations possible in the activated complex. Ion catalysis has been reported to be a characteristic of the outersphere reaction mechanism (Adegite *et al.,* 1977; Ali *et al*., 1990; Idris *et al*., 2015).

Addition of acrylamide to the partially reduced reaction mixture followed by excess methanol did not give any gelatinous precipitate. This implies the absence of free radical in this reaction (Osunlaja *et* al., 2013). Results obtained from comparison of the electronic spectrum of the $[Co(HEDTA)OH_2]$ complex with that of the reaction mixture four minutes after the start of reaction showed no significant shift in λ_{max}, suggesting the absence of spectroscopically detectable intermediate complex formation. Furthermore, Michaelis – Menten plot of $1/k_1$ versus

$1/[N_2H_4]$ was linear and had zero intercept, supporting the absence of intermediate complex, an indication that the reaction occurs via the outer – sphere mechanism.

The positive value of change in entropy of activation ($\Delta S^{\ddagger} = 17.13\ JK^{-1}\ mol^{-1}$) means that the reactant species becomes more disordered at the activated complex, indicating the absence of a bridge linking such reactants together. This supports the suggestion that the reaction follows an outer – sphere mechanistic path (James, 2002).

Taking into account the under listed evidences obtained from this reaction:

a. The zero intercept from Michaelis – Menten plot.

b. The catalysis and inhibition by added anion and cation respectively.

c. The absence of spectroscopically determinable intermediate complex

d. The positive value of change in entropy of activation ($\Delta S^{\ddagger} = 17.13\ JK^{-1}\ mol^{-1}$).

The outer – sphere mechanism is proposed for the reaction. The following plausible mechanistic steps explain the experimental data.

$$\text{Rate} = k_2[N_2H_4][CuCo^{III}(HEDTA)OH^+] \quad (5.32)$$

From Equation 5.28,

$$[CuCo^{III}(HEDTA)OH^+] = K_1[Co^{III}(HEDTA)OH_2][Cu^{2+}][H^+]^{-1} \quad (5.33)$$

Substituting Equations 5.33 Equation 5.32, gives;

$$\text{Rate} = k_2K_1[H^+]^{-1}[Cu^{2+}][Co(HEDTA)OH_2][N_2H_5^+] \quad (5.34)$$

$$= a[H^+]^{-1}[Cu^{2+}][Co(HEDTA)OH_2][N_2H_5^+] \quad (5.35)$$

Equation 5.35 agrees with the experimental rate law in Equation 4.18, where $a = k_3K_1K_2$.

5.5 Comparative Analysis of the Cobalt(III) Reactions Studied

5.5.1 $[Co(EDTA)]^-$ – H_2A and $[Co(EDTA)]^-$ – N_2H_4 system

The rate constant k_2 for the reduction of $[Co(EDTA)]^-$ by H_2A was $(9.88 \pm 0.065) \times 10^{-3}$ $dm^3\ mol^{-1}\ s^{-1}$ this was less than that obtained for the reduction of the same complex by N_2H_4 which was $(1.57 \pm 0.099) \times 10^{-2}$ $dm^3\ mol^{-1}\ s^{-1}$.

5.5.2 $[Co(HEDTA)OH_2]$ – H_2A and $[Co(HEDTA)OH_2]$ – N_2H_4 system

The reduction of $[Co(HEDTA)OH_2]$ by H_2A and N_2H_4 also follows the same trend as that of $[Co(EDTA)]^-$ with similar reductant. The rate constant at of the reduction of $[Co(HEDTA)OH_2]$ by H_2A was $(1.38 \pm 0.014)) \times 10^{-2}$ $dm^{3/2}\ mol^{-1/2}\ s^{-1/2}$, this was far lesser than the rate constant for the reduction of the same complex by N_2H_4 which gave a rate constant of $(9.81 \pm 0.144) \times 10^{-2}$ $dm^3\ mol^{-1}\ s^{-1}$

5.5.3 $[Co(EDTA)]^{-}$ – H_2A and $[Co(HEDTA)OH_2]$ – H_2A system

The rate constant of $(9.88 \pm 0.065) \times 10^{-3}$ dm^3 mol^{-1} s^{-1} obtained for the reduction of $[Co(EDTA)]^{-}$ by H_2A was lower than the rate constant of $(1.38 \pm 0.014) \times 10^{-2}$ $dm^{3/2}$ $mol^{-1/2}$ $s^{-1/2}$ obtained for the reduction of $[Co(HEDTA)OH_2]$ by the same reductant.

$[Co(EDTA)]^{-}$ – N_2H_4 and $[Co(HEDTA)OH_2]$ – N_2H_4 system

Similarly, the trend was consistent as the rate constant of $(1.57 \pm 0.099) \times 10^{-2}$ dm^3 mol^{-1} s^{-1} gotten for the reduction of $[Co(EDTA)]^{-}$ by N_2H_4 was less than the rate constant of $(9.81 \pm 0.144) \times 10^{-2}$ dm^3 mol^{-1} s^{-1} gotten from the reduction of $[Co(HEDTA)OH_2]$ by the same reductant.

The above trend is consistent in the sense that the rate constants for both N_2H_4 reactions are higher than those for H_2A. This could possibly be explained due to their redox potentials, N_2H_4 have a redox potential of – 1.21 V for a complete oxidation (Granot *et al*., 2011) while H_2A has a higher redox potential of +0.19 V (Bradshaw *et al*., 2011). Reductants with a lower redox potential have better reducing ability than those with higher redox potential, hence the enhanced rate noticed for the N_2H_4 systems. Furthermore, it can be seen that the rate constants for the reduction of $[Co(HEDTA)OH_2]$ were greater than those for the $[Co(EDTA)]^{-}$ reactions with the same reductants. This trend is attributed to the nature of ligands attached to each Co(III) central ion, as HEDTA is a penta – dentate ligand, it less stable and thus has a less effect on magnitude of the 10Dq splitting of the overall complex than the EDTA which is hexa – dentate and more stable (James, 2002). This means that the $[Co(HEDTA)OH_2]$ complex has a lesser splitting and can easily be reduced as compared to the $[Co(EDTA)]^{-}$. Again, the larger size of the EDTA ligand compared to the HEDTA means that electron tunneling would be easier in the HEDTA than the EDTA metal complexes (Hamzeh, 2001).

CHAPTER SIX

6.0 SUMMARY, CONCLUSION AND RECOMMENDATION

6.1 Summary

The kinetics of the Cu^{2+} catalysed redox reactions of $[Co(EDTA)]^{-}$ with H_2A and N_2H_4 and $[Co(HEDTA)OH_2]$ with H_2A and N_2H_4 in aqueous acidic solution were successfully studied. The stoichiometry of 2:1 was observed for $[Co(EDTA)]^{-} - H_2A$, $[Co(EDTA)]^{-} - N_2H_4$ and $[Co(HEDTA)OH_2] - N_2H_4$ systems while a stoichiometry of 1:1 was recorded for the $[Co(HEDTA)OH_2] - H_2A$ system respectively.

The reaction was first order with respect to both oxidants and reductants for all the systems, except the $[Co(HEDTA)OH_2] - H_2A$ that showed a first order dependence on the oxidant and a half – order on the reductant. Results from the acid investigations showed an inverse first order for the $[Co(HEDTA)OH_2] - N_2H_4$ system, while changes in $[H^{+}]$ had no effect on the $[Co(EDTA)]^{-} - H_2A$, $[Co(HEDTA)OH_2] - H_2A$ and $[Co(EDTA)]^{-} - N_2H_4$ systems. From the studies on the effects of catalysts, a first order with respect to $[Cu^{2+}]$ was observed for $Co(EDTA)]^{-} - H_2A$, $[Co(EDTA)]^{-} - N_2H_4$ and $[Co(HEDTA)OH_2] - N_2H_4$ systems and a second order for $[Co(HEDTA)OH_2] - H_2A$ system respectively.

The reactions are therefore in conformity with Equations (4.15 – 4.18) and the second order rate constants for the various systems were observed as follows:

$[Co(EDTA)]^{-} - H_2A$: $k_2 = (9.88 \pm 0.065) \times 10^{-3}\ dm^3\ mol^{-1}\ s^{-1}$

$[Co(EDTA)]^{-} - N_2H_4$: $k_2 = (1.57 \pm 0.099) \times 10^{-2}\ dm^3\ mol^{-1}\ s^{-1}$

$[Co(HEDTA)OH_2] - H_2A$: $k_{3/2} = (1.38 \pm 0.014) \times 10^{-2}\ dm^{3/2}\ mol^{-1/2}\ s^{-1/2}$

$[Co(HEDTA)OH_2] - N_2H_4$: $k_2 = (9.81 \pm 0.144) \times 10^{-2}\ dm^3\ mol^{-1}\ s^{-1}$

The $[Co(EDTA)]^-$ – H_2A and $[Co(EDTA)]^-$ – N_2H_4 systems were both sensitive to change in ionic strength while $[Co(HEDTA)OH_2]$ – H_2A and $[Co(HEDTA)OH_2]$ – N_2H_4 systems were not. Except for the $[Co(EDTA)]^-$ – N_2H_4 system, all other systems were sensitive to added anions and cations. There was an observed shift in λ_{max} from 550 – 520 nm for the $[Co(EDTA)]^-$ – N_2H_4 system where as no shift was observed for the other three systems. Free radical was observed only for the $[Co(EDTA)]^-$ – H_2A system.

Records from the temperature studies showed a positive $\Delta H^{\ddagger}$ for all the systems, while a positive $\Delta S^{\ddagger}$ was obtained for the $[Co(HEDTA)OH_2]$ – H_2A and $[Co(HEDTA)OH_2]$ – N_2H_4 systems and a negative $\Delta S^{\ddagger}$ for the $[Co(EDTA)]^-$ – H_2A and $[Co(EDTA)]^-$ – N_2H_4 systems. From the results obtained, it was shown that the $[Co(EDTA)]^-$ – H_2A, and $[Co(HEDTA)OH_2]$ – N_2H_4 systems all undergo an outer – sphere mechanism, $[Co(EDTA)]^-$ – N_2H_4 system undergoes an inner – sphere mechanism while the $[Co(HEDTA)OH_2]$ – H_2A system undergoes both inner – sphere and outer – sphere mechanism. Therefore such mechanisms were proposed for these systems respectively.

6.2 Conclusion

The reduction of both $[Co(EDTA)]^-$ and $[Co(HEDTA)OH_2]$ each by H_2A and N_2H_4, in aqueous acidic medium have been successfully studied spectroscopically. On the basis of the results of these studies, the absence of and/or presence of kinetic and/or spectroscopic evidence for acid dependency, influence of catalyst, complex formation prior to electron transfer, evidence from temperature studies, conformity/non-conformity of the results with Michaelis-Menten plots, and the rationalisation from previous results led to the conclusion that the outer – sphere

mechanism is in play for the $[Co(EDTA)]^{-}$ – H_2A and $[Co(HEDTA)OH_2]$ – N_2H_4 systems, inner – sphere was postulated for the $[Co(EDTA)]^{-}$ – N_2H_4 system, while both inner – sphere and outer – sphere mechanisms are in play for the $[Co(HEDTA)OH_2]$ – H_2A system.

6.3 Recommendation

The kinetics and mechanism of the Cu^{2+} catalysed reduction of $[Co(EDTA)]^{-}$ and $[Co(HEDTA)OH_2]$ by ascorbic acid and hydrazine have been successfully studied in aqueous acidic medium, it is however recommended that:

a. Further studies should be carried out on the reduction of cobalt(III)aminocarboxylato complexes with other reductants using other catalyst aside Cu^{2+} such as Fe^{2+}.

b. Since ascorbic acid and hydrazine monohydrate exists as their highly active forms at higher pH, it would be reasonable to study the kinetics of ascorbic acid and hydrazine monohydrate with other metal complexes in aqueous basic medium.

c. Computational chemistry programs should also be employed in the study of the kinetics and mechanism of these Co(III) complexes and the result should be carefully compared with those generated experimentally from spectrophotometric method, this would check for systematic errors generated experimentally.

REFERENCES

Abdulsalam, S. (2015). *Kinetics and Mechanisms of the Redox Reactions of Crystal Violet with some Oxyanions in Aqueous Acidic Medium* (Unpublished master's dissertation). Ahmadu Bello University, Zaria, Nigeria.

Abdur-Rashid, K., Dasgupta, T. P. and Burgess, J. (1996). Kinetics and Mechanism of the Oxidation of L-ascorbic Acid by *cis*-diaqua Cobalt(III)amine Complexes. *Journal of the Chemical Society, Dalton Transactions,* 1996(7): 1385 – 1391.

Adegite, A., Iyun, J. F. and Ojo, J. F. (1977). Kinetics and Mechanism of Electron Transfer Reaction Between Uranium(III) and some Ruthenium(III)ammines Complexes. *Journal of the Chemical Society, Dalton Transaction,* (1977):115 – 117.

Ali, M., Saha, S. K. and Banerjee, P. (1990). Oxidation of Sulphur(IV) by Dodecatungstocobaltate(III) in Aqueous Acid Solution. *Journal of the Chemical Society, Dalton Transaction,* (1990):187 – 190.

Al-Subu, M. M., El-Halawa, R. A. and Abed, H. M. (1990). Kinetics and Mechanism of Oxidation of Phenylhydrazine and P-Bromophenylhydrazine by Hexacyanoferrate(III) in Acidic Medium. *International Journal of Chemical Kinetics,* 22: 1027 – 1037.

Anca M.M., Constantin, L., Gabriela, C., Simona, I. D., Ioan, G. S. and Alina, C. L. (2015). Synthesis, Characterization and Antimicrobial Activity of Some New Hydrazine Metallic Complexes. *Revista de Chime (Bucharest),* 66(8): 1137 – 1142.

Anweting, B. I. (2012). *Kinetics and Mechanisms of the Oxidation of Nicotinic Acid, L-cysteic Acid, L-aspartic Acid and L-tryptophan by Permanganate Ion in Aqueous Acidic Medium* (Unpublished master's dissertation). Ahmadu Bello University, Zaria, Nigeria.

Arunachalam, P., Sudhir, K. S., Sathyaseelan, V. S., Toleti, S. R., (2015) A Spectrophotometric Method for the Determination Co – EDTA Complexes. *International Journal of Applied Sciences and Biotechnology,* 3(4): 584 – 587.

Asemave, K., Yiase, S. G., Adejo, S. O. and Anhwange, B. A. (2012). Substitution Reaction of trans-dichloro-bis-(ethylenediamine)cobalt(III) Chloride and Phenylalanine- A Kinetics and Mechanism Study. *International Journal of Modern Chemistry,* 1(2): 93 – 101.

Asperger, S. (2003) *Chemical Kinetics and Inorganic Reaction Mechanism 2nd Edition*. Springer Science + Business Media LLC, New York, pp. 3 – 56.

Babasaheb, D. B. and Gavisiddappa, S. G. (2012). Kinetics and Mechanism of Ruthenium(III) Catalyzed Oxidation of D-glucose by 12-tungstocobaltate(III) in Aqueous Hydrochloric Acid Medium. *Advances in Applied Science Research,* 3(2):785 – 792.

Babatunde, O. A. and Ajayi, J. O. (2013). Kinetic Approach to the Reduction of Toluidine Blue by Dithionate Ion in Aqueous Acidic Medium. *Global Journal of Science Frontier Research Chemistry,* 13(8): 20 – 30.

Bamford, C. H. and Tipper, C. F. H. (1972). *Reactions of Metallic Salts and Complexes, and Organometallic Compounds*. Elsevier Publishing Company, Amsterdam – London – New York, p223.

Basab, B. D., Ritam, M., Subrata, M. and Rupendranath, B. (2005). Mechanistic Studies on the Oxidation of Hydrazine by Tris(biguanide)manganese(IV) in Aqueous Acidic Media. *Helvetica Chemica Acta*, 2294 – 2301.

Bazhko, O. (2009). *Application of Redox Titration Techniques for Analysis of Hydrometallurgical Solutions*. Hydrometallurgy Conference, The Southern African Institute of Mining and Metallurgy, Mintek, South Africa.

Berry, R. S., Rice, S. A. and Ross, J. (1980): *Physical Chemistry*. John Wiley & Sons Inc. New York, pp. 1179 – 1185.

Bitziou, E., Snowden, M.E., Joseph, M.B., Leigh, S.J., Covington, J.A., Macpherson, J.V. and Unwin, P.R. (2013). Dual Electrode Micro – Channel Flow Cell for Redox Titrations: Kinetics and Analysis of Homogeneous Ascorbic Acid Oxidation. Journal of Electroanalytical Chemistry, 692(2013): 72 – 79.

Bradshaw, M.P., Barril, C., Clark, A.C., Prenzler, P.D. and Scollary, G.R. (2011). Ascorbic Acid: A Review of its Chemistry and Reactivity in Relation to a Wine Environment. *Critical Review in Food Science and Nutrition*, 51(6): 479 – 498.

Brzyska, W. and Krol, A. (1988). *Polish Journal of Chemistry*, 62:667.

Cantillo, D., Mojtaba, M. M. and Oliver, K. C. (2013). Hydrazine – Mediated Reduction of Nitro and Azide Functionalities Catalyzed by Highly Active and Reusable Magnetic Iron Oxide Nanocrystals. *The Journal of Organic Chemistry*, 78: 4530 − 4542.

Carl, W. R., Richard, J. W. and Lester, P. K. (1975). Kinetics of the Oxidation of Hydrazine by Hydogen Peroxide, Catalyzed by Copper(II). *Ballistic Research Laboratories Momerandum Reports*, 2523.

Carlos B. G., Gabriela P. M. and Christine, F. H. (2000). *American Society of Plant Physiologists.* 123: 335 – 343.

Cookson, F.J., Smith, T.D., Boas, J.F., Hicks, P.R. and Pilbrow, J.R. (1977). *Journal Chemistry Society, Dalton Transactions*, (1977):109.

Curie, C., Cassin, G., Couch, D., Divol, F., Higuchi, K., Le Jean, M., … Mari, S. (2009). Metal Movement Within the Plant: Contribution of Nicotianamine and Yellow Stripe 1-like Transporters. *Annuals of Botany*, 103(1): 1 – 11.

Das, R.S., Singh, B., Mandal, A., Banerjee, R. and Mukhopadhyay, S. (2015). Kinetics of Palladium Nano-Particles Catalyzed Reduction of Methylene Green by Hydrazine: Role of Induction Period in Determining Mechanistic Pathway. *Inorganica Chimica Acta*, 428(2015): 185 – 192.

David, M. S. (1984). Reactions Involving the Hydrazinium Free Radical: Oxidation of Hydrazine by Hexachloroiridate. *Inorganic Chemistry*, 23: 2879 – 2882.

Davies, S. G. (1982). *Organotransition Metal Chemistry: Applications to Organic Synthesis*. Pergamon press, Oxford, pp. 11.

Davis, M. B. (1992). Reactions of L – Ascorbic Acid with Transition Complexes. *Polyhedron*, 11(3): 285 – 321.

Dezsi, I., Agnes, N. and Nagy, D. (1976), After-Effects Observed in ^{57}Co(III)-HEDTA Complex, *Journal de Physique Colloques*, 37(c6), 909 – 911.

Dhas, T. P. A., Mishra, D. K., Mittal, R. K. and Gupta, Y.K. (1991). Kinetics and Mechanism of Oxidation of Hydrazinium Ion with Peroxomonophosphoric Acid in Acid Perchlorate Solutions and Role of Trace Iodide Ions. *International Journal of Chemical Kinetics*, 23: 203 – 213.

El-Zaru, R. A. and Hodali, H. A. (1990). Kinetics of Oxidation of Ascorbic Acid by Octacyanomolybdate(V) in Aqueous Methanol – A Comparative Study. *Polyhedron*, 9(1): 113 – 118.

Gain, S., Mishra, R., Mukhopadhyay, S. and Banerjee, R. (2011). Mechanistic Studies on Oxidation of Hydrogen Peroxide and Hydrazine by a Metal-Bound Superoxide. *Inorganica Chimica Acta*, 373(2011): 311 – 314.

Gamenara, D., Gustavo, A. S., Saenz, M. P. and Pablo, D. (2013). *Redox Biocatalysis: Fundamentals and Applications*. John Wiley & Sons Inc, pp7.

Ghanbari, P. S., Rasoolzadeh, M. and Salimi, M. (2013). Analytical Study of Platinum Group Catalysts Deactivation in Catalytic Propellant in Space Industry. *1st National Industrial Catalyst Conference, Shiraz, Iran.*

Granot, E., Filanovsky, B., Presman, I., Kuras, I. and Patolsky, F. (2011). Hydrazine/Air Direct – Liquid Fuel Cell Based on Nanostructured Copper Anodes. *Journal of Power Sciences*, 204(2011): 116 – 121.

Gromov, V. F., Matveyeva, A. V., Khomikovskii, P. M. and Abkin, A .D. (1966). The Effect of Methanol on the Polymerization of Acrylamide in Aqueous Solution. *Polymer Science U.S.S.R*, 9(7): 1616 – 1623.

Hahn, R. B. and Welcher, F. J. (1963). Inorganic Qualitative Analysis: A Short Course for Introductory Chemistry. *Journal of Chemical Education*, 40(8), 442.

Haim, A. (1983). Electron Transfer Reactions: The Bridge Activated Complex. *Progress in Inorganic Chemistry*, 30: 273 – 357.

Hamzeh, M. A. (2001). Kinetics of Oxidation of L-Ascorbic Acid by Cobalt(III) Complexes. *Journal of the Chemical Society of Pakistan*, 23(2), 69 – 73.

Housecroft, C. E and Sharpe, A. G. (2008). *Inorganic Chemistry Third Edition*. Pearson Education Limited, Edingburgh Gate, England, pp.883.

Idris, S. O., Suleman, J. O., Iyun, J. F. and Osunlaja, A. A. (2015). Reduction of 3,7-Bis(dimethylamino)phenazothionium Chloride by Benzenethiol in Aqueous Nitric Acid Medium: A Mechanistic Approach. *American Chemical Science Journal*, 5(4): 313 – 321.

Iyun, J. F. and Tinuoye, E. O. (1998). A Proceeding of the First Chem. Class Organized by the Chemical Society of Nigeria, Zaria Chapter.

James, H. E. (2002), *Kinetics and Reaction Mechanisms Second Edition*. McGraw – Hill, pp156 – 645.

Jean-Pierre, S. and Paul, B. (2002). *Hydrazine*: *Ullmann's Encyclopedia of Industrial Chemistry*, Wiley-VCH, Weinheim, pp87 – 91.

Jhimli, B., Kabita, D. and Subrata, M. (2004). Mechanistic Studies on Oxidation of Hydrazine by an oxo-diiron(III,III) Complex in Aqueous Acidic Media – Proton Coupled Electron Transfer. *Journal of the Chemical Society, Dalton Transactions*, (2009) 2910 – 2917.

Jiang, Y., Hong-Bin, D., Zhong, Y., Chen, D. and Wang, P. (2015). Complete and Rapid Conversion of Hydrazine Monohydrate to Hydrogen over Supported Ni–Pt Nanoparticles on Mesoporous Ceria for Chemical Hydrogen Storage. *Chemistry-An European Journal*, 21:15439 – 15445.

Jiewei, L., Lianfen, C., Hao, C., Jianyong, Z., Li, Z. and Cheng-Yong, S. (2014). Applications of Metal–Organic Frameworks in Heterogeneous Supramolecular Catalysis. *Chemical Society Review*, 43: 6011 – 6061.

Jones, E. and Hughes, R. E. (1976). Copper Boilers and the Occurrence of Scurvy: An Experimental Approach. *Medical History*, 20(1): 80 – 81.

Joseph, A. L., Joe, J. H. and Raymond, J. T. (2013). Antimicrobial Activity of Metals: Mechanisms, Molecular Targets and Applications. *Nature Reviews Microbiology*, 11: 371–384.

Juan, D., Joseph, J. C. and Garry, R. B. (2012). Ascorbic acid: Chemistry, Biology and the Treatment of Cancer. *Biochemica et Biophysica Acta,* 1826(2): 443 – 457.

Juranic, C., Celap, M.B., Vucelic, D., Maliner, M.J. and Radivojsa, P.N. (2006). A ^{59}Co NMR Study of Co(III) Complexes Containing Aminocarboxylato Ligands. *Journal of Co-ordination Chemistry*, 9(2): 117 – 123.

Karuppiah, N., Krishnan, S. M. and Pilavadi, T. (2015). Kinetics and Mechanism of Electron Transfer Reaction of Single and Double Chain Surfactant Cobalt(III) Complex by $Fe^{2}C$ Ions in Liposome (dipalmitoylphosphotidylcholine) Vesicles. *Phase Transition*, 88(5): 461 – 474.

Khan, M. N. and Sarwar, A. (1999). The Influence of Transition Metal Ions on the Kinetics of Ascorbic Acid Oxidation by Methylene Blue in Strongly Acidic Media. *Turkish Journal of Chemistry*, 25(2001), 433 – 440.

Khan, Z., Kumar, P. and Din, K. (2005). Kinetics of the Reaction of Water Soluble Colloidal MnO_2 by Ascorbic Acid. Journal of Colloid Interface Sciences, 200(2005): 184 – 189.

Khan, Z., Singh, T., Hussian, J.I. and Hashmi, A.A. (2013). Au(III) – CTAB Reduction by Ascorbic Acid: Preparation and Characterization of Gold Nanoparticles. Colloid and Surfaces B: Biointerfaces, 104(2013): 11 – 17.

Kimura, M., Yamamoto, M. and Yamabe, S. (1982). Kinetics and Mechanism of the Oxidation of L-ascorbic Acid by tris(1,10-phenanthroline)iron(III) Complexes in

Aqueous Solution. *Journal of the Chemical Society, Dalton Trasnsactions,* 1982: 423 – 427.

Kustin, K. and Toppen, D. L. (1973). Reduction of Vanadium(V) by L – Ascorbic Acid. *Inorganic Chemistry*, 12: 1404 – 1407.

Lachapelle, M. Y. and Drouin, G. (2010). Inactivation Dates of the Human and Guinea Pig Vitamin C Genes. *Genetica*, 139(2): 199–207.

Lappin, A. G., Laranjeira, M. C. M. and Youde-Owei, L. (1981). *Journal of the Chemical Society, Dalton Transactions*,(1981): 721.

Larsen, J. W., John, J., Matthew, S. and John, L. S. (2001). Carbon – Catalyzed Decompositions of Hydrazine and Hydroxylamine. *Carbon*, 39: 473 – 481.

Laurence, G. S. and Ellis, K. J. (1972). The Detection of a Complex Intermediate in the Oxidation of Ascorbic Acid by Ferric Ion. *Journal of the Chemical Society, Dalton Transactions*, 1972(15): 1667 – 1670.

Lawrence, M.A.W., Maragh, P.T. and Dasgupta, T.P. (2012). Mechanistic Studies on the Intra-molecular Electron Transfer in the Adduct Species of some Oxo-centered Trinuclear Iron(III)/Chromium(III) Cations and L-Ascorbic Acid in Aqueous Acetate Buffer. *Inorganica Chimica Acta*, 388(2012): 88 – 97.

Laxmi, N. J., Kirthi, S. B., Noorjahan, M. S., Sharanappa, T. N. and Shivamurti, A.C. (2013). Oxidation of Ascorbic Acid by Hexacyanoferrate(III) in Aqueous Perchloric Acid Medium – A Kinetic and Mechanistic Study. *Journal of Chemical and Pharmaceutical Research*, 5(4):290 – 300.

Leal, J. M., Domingo, P. L., Gercia, B. and Ibeas, S. (1993). Alkali – Metal Ion Catalysis of the Oxidation of L-ascorbic Acid by Hexacyanoferrate(III) in Strongly Acidic Media. *Journal of the Chemical Society, Faraday Transactions.* 89(19): 3571 – 3577.

Lemma, K., House, D.A., Retta, N. and Elding, L.I. (2002). Kinetics and Mechanism of Reduction of Halo and Haloam(m)ineplatinum(IV) Complexes by L-Ascorbate. *Inorganica Chimica Acta*, 331(2002): 98 – 108.

Lim, P. K. and Zhong, Y. (1989). The Copper-Catalyzed Redox Reaction between Aqueous Hydrogen Peroxide and Hydrazine. 2. Reaction Mechanism, Model Analysis, and a Comparison of Model and Experimental Results. *Journal of the American Chemical Society*, 111: 8404 – 8410.

Liu, C., Gorby, Y. A., Zachara, J. M., Fredrickson, J. K. and Brown, C. F. (2002). Reduction Kinetics of Fe(III), Co(III), U(VI), Cr(VI), and Tc(VII) in Cultures of Dissimilatory Metal – Reducing Bacteria. *Biotechnology and Bioengineering*, 80(6): 637 – 649.

Lohdip, Y. N. (1989). Kinetics *and Mechanism of the Oxidation – Reduction Reactions of Diaquotetrakis(2,2'-Bipyridine-μ-oxo-diruthenium(III) Ion in Acid Medium* (Unpublished master's dissertation). Ahmadu Bello University, Zaria, Nigeria.

Luty-Blocho, M., Paclawski, K., Wojnicki, M. and Fitzner, K. (2013). The Kinetics of Redox Reaction of Gold(III) Chloride complex Ions with L-Ascorbic Acid. *Inorganica Chimica Acta*, 395(2013):189 – 196.

Maity, D., Mijanuddin, M., Drew, M.G.B., Marek, J., Mondal, P.C., Pahari, B. and Ali, M. (2007). Oxovanadium(V) Complexes of Bis(phenolate) Ligands with Acetylacetone as co-Ligand: Synthesis, Crystal Structure, Electrochemical and Kinetics Studies on the Oxidation of Ascorbic Acid. Polyhedron, 26(2007): 4494 – 4502.

Majumdar, T., Pahari, S., Mandal, H. K. and Mohapatra, A. (2010). Kinetic studies on the reaction between $[Co(NH_3)_5N_3]Cl_2$ and ascorbic acid: Effect of surfactant, polymer and their mixture. *Journal of Molecular Liquids*, 153(2 – 3): 101 – 106.

Mandal, K., Banerjee, R. and Mukhopadhyay, S. (2013). Kinetics of Reduction of μ-amido-μ-superoxo-bis[tetraaminecobalt(III)]$^{4+}$ Complex with Hydroxylamine Derivatives. Inorganica Chimica Acta, 394(2013): 691 – 695.

Manolis, J. M. and Mercouri, G. K. (2009). Use of Hydrazine in the Hydrothermal Synthesis of Chalcogenides: the Neutral Framework Material $[Mn_2SnS_4(N_2H_4)_2]$. *Inorganic Chemistry*, 48(11): 4658–4660.

Max, L., Paul, R. and JoÈrg, W. (1998). Reduction of Aromatic Nitro Compounds with Hydrazine Hydrate in the Presence of an Iron Oxide Hydroxide Catalyst. I. The Reduction of Monosubstituted Nitrobenzenes with Hydrazine Hydrate in the presence of Ferrihydrite. *Applied Catalysis.* 172:141–148.

Max, L., Ronny, R. and Paul, R. (1999). Reduction of Aromatic Nitro Compounds with Hydrazine Hydrate in the Presence of an Iron Oxide/Hydroxide Catalyst. III. The Selective Reduction of Nitro Groups in Aromatic Azo Compounds. *Applied Catalysis*, 17 (1999):9 – 14.

Mehrota, U. S., Agrawal, M. C. and Mushran, S. P. (1970). Reduction of Hexachloroplatinate by Ascorbic Acid. *Journal of Inorganic and Nuclear Chemistry*, 32(7): 2325 – 2329.

Micheal, G. M., Gregory, A. U. and Sue, E. B. (1978). Oxidation of Hydrazine in Aqueous Solution. *Environmental sciences Research Division*.

Miessler, G. L., Fischer, P. J. and Tarr, D. A. (2014). *Inorganic Chemistry Fifth Edition*. Pearson Education, Inc New York, pp 462 – 465.

Mohanty, B., Behera, J., Acharya, S., Mohanty, P. and Patnaik, A. K. (2014). Kinetics and Mechanism of Oxidation of GSH by cis-(diaqua)-bis-(ethylenediamine)cobalt(III) Ion. *International Journal of Advanced Chemistry*, 2(1): 39 – 43.

Mondal, A. and Banerjee, R. (2009). Kinetics and Mechanism of the Uncatalysed Oxidation of Hydrazine with Superoxide Co-Ordinated to Cobalt(III). *Indian Journal of Chemistry*, 48(a): 645 – 649.

Mondal, A., De, P., Mukhopadhyay, S., Banerjee, R., Kar, P., Jose, A.D. and Das, A. (2009). Kinetics of Oxidation of Quinol and Ascorbic Acid with the Phen Substituted Semiquinone Ligand, (5,6-dioxlene-1,10-phenanthroline-O,O) Bound to the $Ru(bipy)_2$ Moiety. *Polyhedron*, 28(2009): 2655 – 2660.

Mshelia, M. S., Iyun, J. F., Uzairu, A. and Idris, S. O. (2010). Kinetics and Mechanism of the Oxidation of Hydrazine Dihydrochloride by Aqueous Iodine. *Journal of American Science*, 6(9):293 – 296.

Muhammad, A. A., Adnan, A., Aziz, U. R., Khadija, N., Sabahat, Z. S., Khalid, M. K., … Syeda, A. E. (2013). Synthesis, Structural Characterization and Enzyme Inhibition Studies on 5-(2-nitrostyryl)-1,3,4-oxadiazole-2-thiol Derivatives. *Journal of the Chilean Chemical Society*, 58(4): 2186 – 2190.

Nagaraj, K., Murugan, K. S. and Thangamuniyandi, P. (2015). Kinetics and Mechanism of Electron Transfer Reaction of Single and Double Chain Surfactant Cobalt(III) Complex by Fe^{2+} Ions in Liposome(dipalmitoylphosphotidylcholine) Vesicles. *Phase Transitions*, 88(5): 461 – 474.

Narendra, K. S., Riya, S. and Prem, D. S. (2014). Kinetics and Mechanism of Oxidation of L – Ascorbic Acid by Silver (I) in Acid Perchlorate Medium. *International Journal of Scientific Research*, 3(7): 62 – 66.

Olayinka, A. O., Maipelo, G. and Ngonye, S. (2006). Non-Bridging Ligand Effects on the Kinetics of Reduction of Chloro- and Azido-Pentaamminecobalt(III) by some polypyridyl Complexes of Ruthenium(II). *Bulletin of the Chemical Society of Ethiopia*, 20(2), 227 – 234.

Onu, A. D. and Iyun, J. F. (2000). Redox Kinetics of Monomethyl Fuchsin by Dithionite Ion in Aqueous Hydrochloric Acid. *Nigerian Journal of Chemical Research*, 5:33 – 36.

Onu, A. D., Iyun, J. F. and Idris, S.O. (2015). Kinetics and Stoichiometry of the Reduction of Hydrogen Peroxide by an Aminocarboxylactocobaltate(II) Complex in Aqueous Medium. *Open Journal of Inorganic Chemistry*, 5:75 – 82.

Onu, A. D. (2010). *Kinetics and Mechanism of the Reaction of two Aminocarboxylatocobaltate(II) Complexes with some Oxy – Anions and Hydrogen Peroxide in Aqueous Perchloric Acid Medium* (Unpublished doctorial thesis). Ahmadu Bello University, Zaria, Nigeria.

Onu, A.D., Iyun, J.F. and Idris, S.O. (2015). Kinetics and Stoichiometry of the Reduction of Hydrdogen Peroxide by Aminocarboxylatocobaltate(II) Complex in Aqueous Medium. *Open Journal of Inorganic Chemistry*, 5: 75 – 82.

Onu, A. D., Iyun, J. F. and Idris, S.O. (2016). Oxidation of Ethylenediaminetetraactato-cobaltate(II) Complex by Hydrogen Peroxide in Aqueous Acidic Medium: A Kinetic Study. *Journal of the Nigerian Chemical Society*, 41(2): 81 – 86.

Osunlaja, A. A., Idris, S. O. and Iyun, J. F. (2013). Kinetics and Mechanism of Thiourea Oxidation by Oxygenated $[Co_2(O_2)(NH_3)10]^{5+}$ Complex. *Journal of Chemical and Pharmaceutical Research*, 5(2):328 – 336.

Pap, J.S., Szyuriel, L., Rowinska-Zyrek, M., Nikitin, K., Fritsky, I.O. and Kozlowski, A. (2011). An Efficient Copper(II) Catalyst in the Four Electron Reduction of Molecular Oxygen by L-Ascorbic Acid. Journal of Molecular Catalysis A: Chemical, 334(2011): 77 – 82.

Paraneeiswaran, A., Sudhir, K. S., Prashanth, K. and Subba, R. T. (2014). Microbial Reduction of [Co(III)-EDTA]$^{-}$ by *Bacillus licheniformis* SPB-2 Strain Isolated from a Solar Salt Pan. *Journal of Hazardous Materials*, 283:582–590.

Paraneeiswara, N. A., Sudhir, K. S., Subba, R. T. and Prashanth, K. (2015). Removal of Toxic Co-EDTA Complex by a Halophilic Solar-Salt-Pan Isolate *Pseudomonas aeruginosa* SPB-1. *Chemosphere,* 95:503–510.

Paraneeiswaran, A., Sudhir, K. S., Rajesh, K. and Subba, R. T. (2016). Reduction of [Co(III)–EDTA]$^{-}$ Complex by a Novel Process Using Phototrophic Granules: a Step Towards Sustainable Bioremediation. *Royal Society of Chemistry Advances*, 6: 43656–43662.

Patapati, S. R., Nabeen, K. R. and Rama, K. P. (1986). Kinetics and Mechanism of Oxidation of Hydrarine by Tri-iodide Ion in Aqueous Acidic Media. *Journal of the Chemical Society, Dalton Transactions*, (1986):1189 – 1192.

Patil, K. C. and Tanu, M. R. (2014). *Inorganic Hydrazine Derivatives Synthesis, Properties and Applications*. John Wiley & Sons, Ltd, United Kingdom, pp 219 – 252.

Pelizzetti, E., Mentasi, E. and Pramauro, E. (1978). Kinetics and Mechanism of Oxidation of Ascorbic Acid by Manganese(III) in Aqueous Acidic Perchlorate Media. *Journal of the Chemical Society, Dalton Transactions,* 1978: 61 – 63.

Perveen, A., Nezamoleslam, T. and Iftikhar, I. N. (2013). Preparation of Cobalt(III) complexes with trans-1,2-diaminocyclohexane-N,N,N',N'-tetraacetatic acid (CDTA) and ethylenediaminetetraacetic acid (EDTA). *African Journal of Pure and Applied Chemistry,* 7(6): 218 – 222.

Peter, T. A. D., Mishra, D. K., Mittal, R. K. and Gupta, Y. K. (1991). Kinetics and Mechanism of Oxidation of Hydrazinium Ion with Peroxomonophosphoric Acid in Acid Perchlorate Solutions and Role of Trace Iodide Ions. *International Journal of Chemical Kinetics*, 23: 203 – 213.

Ravi, E. and Brian, P. (2012). Synthesis of Nickel Nanoparticles by Hydrazine Reduction: Mechanistic Study and Continuous Flow Synthesis. *Journal of Nanoparticle Research,* (2012) 14:800.

Rehana, S., Sameera, R. K. and Maria, A. (2012). Effect of Ionic Strength on the Kinetics of Oxidation of Ascorbic Acid by Methylene Green in Aqueous Methanol System. *Asian Journal of Chemistry*, 24(8): 3745 – 3750.

Richard C. O. and Renfrow W. B. (1952). A qualitative Test for Ammonia in Aqueous Solution. *Journal of Chemistry Education*, 29(2): 94.

Rupa, S., Aditya, P. and Raj, N. M. (1999). Outer – Sphere Mechanism of the Oxidation of Hydrazine and Hydrazinium Ion by 12-tungstocobaltate(III) Ion in Acetic – Acetic Acid Buffer: Marcus Treatment. *Indian Journal of Chemistry*, 38(a): 680 – 685.

Sadagopa, V. M. R., Sundaram, S. and Venkatasubramanian, N. (1975). Oxidation of Hydrazine by Cr(VI) Oxide: Kinetic and Mechanistic Studies in the Presence of Complexing Agents. *Inorganica Chimica Acta,* 13 (1975): 133 – 139.

Sadhana, S. S., Mohanty, D. P. and Pattnaik, A. K. (2014). Catalytic Effect on the Electron Transfer Reactions of L – Ascorbic acid with Co(III) Complex in Aqueous Acid Medium. *Chemical Science Review and Letters*, 3(12):774 – 783.

Sadhana, S., Patnaik, A. K., Das, S. P. and Mohanty, P. (2015). Kinetics and Mechanistic Study of Redox Reaction of Cobalt (III) Complex with L-Ascorbic Acid in Aqueous Acid Medium. *American Chemical Science Journal*, 9(2), 1 – 10.

Saha, B., Gangopadhyay, S., Ali, M. and Banarjee, P. (1995). Kinetic Studies on the Reduction of Nickel(IV) and nickel(III) Oxime–imine Complexes by Ascorbic Acid. *Journal of the Chemical Society, Dalton Transactions*, (7):1083 – 1088.

Sailani, R., Dubey, S., Khandelwal, C.L., Sharma, P.D. and Khan, P. (2011). Kinetics and Mechanism of Oxidation of L-ascorbic Acid by Peroxomonosulphate in Acid Perchlorate Medium. Role of Copper(II) as a Trace Metal-Ion Catalyst. *Rendus Chimie*, 14(2011): 1088 – 1094.

Sanjay, K. S. and Qiang, X. (2013). Nanocatalysts for Hydrogen Generation from Hydrazine. *Catalysis Science and Technology*, 3:1889 – 1900.

Scott, E. J. Y. and Chester, A. W. (1972). Kinetics of the Cobalt-Catalyzed Autoxidation of Toluene in Acetic Acid: Role of Cobalt. *Journal of Physical Chemistry*, 76 (11), 1520–1524.

Sekhon, B. S. (2003). Chelates for Micronutrient among Crops. *Resonance*, 8(7): 46 – 53.

Shahram, G. P., Mozaffar, S. and Maryam, R. (2014). A Review on Decomposition of Hydrazine and Its Kinetics as a Novel Approach for CO-Free H_2 Production. *Researches and Applications in Mechanical Engineering*, Volume 3.

Sharpe, A. G. (1981). *Inorganic Chemistry, 1st edition*. Longman, London. p518.

Sherrell, C. G. (1990). Effect of Cobalt Application on the Cobalt Status of Pastures 3: Comparison of Chelate and Sulphate as Cobalt Source for Top Dressing Deficient Pastures. *New Zealand Journal of Agricultural Research*, 33(2): 313 – 317.

Shirin, N. O., Changlin, Z., Sang, Y. H., Harry, M. C. and Zhenmeng, P. (2016). Synthesis and Property of a Helwingia-structured Nickel Nitride/Nickel Hydroxide Nanocatalyst in Hydrazine Decomposition. *Royal Society of Chemistry Advances*, 6:38494–38498.

Singh, B., Das, R.S., Banerjee, R. and Mukhopadhyay, S. (2014). Uncatalyzed and Copper(II) Catalyzed Oxidation of Glutathione by $Co(III)_2$ Bound Superoxide Complex. *Inorganica Chimica Acta*, 418(2014): 51 – 58.

Singh, R., Dong, H., Liu, D., Marts, R.A., Tierney, D.L. and Almquist, C.B. (2015). $[Cobalt(III)\text{-}EDTA]^-$ Reduction by Thermophilic Methanogen *Methanothermobacter thermautotrophicus*. *Chemical Geology*, 411(2015): 49 – 56.

Snehalatha, T., Rajanna, K. C., Saiprakash, P. K., (1997). Methylene Blue–Ascorbic Acid an Undergraduate Experiment in Kinetics. *Journal of Chemical Education*, 74(2): 228 – 233.

Srinivas, B., Reddy, R. M. and Chandra, A. V. (2007). The Anation Kinetics of cis[Co(en)2(H2O)2](NO3)3 by Anthranilic Acid in Aqueous Medium. *Asian Journal of Chemistry*, 19(4), 2586 – 2594.

Streszewski, B., Jaworski, W., Konrad, S. and Krzysztof, P. (2014). Kinetics and Mechanism of Redox Reaction between Tetrachloroaurate(III) Ions and Hydrazine. *International Journal of Chemical Kinetics*, 1–10.

Suggs, H. J., Luskus, L. J., Kilian, H. J. and Mokry, J. W. (1979). Exhaust Gas Composition of the F-16 Emergency Power Unit (Technical report). *USAF*.

Sultan, S. M. S., Al-zamil, Z. I., Al-hajjaji, A. M., Al-tamrah, S. A. and Aziz, A.A.M. (1985). A Kinetic Study on the Determination of Hydrazine by Iodine in Sulphuric Acid Media. *Journal of the Chemical Society of Pakistan*, 7(2): 93 – 99.

Szabolcs, S., Gyorgy, P. and Laszlo, W. (2005). Cobalt(III) EDTA Complex Removal from Aqueous Alkaline Borate Solution by Nanofiltration. *Desalination*. 175:179 – 185.

Thakuria, M. B. and Gupta, Y. K. (1975). Kinetics and Mechanism of Electron Transfer Reactions of Aqueous and Co-ordinated Thallium(III), Part II: Reduction of Hexa-aquathallium(III) by Hydrazine. *Journal of the Chemical Society, Dalton Transactions*, (1975): 2541 – 2545.

Tipson, R. S. (1945). A Qualitative Test for Dehydroascorbic Acid. *Journal of the American Pharmaceutical Association*, 34(7): 190 – 192.

Tobe M. L, and Burgess, J. (1999). *Inorganic Reaction Mechanisms*, Addison Wesley Longman: New York; chpt. 4 and 9.

Tsukahara, K., Izumitani, T. and Yamamoto, Y. (1982). The Reduction of Cobalt(III) Complexes by Ascorbic Acid. II. The Kinetics and Mechanism of the Reaction of Diaqua and Aquahydroxo Macrocyclic N4 Complexes. *Bulletin of the Chemical Society of Japan*, 55(1): 130 – 135.

Twigg M. V. (1983). *Mechanisms of Inorganic and Organometallic Reactions vol 1*. Plenum press New York, pp.51 – 52.

Twigg M. V. (1984). *Mechanisms of Inorganic and Organometallic Reactions vol 2*. Plenum press New York, pp.11 – 55.

Vieira, R., Pham-Huu, C., Keller, N. and Ledoux, M. J. (2002). New Carbon Nanofiber/Graphite Felt Composite for Use as a Catalyst Support for Hydrazine Catalytic Decomposition. *Chemical Communications*, (9): 954–955.

Wagnerova, D. M., Schwertnerova, E. and Veprek-siska, J. (1973). *Collection of Czechoslovak Chemical Communications*, 38(1973):756.

Wang, Y., Lau, K., Lam, W. Y., Man, W., Leung, C. and Lau, T. (2009). Kinetics and Mechanism of the Oxidation of Ascorbic Acid in Aqueous Solutions by a *trans*-Dioxoruthenium(VI) Complex. *Inorganic Chemistry*, 48(1): 400 – 406.

Wilkins, G. R. (2002): *Kinetics and Mechanism of Reactions of Transition Metal Complexes 2nd Thoroughly Revised Edition*. Wiley-VCH Verlag GmbH & Co, pp. 73 – 275.

William, H. J., Donald, R. S. and Thomas, W.S. (1991). Kinetics of the Aqueous Cobalt(II)/Cobalt(III)/EDTA System at Variable Pressure. *Inorganic Chemistry*, 31(3):507 – 511.

Zagal, J. H., Sergio, L. and Soledad, U. (1986). A Mechanistic Study of the Electro-Oxidation of Hydrazine on Phthalocyanines of Vo, Cr, Mn, Ni, Cu and Zn Attached to Graphite Electrodes. *Journal of Electroanalytical Chemistry*, 210 (1986): 95 – 110.

Zheng, M., Cheng, R., Chen, X., Li, N., Li, L., Wang, X. and Zhang, T. (2005). "A Novel Approach for CO-free H_2 Production Via Catalytic Decomposition of Hydrazine". *International Journal of Hydrogen Energy*, 30:1081 – 1089.